Behavior and Capacity of 12-Inch Hollowcore Under Concentrated Point Load

Jenna J. Powers

Civil and Architectural Engineering and Construction Management Department

Milwaukee School of Engineering

Author Note

Jenna J. Powers, Civil and Architectural Engineering and Construction Management Department, Milwaukee School of Engineering.

A report submitted in February 2021 to the faculty of the Milwaukee School of Engineering in partial fulfillment of the requirements for the degree of Master of Science in Architectural Engineering.

Correspondence concerning this article should be addressed to Jenna Powers, 1025 North Broadway, Milwaukee, WI 53202. E-mail: powers9027@gmail.com

Abstract

Elematic hollowcore is a machine extruded, precast, prestressed structural member. Prefabrication of these members allows for controlled design parameters, speed of construction, and versatility. However, with the ever-evolving success of these products, it is crucial for designers to have adequate information about their behavior. The objective of this paper is to report the results of an investigation entailing the observation and quantitative measurements of failure modes of 12-inch elematic hollowcore. A review of relevant literature provided comprehension of the common behavior and failure modes of hollowcore. Seven 12-inch polygon voided hollowcore, supplied by Mid-States Concrete Industries, were tested with a concentrated load at midspan. Applied loads, moments, and deflections were observed. Results from this research illustrate the comparison between modern codes and produced specimen. The test specimens had similar results to ACI predictions for mode of failure, and cracking, nominal, and maximum probable moments, thus validating the testing procedure and results. Future research with various testing parameters (e.g., span, concrete strength, prestressing configuration) that would result in shear failure would present validity of the shear calculations. Additionally, punching shear should be researched to observe the difference in crack patterns between 8-inch and 12-inch hollowcore.

Keywords: behavioral properties, concentrated load, concrete, elematic, flexure, flexure shear strength, hollowcore, load capacity, mechanical properties, Mid-States Concrete Industries, moment curvature, point load, shear, Spancrete, testing, web shear strength

Acknowledgements

Many people helped make this thesis possible. First, I would like to thank Mid-States Concrete Industries for providing the testing specimens and the Milwaukee School of Engineering for providing testing equipment. Without either, this thesis would not have been possible.

Without the wisdom and patience of my advisor, Todd Davis, Ph.D., this project would not have been the same. Thank you to Chris Raebel, Ph.D. and Douglas Stahl, Ph.D. for guidance throughout the entire process. Thank you also to Jeff MacDonald, who assisted in material acquisition and testing. Additionally, I would like to thank everyone who helped disassemble and reassemble the test frames in the lab.

Finally, I am grateful for my friends and family, who were understanding of my time limitations because of working on this thesis. They were more than generous in their support. I look forward to having more time for them now.

Table of Contents

List of Figures

List of Tables

Nomenclature

Symbols

A – cross-sectional area of member

A_{ps} – area of prestressing steel

b_o – perimeter of critical section for two-way shear

b_w – web width

d – depth of critical section

d_p – distance from extreme compression fiber to the centroid of prestressing reinforcement

d_{ps} – depth of prestressing steel

E_c – concrete modulus of elasticity

f_{pc} – compressive stress in concrete

f_{rup} – actual strength of reinforcement above yielding

$f'c$ – specified compressive strength of concrete

I – moment of inertia of section about centroidal axis

I_{cr} – moment of inertia of cracked section transformed to concrete

I_e – effective moment of inertia for calculation of deflection

I^*_e – alternative effective moment of inertia for calculation of deflection

I_g –moment of inertia of gross concrete section about centroidal axis, neglecting reinforcement

L – distance between supports

Length – length of member

M_a – maximum moment in member due to service loads at stage of deflection

M_{cre} – moment causing flexural cracking at section due to externally applied loads

M_D –moment in member due to self-weight

M_{max} – maximum factored moment at section due to externally applied loads

M_n – nominal flexural strength at section

M_{rup} – maximum probable flexural strength at section

n – modular ratio

P_{cr} – superimposed force at cracking

P_n – superimposed force at nominal

V_d – shear force at section due to unfactored dead load

V_i – factored shear force at section due to externally applied loads occurring simultaneously with

V_p – vertical component of effective prestress force at section

w_D – uniform weight of member

y_g – distance from centroidal axis of gross transformed section, to compression face

y_o – distance from centroidal axis of gross section, to compression face

y_t – distance from centroidal axis of gross section, neglecting reinforcement, to tension face

α_s – constant value

β – ratio of the long side to the short side of the punching shear area

ρ_p – ratio of A_{ps} to bd

λ – modification factor to reflect the reduced mechanical properties of lightweight concrete relative to normalweight concrete of the same compressive strength

Abbreviations

In – inches

Mpsi – megapounds per square inch

Psi – pounds per square inch

Ksi – kips per square inch

Behavior and Capacity of 12-Inch Hollowcore Under Concentrated Point Load

Precast concrete, a leading material in today's construction, is structural, prefabricated members, such as wall panels, hollowcore, beams, and columns. Prefabrication allows for controlled design parameters, speed of construction, and versatility. However, with the ever-evolving success of these products, it is crucial for designers to have adequate information about their behavior.

To contribute to the knowledge base about the behavioral properties of hollowcore slabs, an experimental testing program has been conducted at the Milwaukee School of Engineering. This paper features background information on precast, prestressed concrete, and hollowcore products produced by Mid-States Concrete Industries (MCI) and Spancrete. This paper also presents the results of a review on the capacity of 12-inch hollowcore slabs provided by MCI. In order to analyze the validity of the test results, the paper has been organized in terms of background information, calculations for specimens, and testing. First, background information describing the industry standard for point load capacity from Spancrete is introduced. Second, the testing regimen and results of testing MCI's 12-inch hollowcore are discussed. Third, the conclusions concerning the validity of the prediction of capacities and deflections are stated. Finally, recommendations are provided for future research based on the experimental findings and analytical comparisons.

Background

Concrete hollowcore plank (hollowcore) is a common type of structural element for floors and roofs. It is a precast, prestressed component with void extrusions through the span of a member. The voids reduce the dead load, while generating in an efficient strength to depth ratio. Although the strand provides flexural capacity, the lack of transverse shear reinforcement can

cause shear capacity to govern a design (ACI, 2014). As for the shape of the members, they can be sized for most framing layouts while providing strength, durability, and resistance to weather and fire. Typically, hollowcore ranges in depths of 8-inches to 16-inches with a width of 48-inches. However, filler pieces[1] provide more precise layouts. Figure 1 shows typical hollowcore slabs.

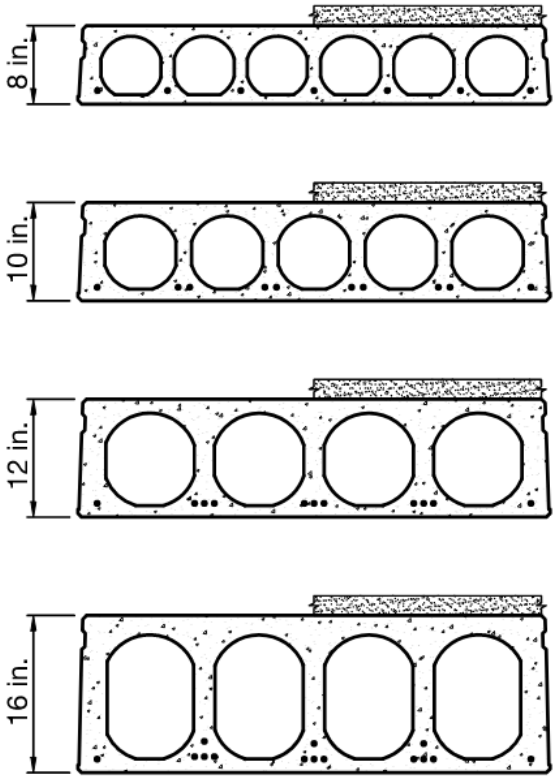

Figure 1. Hollowcore depths. Adapted from "PCI Design Handbook: Precast and Prestressed Concrete" by Precast/Prestressed Concrete Institute, 2017, p. 3-32.

[1] A filler piece is hollowcore that is less than 48-inches in width. These pieces come in specified widths that are determined by the manufacturer.

Precast, Prestressed Concrete

As an alternative to cast-in-place concrete, precast concrete refers to the manufacturing of concrete members at a plant and transporting those members to the construction site. This provides a controlled environment throughout the manufacturing of the members.

Because precast members require lifting from the form and truck, the members have requirements for shipping and handling. These requirements are regulated by the Precast/Prestressed Concrete Institute (PCI), which is a technical institute and trade association of councils and committees that provides design standards (PCI, 2017). PCI also provides literature on the design, fabrication, and erection of precast and prestressed members (PCI, 2017).

As for prestressing, it is similar to mild reinforcement such that it provides flexural strength (PCI, 2017). Concrete is strong in compression but weak in tension (Wight, 2016). Incorporating reinforcing counteracts the tensile stresses in service that can cause cracking and failure. Prestressing consists of stretched steel strands made up of twisted cables located at certain positions in the form (PCI, 2017). The concrete is then cast around the strand and cured such that the concrete and strand bond. Once the concrete reaches an optimal strength, the strands are cut from the frame, which creates camber in the hollowcore because of an introduced compressive force in the concrete. This is beneficial in the design because when the member is loaded, the total deflection is less (PCI, 2017).

Figure 2 demonstrates the effects of a non-prestressed beam versus a prestressed beam. The left beams are non-prestressed. When the non-prestressed beam has a load applied at midspan, it deflects. Similarly, on the right, the prestressed member deflects. However, camber is

introduced to the beams as the tendons are initially stressed, which results in a total deflection that is less than the non-prestressed beam.

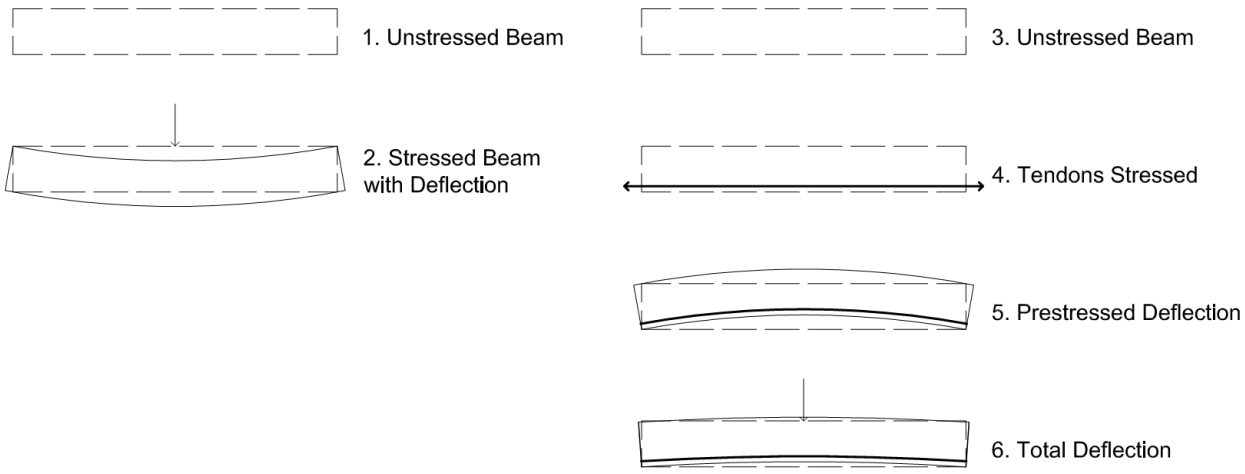

Figure 2. Comparison of non-prestressed and prestressed beams.

Note. In Figure 2, 1 = Non-prestressed beam without load, 2 = Non-prestressed beam with load, 3 = Non-prestressed beam without load, 4 = Prestressed beam without load prior to strand cutting, 5 = Unloaded prestressed beam with camber after strand cutting; 6 = Prestressed beam with load.

Spancrete

Spancrete is a precast manufacturer. Additionally, they are the licensing organization for load tables used in PCI MNL-126-15E, which provides superimposed live load capacities for various member spans, cambers, strand layouts, and structural topping (Spancrete, n.d.). The load tables are for material properties of 6,000 psi compressive strength and 250 ksi or 270 ksi prestressing strands (Spancrete, n.d.).

Mid-States Concrete Industries

Mid-States Concrete Industries (MCI) is a precast design-build firm located in South Beloit, Illinois. Their void forms vary from Spancrete, thus resulting in different capacities from the standard load tables. Figure 3 and Figure 4 show the difference in the cross-sectional shape of Spancrete's and MCI's 12-inch hollowcore. MCI has fewer voids that are greater in width,

while Spancrete has more narrow voids. MCI has thicker webs than Spancrete, while Spancrete has thicker flanges.

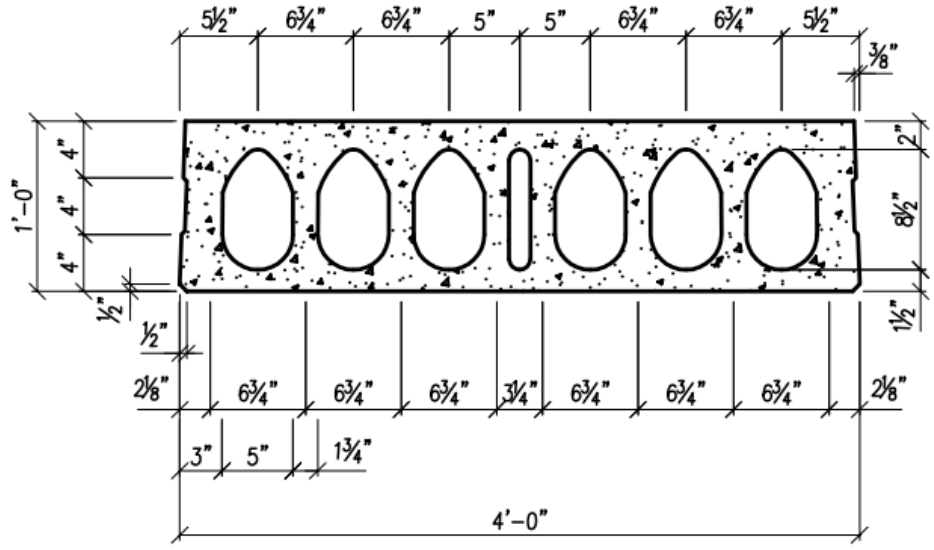

Figure 3. Spancrete's 12-inch hollowcore cross-section. Adapted from "Spancrete Cross-Sections" by Spancrete, (n.d.). Retrieved from https://www.spancrete.com/application/files/1915/3013/0978/Hollowcore_Cross_Sections.pdf

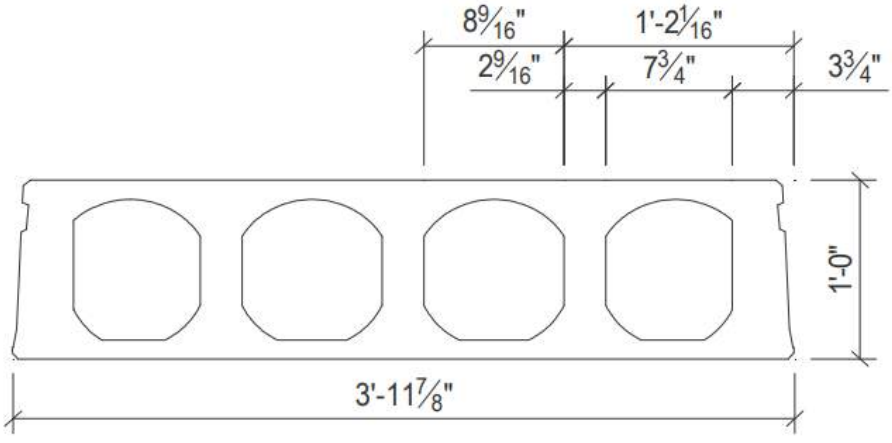

Figure 4. MCI's 12-inch hollowcore cross-section. Adapted from "Safe Load Table" by Mid-States Concrete Industries, (n.d.). Retrieved from https://static1.squarespace.com/static/59ee03b6017db2f97fb52c4f/t/5ba1340303ce64b9d5007457/1537291267660/12x48_NT2H.pdf

Hollowcore Cracking

Cracking of concrete members can cause issues related to shear capacity, debonding between the concrete and reinforcement, and corrosion propagation, which can lead to durability issues and failure of the member (Parkhats, 2018). In precast concrete, these issues can occur from casting, stripping, shipping, or loading. Figure 5 shows various types and locations of cracks that are associated with hollowcore.

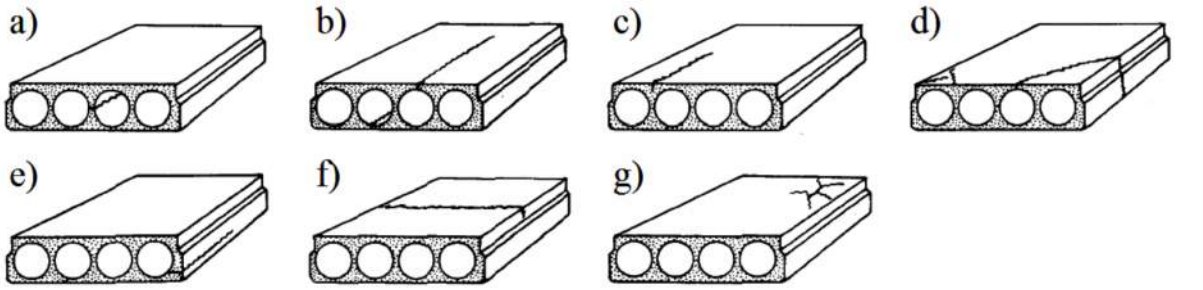

Figure 5. Cracks in prestressed hollowcore. Adapted from "Problem of Cracks in Prestressed Hollow Core Slabs" by V. Parkhats, May 2018, p. 6. Retrieved from https://www.researchgate.net/

Each of the crack patterns can be caused by a multitude of reasons; the following is a brief overview of some of these causes from Parkhats (2018, May). A web crack, shown in Figure 5a, is caused by excessive prestressing relative to the cross-sectional area of the member. It is also caused by insufficient release strength of the strands, expansion of the void forms, insufficient mix vibration, and bed surface to member bonding upon stripping. The longitudinal cracks at the voids in Figure 5b result from placement of the strands, insufficient flange thickness, and improper handling. Figure 5c shows longitudinal cracks in the webs, which can result from shrinkage because of the concrete mix and curing, and subsidence above the void.

The cracks at the corners in Figure 5d can be caused by excessive tension in the strands during stripping, and uneven handling and dunnage. Figure 5e shows web cracks near the strands, which is caused by bursting stresses, improperly placed strand masking, poor concrete

consolidation near strands, and inadequate layer bonding. The transverse cracks in Figure 5f are caused by longitudinal shrinkage, tension in the top fibers of the member, and delayed detensioning. Lastly, Figure 5g shows miscellaneous cracks, which can be caused by the concrete mix, surface shrinkage, and improper troweling.

Deflection

Deflection is the amount a member is displaced from a load. Deflection calculations depend on the classification of the prestressed flexural member (ACI, 2014). In prestressed concrete, the classifications are Class U, Class T, and Class C, depending on the extreme stress in the precompressed tension zone under service loads. The stress limits can be found in ACI 318-14 (2014) Section 24.5.2.1. Class U assumes uncracked behavior. Class C assumes cracked behavior. Class T is a transition between Class U and Class C. In order to calculate the deflection of Class U, it is based on the gross section, whereas the deflection for Class C and Class T are based on a cracked section and require a bilinear analysis.

The following are several methods for computing expected deflections. This paper looks at using the effective moment of inertia method, the bilinear method, and the I_e* method. Each of these deflection methods distinguish between the gross moment of inertia and cracked moment of inertia. The transformed gross moment of inertia is based on the uncracked cross-sectional dimensions. This is calculated using the parallel axis theorem for a composite shape from the concrete and steel reinforcement:

$$\mathbf{I}_{\boldsymbol{g}} = \mathbf{I} + \boldsymbol{A} * \left(\boldsymbol{y}_{\boldsymbol{g}} - \boldsymbol{y}_{\boldsymbol{o}}\right)^{\mathbf{2}} + (\boldsymbol{n} - \mathbf{1}) * \boldsymbol{A}_{\boldsymbol{ps}} * (\boldsymbol{d}_{\boldsymbol{ps}} - \boldsymbol{y}_{\boldsymbol{g}})^{\mathbf{2}}. \quad (1)$$

The cracked moment of inertia is reduced to account for the reduced cross-section after cracking. This is calculated as from PCI equation 5-110:

$$\mathbf{I}_{cr} = \boldsymbol{n} * \boldsymbol{A}_{ps} * \boldsymbol{d}_{p}^{2} * (\mathbf{1} - \mathbf{1.6}\sqrt{\boldsymbol{n} * \boldsymbol{\rho}_{p}}) . \quad (2)$$

The load-deflection relationship can be seen in Figure 6:

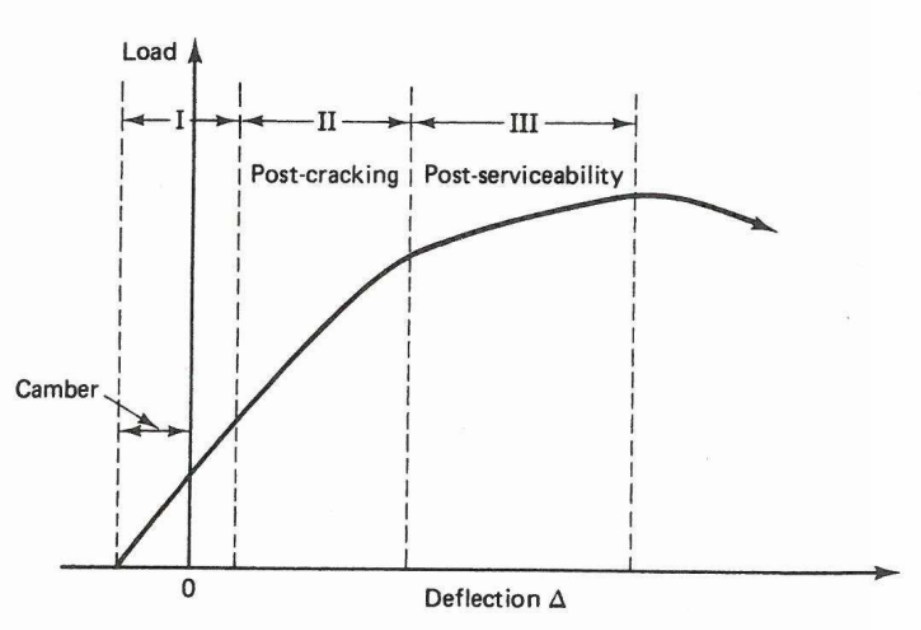

Figure 6. Load-deflection relationship. Adapted from *Prestressed Concrete: A Fundamental Approach* by E. Nawy, 2006, United Kingdom: Pearson/Prentice Hall, p. 420.

Region I of Figure 6 shows where the member is precracked. This is when the gross moment of inertia is applicable in deflection calculations. Region II shows the member after cracking, which is where the cracked moment of inertia is used for calculations. Region III shows the postservicabilitiy stage. Figure 7 illustrates the reduced cross-section after cracking.

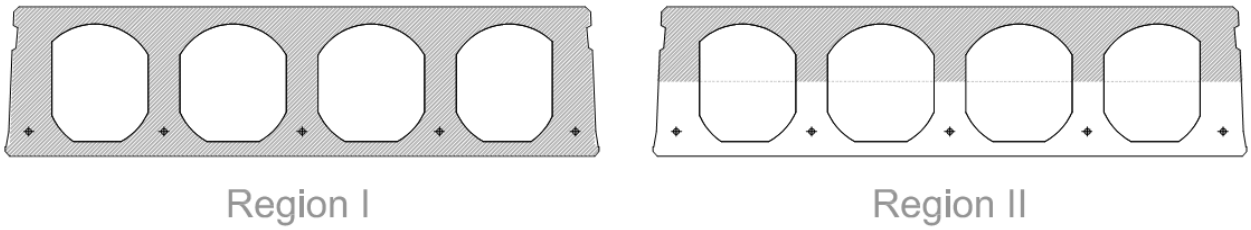

Figure 7. Cross-sectional before and after cracking.

Similarly, Figure 8 shows that the bilinear method uses the gross moment of inertia until cracking and then the cracked moment of inertia, while the I_e* method uses a modified moment of inertia.

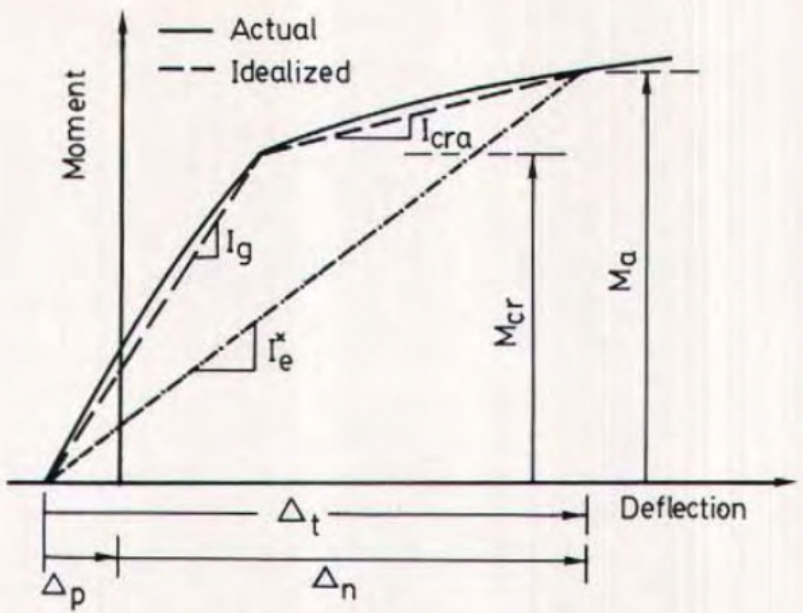

Figure 8. Bilinear and I_e* methods of deflection. Adapted from "Deflection of Progressively Cracking Partially Prestressed Concrete Flexural Members" by A. Alameh and M. Harajli, 1989, p. 96.

The effective moment of inertia method for calculating deflections is to "provide a transition between the upper and lower bounds of I_g and I_{cr} as a function of the ration M_{cr}/M_a" (ACI-318-14), where M_a is calculated via moment curvature, and M_{cr} is calculated using equation 14. ACI 318-14 (2014) also states that this method should only be used for nonprestressed members. Although this method matches the other methods until cracking, the approximation of moments after cracking is not the same between methods. This is because the moment of inertia will decrease as the moment increases above cracking and will be between the two extremes of the gross and cracked moment of inertias. ACI 318-14 (2014) equation 24.2.3.5a provides the effective moment of inertia calculation for nonprestressed members:

$$\mathbf{I}_e = \left(\frac{M_{cr}}{M_a}\right)^3 * I_g + \left[1 - \left(\frac{M_{cr}}{M_a}\right)^3\right] * I_{cr}. \quad (3)$$

The deflection for a member after cracking caused by a superimposed load, which is the first term, and self-weight, which is the second term, at midspan is calculated as:

$$\Delta_{\mathbf{I}_e} = \frac{P * L^3}{48 * E_c * I_e} + \frac{5 * w * L^4}{384 * E_c * I_e}. \quad (4)$$

An alternative method to the effective moment of inertia method is the I_e* method. This follows the secant modulus for the transition between the gross and cracked moment of inertias. For calculating deflections after cracking, this method calculates a moment of inertia between the gross and cracked moment of inertia as follows (Alameh & Harajli, 1989):

$$\mathbf{I}^*_{\mathbf{e}} = \frac{I_{cr}}{1 - \frac{M_{cr}}{M_a} * (1 - \frac{I_{cr}}{I_{gr}})}. \quad (5)$$

The deflection for a member after cracking caused by self-weight and a superimposed load at midspan is calculated as:

$$\Delta_{\mathbf{I}^*_{\mathbf{e}}} = \frac{5 * M_D * L^2}{48 * E_c * \mathbf{I}^*_{\mathbf{e}}} + \frac{(M_a - M_D) * L^2}{12 * E_c * \mathbf{I}^*_{\mathbf{e}}}. \quad (6)$$

The bilinear method has two parts to the deflection calculation. The first portion of the equation is for the deflection at cracking using the gross moment of inertia. The second portion of the equation is the additional deflection because of the cracked moment of inertia based on the additional load after cracking. Equation (7) is the total deflection of a member subjected to self-weight and a concentrated load at midspan:

$$\Delta_{Bilinear} = \frac{M_{cr} * L^2}{12 * E_c * I_{\mathbf{g}}} + \frac{(M_a - M_{cr}) * L^2}{12 * E_c * I_{cr}}. \quad (7)$$

Failure Modes

Failure modes are the ways in which a member fails. Common failure modes include flexural and shear failures for prestressed concrete hollowcore. The following sections describe these failure modes in depth.

Shear Failure

Shear strength is based on the amount of prestressing, concrete compressive strength, cross-sectional geometry, depth, and span to depth ratio (Tawadrous, 2018). There are three shear failure modes (web shear, flexural shear, and punching shear) and each control in different loading situations and locations on the member (ACI, 2014). The governing shear depends on the load application's shear demand relative to the capacity along the member's length (ACI, 2014).

Figure 9 shows a generic shear capacity envelope along the length of a member. This is not applicable for all hollowcore. Near the supports, which is indicated in red, web shear controls and creates a truncated plateau in the shear capacity limit. This controls but is higher than flexural shear. However, the tension that creates the flexural shear is not at the end of the member; therefore, flexure shear doesn't occur there. Towards the middle of the member, which is indicated in blue, flexure shear controls and creates a lower truncated plateau in the shear capacity. The curved segment that connects these two plateaus, which is indicated in black, is the transition between web shear and flexure shear. This transition is where tensile stresses develop with an increase in distance from the support.

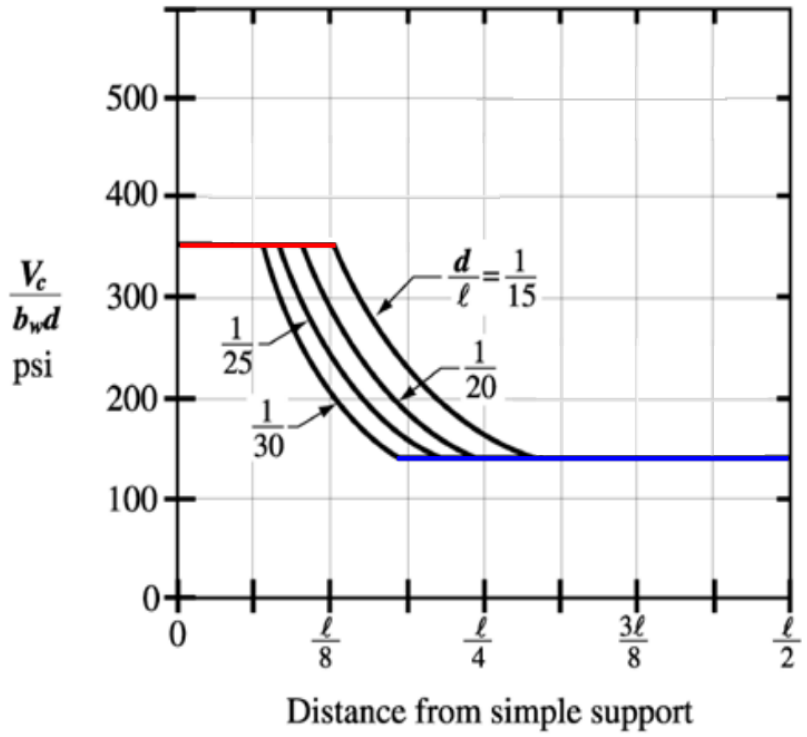

Figure 9. Cracks in prestressed hollowcore. Modified from "Building Code Requirements for Structural Concrete (ACI 318-14) [and] Commentary on Building Code Requirements for Structural Concrete (ACI 318R-14)" by ACI Committee 318, 2014, p. 356.

Web Shear. When the tensile strength is exceeded by the maximum principal stress in the concrete, a crack will develop perpendicular to the maximum principal stress (Wight, 2016). The initiation of a tensile crack near mid-height of the member results in a diagonal crack from the extreme fibers of the flanges. The location of the crack is perpendicular to the direction of the principal tensile stress and generally is near the support (Celal, 2012). This typically occurs in deep flexural members with thin webs.

For prestressed members, web shear is calculated by ACI 318-14 (2014) equation 22.5.8.3.2:

$$\mathbf{V_{cw}} = \left(\mathbf{3.5}\boldsymbol{\lambda}\sqrt{\boldsymbol{f'c}} + \mathbf{0.3}\boldsymbol{f_{pc}}\right)\boldsymbol{b_w d_p} + \boldsymbol{V_p}\,. \tag{8}$$

This shear is assumed to occur when the principal tensile stress created by the shear is approximately $\mathbf{4\lambda\sqrt{f'c}}$ (ACI 318-14, 2014). Additionally, the depth of the distance from the extreme compression fiber to the centroid of the prestressing reinforcement "need not be taken less than **0.80h**" (ACI 318-14, 2014, p. 357).

Flexure-Shear. The following is a brief overview of flexure failure from Wight (2016). Flexure-shear results from the crack originating because of the deflection from flexure and then propagates vertically towards the compression side of the member. This occurs where there is an increase in flexure in the member. As the deflection increases, the concrete's tension capacity is exceeded, which causes a crack to develop, and the concrete in compression exceeds the ultimate compression strength, which causes failure in the member. This type of failure occurs more in shallow or lightly prestressed hollowcore (Wu, 2015). For prestressed members, flexure shear is the greater of ACI 318-14 (2014) equations 22.5.8.3.1a and 22.5.8.3.1b:

$$\mathbf{V_{ci}} = \mathbf{0.6\lambda\sqrt{f'c}b_w d_p} + \boldsymbol{V_d} + \frac{\boldsymbol{V_i M_{cre}}}{\boldsymbol{M_{max}}}, \tag{9}$$

$$\mathbf{V_{ci}} = \mathbf{1.7\lambda\sqrt{f'c}b_w d_p}. \tag{10}$$

The commentary from ACI 3.18-14 (2014) states that $\boldsymbol{M_{cre}}$ uses the section properties associated with resisting the externally applied loads for $\boldsymbol{I}$ and $\boldsymbol{y_t}$. Also, $\mathbf{V_{ci}}$ contains $\frac{\boldsymbol{V_i M_{cre}}}{\boldsymbol{M_{max}}}$ to signify the shear required to cause a flexural crack.

Punching Shear. Punching shear is a conical failure surface from diagonal tension cracks (ACI, 2014). These cracks result from the presence of a concentrated load that exceeds the capacity of the material's thickness and reinforcement (Wight, 2016). The *PCI Manual for the Design of Hollow Core Slabs and Walls* (2015) does not offer much guidance in checking for punching shear, other than saying that "[t]he magnitude of concentrated loads must be limited to

preclude such failures. These limits are best established by test for each hollow core slab system" (p. 3-3).

In the absence of testing data, the punching shear capacity of the hollowcore in this research project was calculated with the concentrated load acting directly over a void. According to ACI 318-14 (2014), prestressed two-way members have the shear stress calculated in accordance to either section 22.6.5.2 or 22.6.5.5. This includes the calculation of the shear stress ($\boldsymbol{v_c}$) via the minimum of Equation (11) and (12):

$$\mathbf{3.5}\,\boldsymbol{\lambda}\sqrt{\boldsymbol{f'c}} + \mathbf{0.3}\,\frac{\boldsymbol{f_{pc}}}{2} + \frac{\boldsymbol{V_p}}{\boldsymbol{b_o * d}}, \tag{11}$$

$$\left(\mathbf{1.5} + \frac{\boldsymbol{\alpha_s d}}{\boldsymbol{b_o}}\right)\boldsymbol{\lambda}\sqrt{\boldsymbol{f'c}} \; + \; \mathbf{0.3}\,\frac{\boldsymbol{f_{pc}}}{2} + \frac{\boldsymbol{V_p}}{\boldsymbol{b_o * d}}. \tag{12}$$

The compressive strength after prestresses losses term is the average of the stress in both directions, since there was no stress in the transverse direction, the average is the stress in the longitudinal direction divided by two. The ACI 3.18-14 (2014) commentary explains the use for section 22.6.5.5 for prestressed members that satisfy the conditions in 22.6.5.4:

> For prestressed two-way members, modified forms of expressions (b) and (c) in Table 22.6.5.2 are specified. Research (ACI 423.3R) indicates that the shear strength of two-way prestressed slabs around interior columns is conservatively calculated by the expressions in 22.6.5.5, where $\boldsymbol{v_c}$ corresponds to a diagonal tension failure of the concrete initiating at the critical section defined in 22.6.4.1. The mode of failure differs from a punching shear failure around the perimeter of the loaded area of a nonprestressed slab calculated using expression (b) in Table 22.6.5.2. Consequently, the expression in 22.6.5.5 differ from those for nonprestressed slabs. (p.365)

The punching shear capacity is the minimum shear stress ($\boldsymbol{v_c}$) multiplied by the area created by the critical shear-perimeter ($\boldsymbol{b_o}$):

$$\mathbf{V_n} = \boldsymbol{v_c b_o d}\ . \tag{13}$$

As seen in Figure 10, the concentrated load in this capstone investigation was centered over a void. The concentrated load was applied over a 4-inch by 4-inch area to replicate a typical concentrated load created by a hollow structural section (HSS). The critical shear-perimeter was defined as a square with a side equal to the width of the concentrated load plus half of each side distance to the edge of the void. The depth ($\boldsymbol{d}$) was the thickness of the flange directly below the critical shear perimeter.

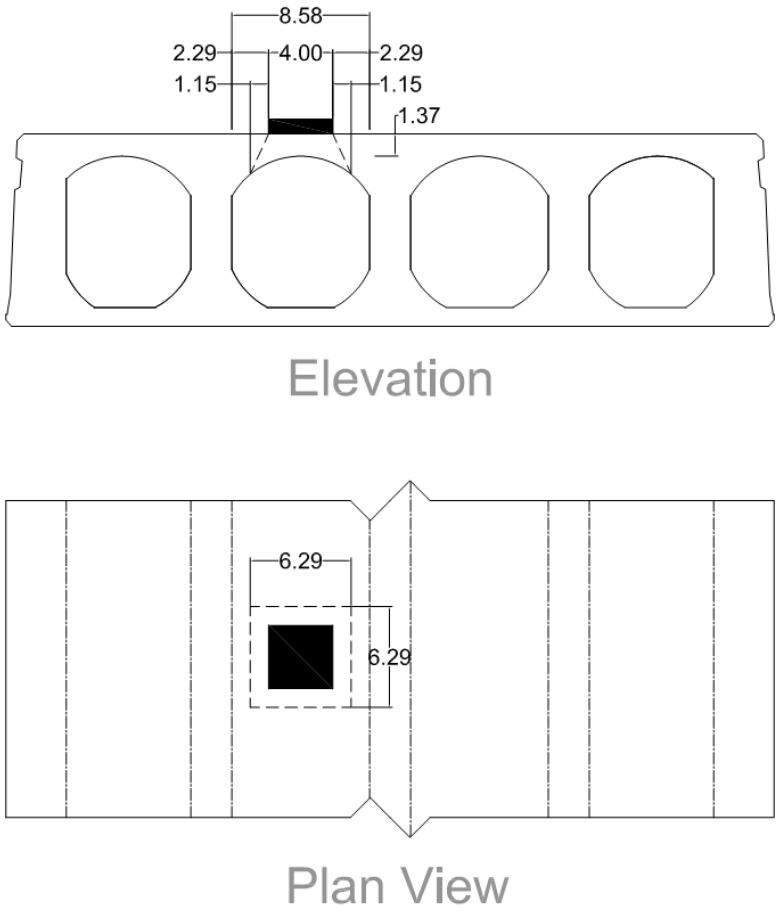

Figure 10. Punching shear.

Flexure Failure

The following is a brief overview of flexure failure from PCI (2017). Flexure failure can be distinguished by the development of cracks on the tension side that extend to the compression side. This occurs after the reinforcement has yielded. A few notable moments are at cracking and nominal. When the tensile stress at the bottom of the concrete member reaches the modulus of rupture, the concrete cracks. The cracking moment is when the tensile stress is equivalent to the modulus of rupture. For prestressed concrete, the cracking moment is calculated by PCI equation 5-6a:

$$\boldsymbol{M_{cr} = S_b \left(\frac{P_e}{A} + \frac{P_e e}{S_b} + f_r \right).} \quad (14)$$

The nominal moment is a computed value for a member's flexural capacity that can be resisted before failure caused by the applied load. For prestressed members, Figure 5.2.2 in PCI MNL-120-17 shows which equations to use. Equation (15) was applicable for the test specimen:

$$\boldsymbol{M_n = A_{ps} f_{ps} \left(d_{ps} - \frac{a}{2} \right).} \quad (15)$$

This doesn't include the portions of the equation for compression reinforcement or mild reinforcement, because those were not applicable for these tests.

The maximum probable moment is the flexural capacity for the actual strength of the prestressed strand, which is above yielding. The tested maximum stress in the strands was 287.0 ksi versus the stress of 266.0 ksi, which is assumed for yielding. Equation (16) was used to calculate the maximum probable moment:

$$\boldsymbol{M_{rup} = A_{ps} f_{rup} \left(d_{ps} - \frac{a}{2} \right).} \quad (16)$$

Controlling Failure Mode

In order to predict the superimposed load to reach the first limit state for the hollowcore, a series of calculations was performed, which can be found in Appendix A. First, a moment curvature analysis was conducted in order to find the load-deformation behavior given the cross-sectional, concrete, and strand properties.

Critical points such as cracking moment and nominal moment were compared to estimates from ACI. The moment curvature method allows the load-deformation behavior of concrete to be determined by using nonlinear stress-strain relationships (Matthews, 2001). Figure 11 shows the relationship of the moment curvature analysis.

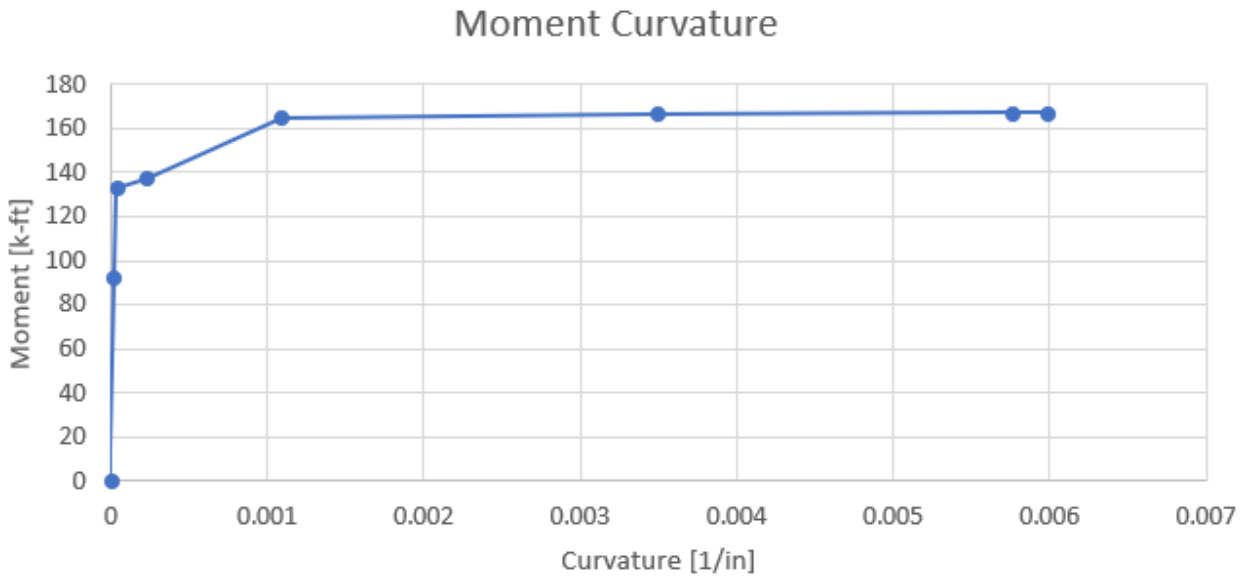

Figure 11. Moment curvature without self-weight.

In order for direct comparison between the test results, moment curvature, and ACI calculations, the tests needed the self-weight of the member to be added into the results.

The largest superimposed concentrated load at midspan from the moment curvature analysis was then used as a baseline in determining the applied shear diagram, which was used to

determine the shear capacity diagram. From AISC (2017), Equation (17) shows the shear equation used for a simply supported member including self-weight with respect to the distance (x) from the support:

$$V = \frac{P + w_D * Length}{2} - w_d * x. \quad (17)$$

First, the superimposed applied load to cause flexural failure and punching shear failure was determined, which were 35.0 kips and 43.1 kips, respectively. The superimposed load at midspan to cause flexural failure was lower than the load to cause punching shear; thus the 35.0 kips was used in calculating the shear capacity envelope. Calculations for these values are found in Appendix A. Figure 12 shows that web shear and flexure shear are not the governing failure modes under the superimposed applied load of 35.0 kips at midspan since the demand is less than the capacity.

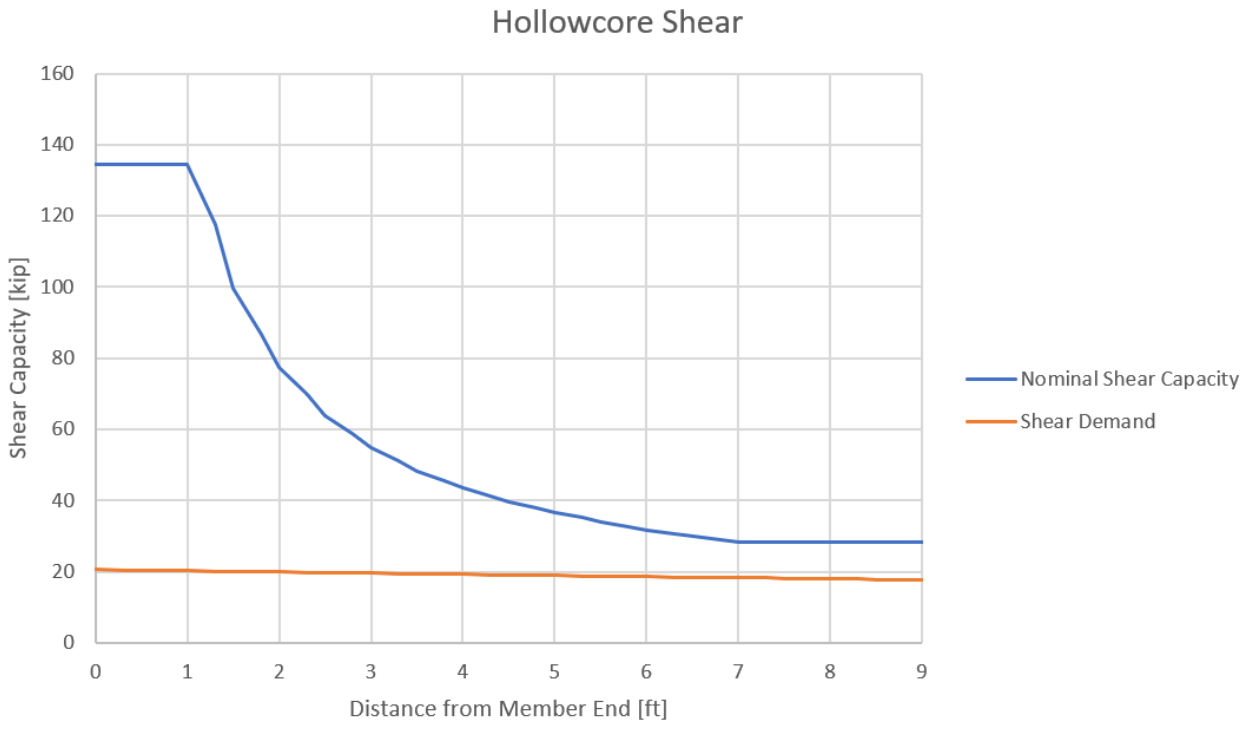

Figure 12. Shear envelope and member capacity.

The preliminary calculations for the 12-inch hollowcore were validated by comparing the predictions to testing of 8-inch hollowcore at another laboratory. These calculations included a limit state prediction by evaluating web shear, flexure shear, and punching shear, as well as the load-deformation. From this, punching shear was predicted to govern. This supports the results from the tests, which failed at the predicted load and exhibited longitudinal cracks through the voids. Since the calculations suggest the mode of failure as punching shear, and the specimens exhibited longitudinal cracks, it is postulated that punching through the flange of the member initiated a crack that propagated longitudinally through the flange of the void.

Predicted Behavior

From this research, the 12-inch hollow core was predicted to fail in flexure at a concentrated superimposed load at midspan of 35.0 kips. This was because in order for the expected load to cause a flexural failure, the shear demand was lower than the shear capacities in flexure-shear and web shear. Since the demand was less than the capacity, shear was not expected to govern. Furthermore, the load to cause punching shear (43.1 kips) was greater than the load to cause a flexure failure, so punching shear would also not govern. The capacity between the center and offset tests is not expected to differ. A summary from the preliminary calculations for moments, superimposed loads, and deflections are seen in Table 1.

Table 1

Preliminary Summary

	Moment [k-ft]	Superimposed Load [k]	I^*_e Method [in]	Bilinear Method [in]
Cracking	133.0	25.1	0.23	0.23
Nominal	164.0	31.7	1.06	1.04
Maximum Probable	177.0	34.4	1.40	1.37

Since the bilinear method is recognized by ACI, it will be used moving forward for deflection.

Methods

Experimental Program

Seven tests were conducted in total. Three tests had the concentrated load centered at midspan in both the transverse and longitudinal directions of the hollowcore. Four tests had the concentrated load centered at midspan in the longitudinal direction and directly over a void in the transverse direction. This offset in the transverse direction was to verify that punching shear would not govern. The tests were labeled “Center #1-3” and “Offset #1-4”.

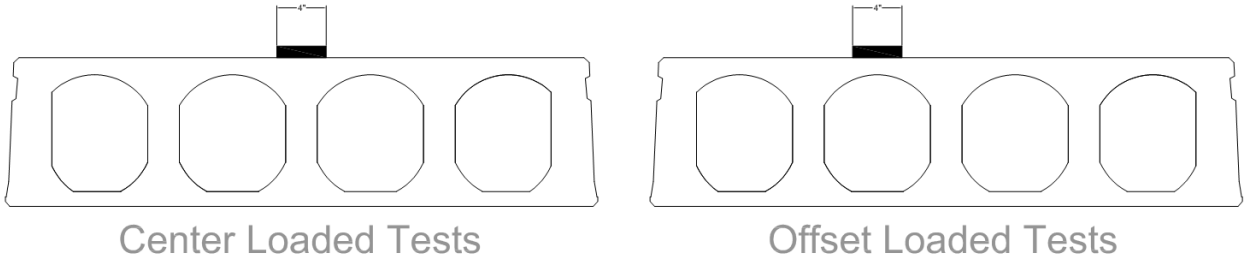

Figure 13. Location of concentrated load.

Test Samples

The experimental program was based on measuring and analyzing the force supported by 20-feet long by 4-feet wide by 12-inches thick hollowcore reinforced with five 0.5-inch diameter, seven-wire, 270 ksi, low-relaxation prestressed strands. Figure 14 shows the cross-section of the test subjects, as well as strand layout. This is a standard cross-section used that has the lightest strand pattern for the 12-inch hollowcore.

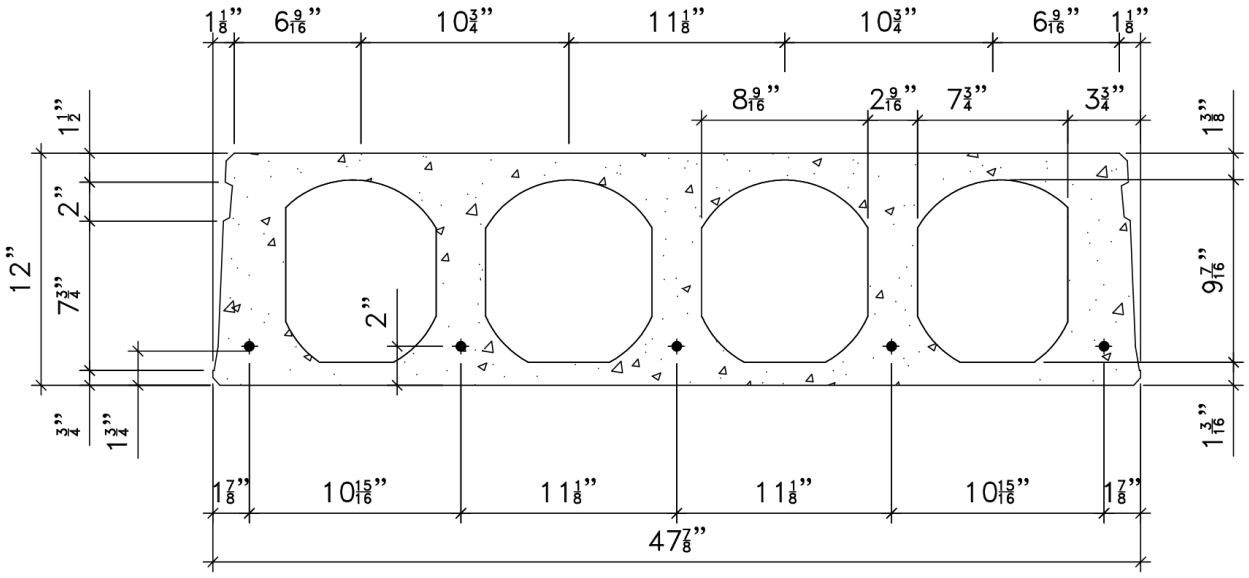

Figure 14. MCI's 12-inch hollowcore cross-section with 1.75-58 stranding. Adapted from "Cross Sections & Strand Configurations" by Mid-States Concrete Industries, (n.d.). Retrieved from https://www.msprecast.com/cross-sections-strand-patterns

The manufacturer provided the following properties of the strand:

- a diameter of 0.5 in,
- a cross-sectional area of 0.22 in^2,
- a nominal strength of 270 ksi,
- a yield point between 54.7 kips and 55.9 kips,
- a modulus of elasticity of 28.6 Mpsi, and
- a prestressing force of 65% of the nominal strand strength.

Additionally, the concrete mixture contained 3.80% fly ash compared to the total mixture weight and had a strength of 3,532 psi at 8 days and 11,150 psi at 28 days.

Setup and Equipment

The testing equipment consisted of a reaction test frame for hollowcore bearing and load application. The test frame consisted of various steel members, including wide flange beams and columns, and angles. The hollowcore supports were wood 2x4s centered on wide flange beams

that were attached to the base of the frame. Figure 15 shows the test frame setup. Dimensioned drawings of the test frame are found in Appendix B.

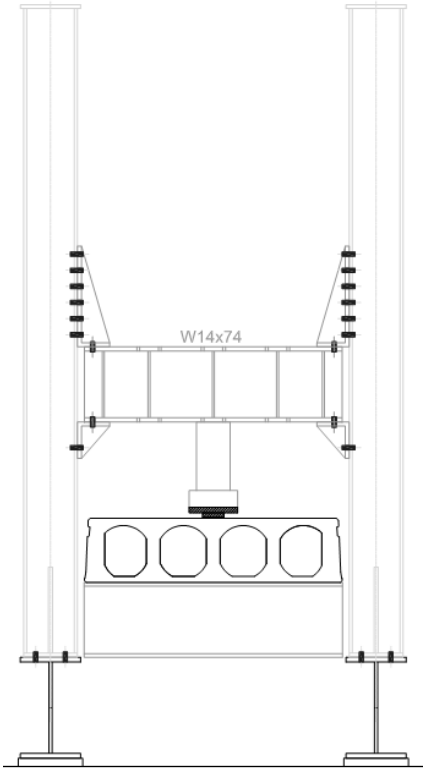

Figure 15. Test frame setup.

The concentrated load at midspan was applied with an RRH-606 Hollow Plunger Cylinder and measured with a Sensotec Model 41 precision pancake load cell. The load cell was bearing on a square steel plate with a width of 9-inches and thickness of 2-inches, which was bearing on a square steel plate with a width of 4-inches and thickness of 1-inch. This was set on a Neoprene square pad that was 4-inches in width, and 0.5-inch thick to create the desired concentrated load without creating concrete crushing in the compression zone, as well as to provide adequate bearing on the rough concrete top surface. Figure 16 shows the configuration of each of these members.

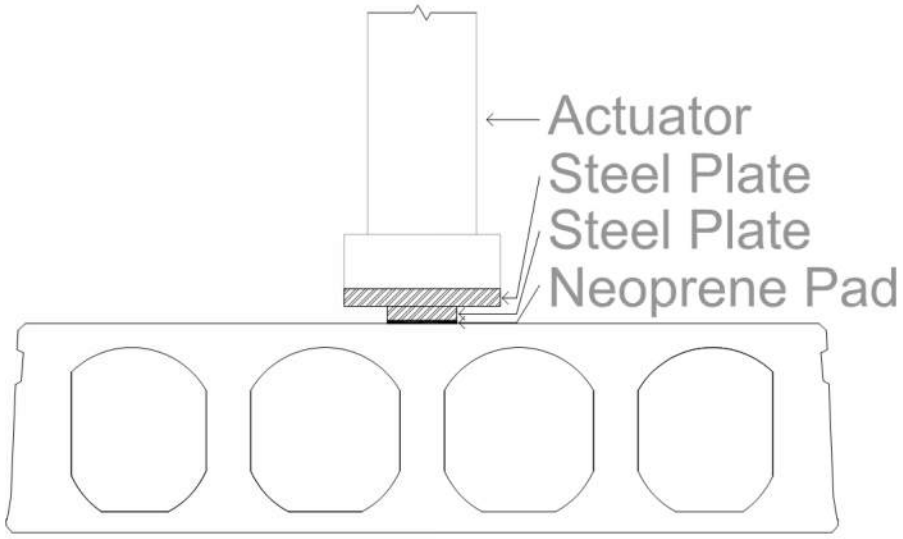

Figure 16. Actuator and plate stepdown to 4-inch concentrated load.

Six Sensotec VL7A linear variable differential transformers (LVDT) with a 6-inch throw measured the top surface of the hollowcore's deflection during the loading and unloading process. Two LVDTs were located above the supports at each end of the hollowcore, as well as at midspan. Each of these set of two LVDTs had one located on one side of the transverse span, and one on the other side of the transverse span, which was approximately four-feet between them.

The LVDTs were attached to an independent frame that was attached to the floor and wall such that the deflection of the steel frame upon loading would not alter the deflection recorded by the LVDTs. The resulting deflection of the plank was calculated by mathematically removing any displacement of the supports caused by deflection of the reaction frame. Figures 17 and 18 show the setup of the LVDTs on the independent frame at midspan and at a support.

Figure 17. LVDT setup at midspan.

Figure 18. LVDT setup at ends.

Testing Technique

Prior to loading the hollowcore into the test frame, reference measurements on the support beams and the hollowcore were taken in order to better align the piece in the frame. In order to load the hollowcore into the test frame, the frame required partial disassembly of the beam and column. This allowed the hollowcore to be positioned into the test frame using an overhead crane in order to align with the placement of the loading point from the actuator and load cell.

Upon adequate placement, the steel frame was completely reassembled, the load cell and actuator were reinstalled, and the wooden supports for the LVDTs were fixed into place. The LVDTs were attached at designated locations via clamps. Once setup was complete, the LVDTs were verified using LabVIEW to ensure they were recording properly. After equipment testing, testing commenced.

The actuator was operated by slowly pulsing the control button. This allowed for incremental loading on the specimen. While increasing the load applied to the hollowcore, a load versus displacement graph was generated and displayed in LabVIEW. Once the hollowcore reached failure, the hollowcore was unloaded. These test results were saved and exported to Microsoft Excel (Excel). Because the load cell was not tared and the signal was truncated at a certain level during testing of the center loaded specimens, the load was removed after cracking and then reapplied until the nominal load. The two data sets for each test specimen were later combined.

Results

The following sections are organized by concrete, strand slip, and overall data results of the seven hollowcore specimens. These include a description of what occurred during the tests,

along with pictures, and graphs. For each of the tests, cracking and strand slip occurred, as well as similar cracking and nominal moments.

Crack Patterns

Each of the hollowcore members had transverse cracking on the tension side. As for the cracks that developed on the sides of each member, the cracks continued from the tension side up towards the top of the member. Near the compression zone, the cracks forked to each side and began running longitudinally to the member. Offset #1 shows this general condition in Figure 19.

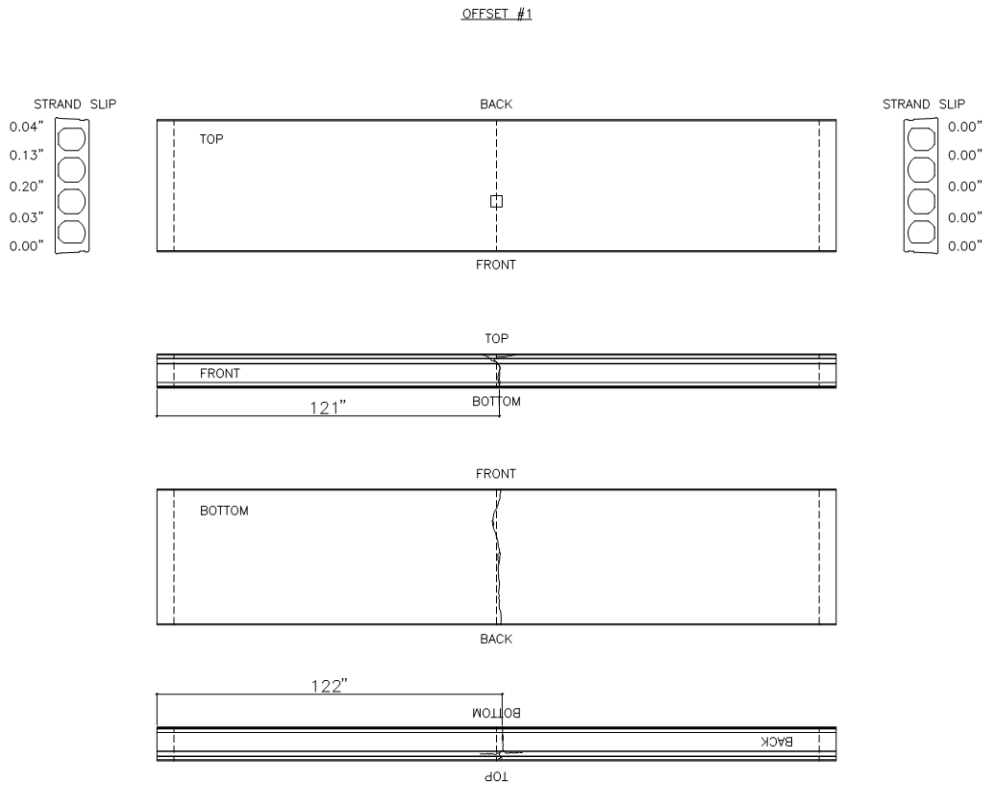

Figure 19. Offset #1 crack patterns and strand slip.

Although most of the tests resulted in a similar crack pattern, Center #1 and Offset #2 were outliers. Figure 20 shows that Center #1 had two transverse cracks running along the tension side, as opposed to the typical one transverse crack. Figure 21 shows that Offset #2 had a

crack on the tension side that forked and caused two separate transverse cracks that led to two cracks on the side of the member. This varied greatly from every other test since the other six tests only had one transverse crack.

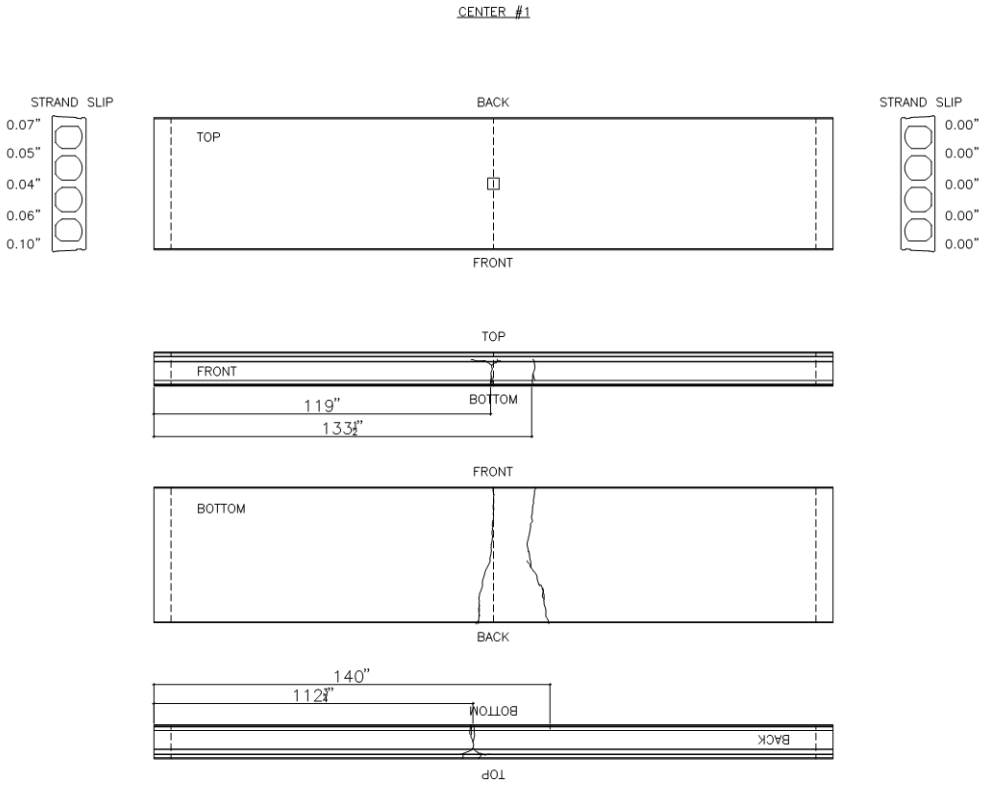

Figure 20. Center #1 crack patterns and strand slip.

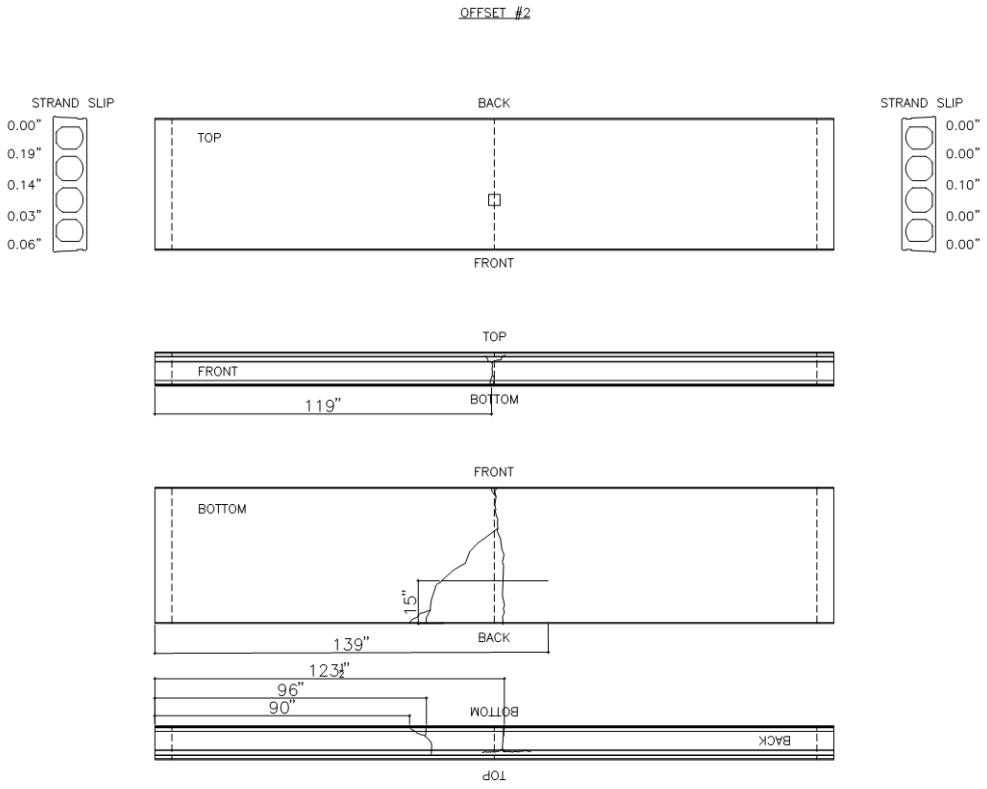

Figure 21. Offset #2 crack patterns and strand slip.

Strand Slip

Strand slip was measured from the face of the strand to the face of the concrete using a caliper after the specimens were unloaded and removed from the test frame. All five strands on both ends of each specimen were recorded. Table 2 shows the average strand slip for each of the five strands on both ends of the hollowcore specimen. The individual strand slips can be found in Appendix B.

Table 2

Strand Slip

Specimen	Average Slip [in]
Center #1	0.032
Center #2	0.075
Center #3	0.070
Offset #1	0.040
Offset #2	0.052
Offset #3	0.045
Offset #4	0.088

Since the strand was not measured during testing, it was postulated that strand slip occurred after the nominal load was reached and the actuator continued to push on the specimen. The load versus displacement graphs step down after the nominal load was reached, which may suggest the strands slipping during that time.

Deflection

As the load was applied, the hollowcore began to deflect. Each specimen started with 5/16-inch camber created by the prestressing forces from the strands, which is the camber from prestressing plus the deflection caused by the self-weight. The deflection seen in each test is the overall deflection from initial position, which already contains camber and deflection caused by self-weight, to the final position of failure. Table 3 shows the deflection caused by the superimposed load for each of the specimen.

Table 3

Superimposed Load Deflection of Test Specimens

Specimen	Deflection [in]
Center #1	1.99
Center #2	1.69
Center #3	2.17
Offset #1	2.11
Offset #2	1.78
Offset #3	1.99
Offset #4	2.08

Load versus displacement graphs were created from the LabVIEW outputs. Figure 22 and Figure 23 show a compilation of the load versus displacements for each type of test, Center and Offset. Each specimen had relatively the same cracking and nominal moments.

In Figure 23, there was variation in Offset 2's data. At approximately a displacement of 0.28-inch, Offset 2's data increases in load more rapidly than in the other tests. This resulted in a higher nominal load and a smaller total deflection. However, it follows the same trend as the other Offset specimen, meaning that the curvature of the load versus displacement is consistent between all four tests. As noted before, the load cell wasn't tared during the Center tests, so Figure 22 has six sets of data for the three tests. Each specimen's two sets of data were made in shades of the same color in order to more easily see the link between the two sets of data. The instrumentation issue did not affect the outcome of the results, which are still valid. The issue only caused a gap in the data between the transition from after cracking to the nominal moment.

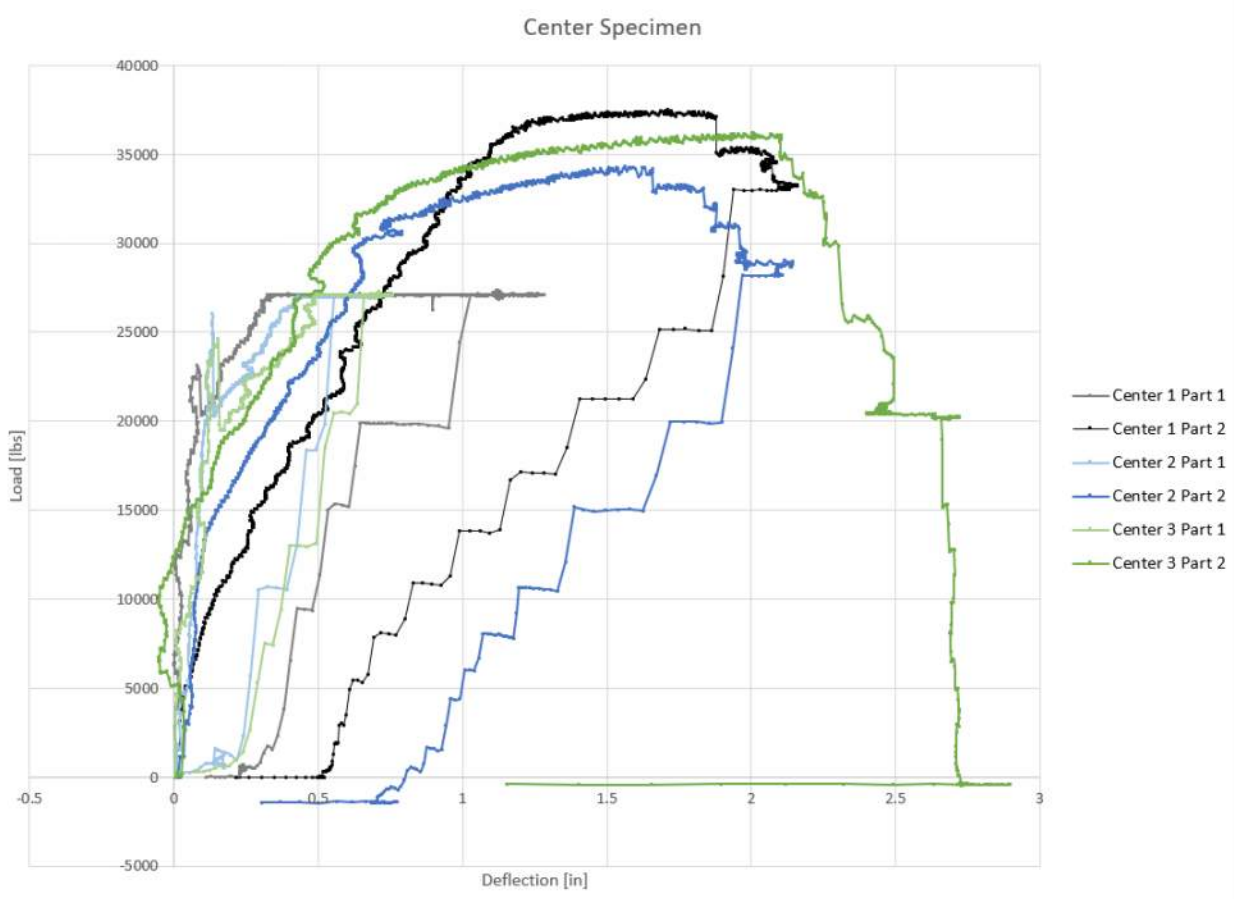

Figure 22. Load versus displacement for center tests.

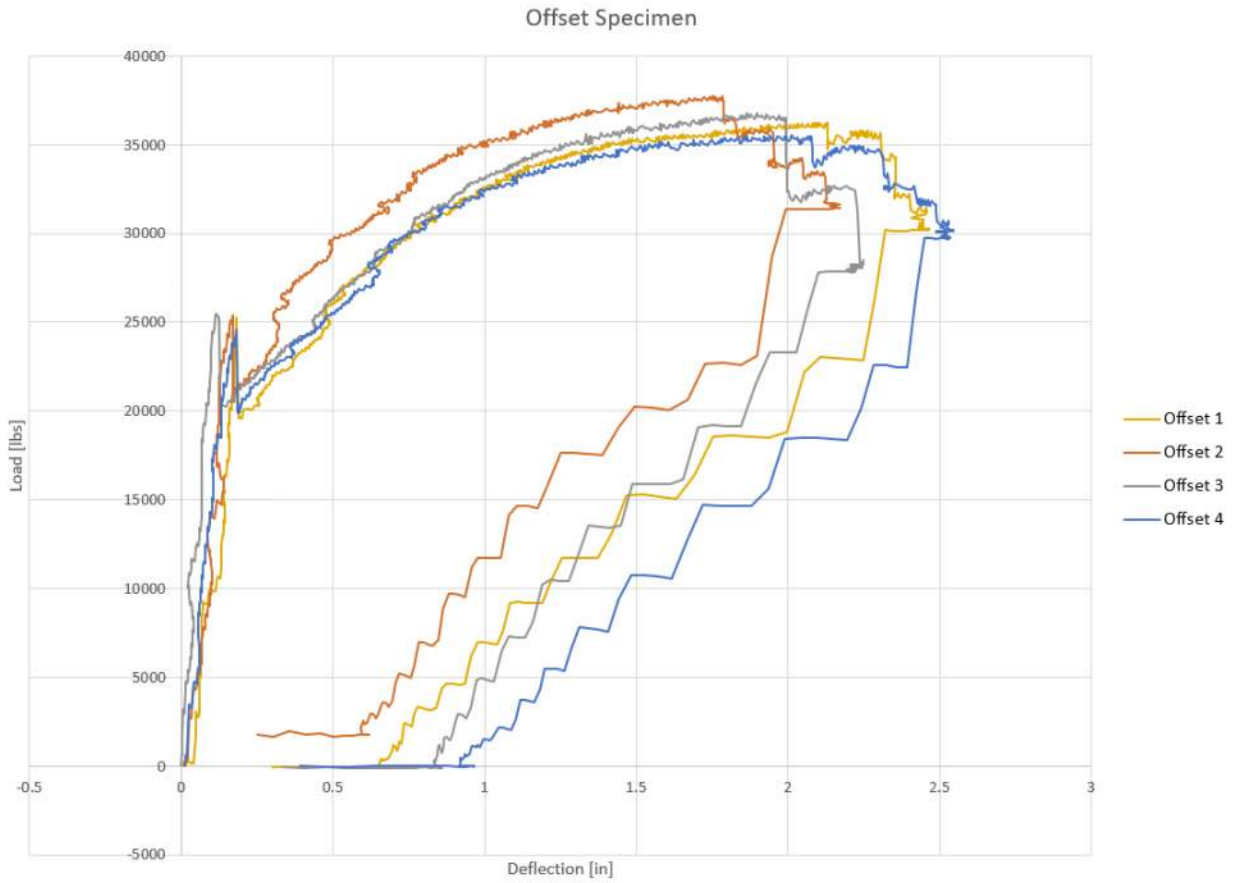

Figure 23. Load versus displacement for offset tests.

Discussion and Conclusions

After reviewing existing literature and conducting physical testing, conclusions may be made with respect to the capacity of 12-inch elematic hollowcore. Testing verified the ACI 318-14 (2014) prediction that flexure failure will occur. Preliminary calculations of moment curvature, PCI, and ACI were conducted to determine the validity of code-based calculations. Based on the testing, the results of both the center and offset tests aligned with the proposed calculation methods by ACI and PCI. The following information is a summary of the comparisons between the tests and the code.

Table 4 shows the cracking moments of each specimen, along with the predictions from ACI 318-14 (2014), while Table 5 shows the nominal and maximum probable moments. These tables show the accuracy of the ACI calculations for cracking and nominal moments relative to the tests. The tests' moments are higher than the ACI nominal and maximum probable moments because the tests stressed the steel past yielding, when ACI assumes the maximum value as the yielded stress. The strands slipped before snapping, which makes the system more ductile, resulting in an increase in deflection without increasing capacity. The moments include both the superimposed loads and self-weight for the experimental data, which were calculated using Equation (18) (AISC, 2017):

$$\boldsymbol{M = \frac{P * L}{4} + \frac{w_d * L^2}{8}.} \tag{18}$$

Table 4

Specimens' Cracking Moments

Specimen	Experimental [k·ft]	Average Experimental [k·ft]	ACI [k·ft]	$\frac{\text{Average Exprimental}}{\text{ACI}}$
Center #1	123.5	129.9	133.0	0.977
Center #2	137.5			
Center #3	128.9			
Offset #1	133.7	133.3		1.00
Offset #2	134.3			
Offset #3	134.5			
Offset #4	130.6			

Table 5

Specimens' Nominal and Maximum Probable Moments

Specimen	Experimental [k·ft]	Average Experimental [k·ft]	ACI Nominal [k·ft]	ACI Max Probable [k·ft]	$\frac{\text{Avg Exp.}}{\text{ACI Nominal}}$	$\frac{\text{Avg Exp.}}{\text{ACI Max Prob.}}$
Center #1	191.7	184.6	164.0	177.0	1.126	1.043
Center #2	176.6					
Center #3	185.6					
Offset #1	185.8	187.3			1.142	1.058
Offset #2	192.8					
Offset #3	188.3					
Offset #4	182.4					

Additionally, moment versus displacement graphs were created to show the accuracy between the tests and the bilinear deflection calculations. Although the load versus displacement graphs are more common, the moment versus displacement graphs were plotted since this is more relevant to MCI. Figure 24 and Figure 25 show the moment-displacement relationships of the bilinear method relative to the testing data. The testing data does not start at zero because the graphs incorporated the additional moment caused by self-weight, which the test results didn't include because only the superimposed load was measured.

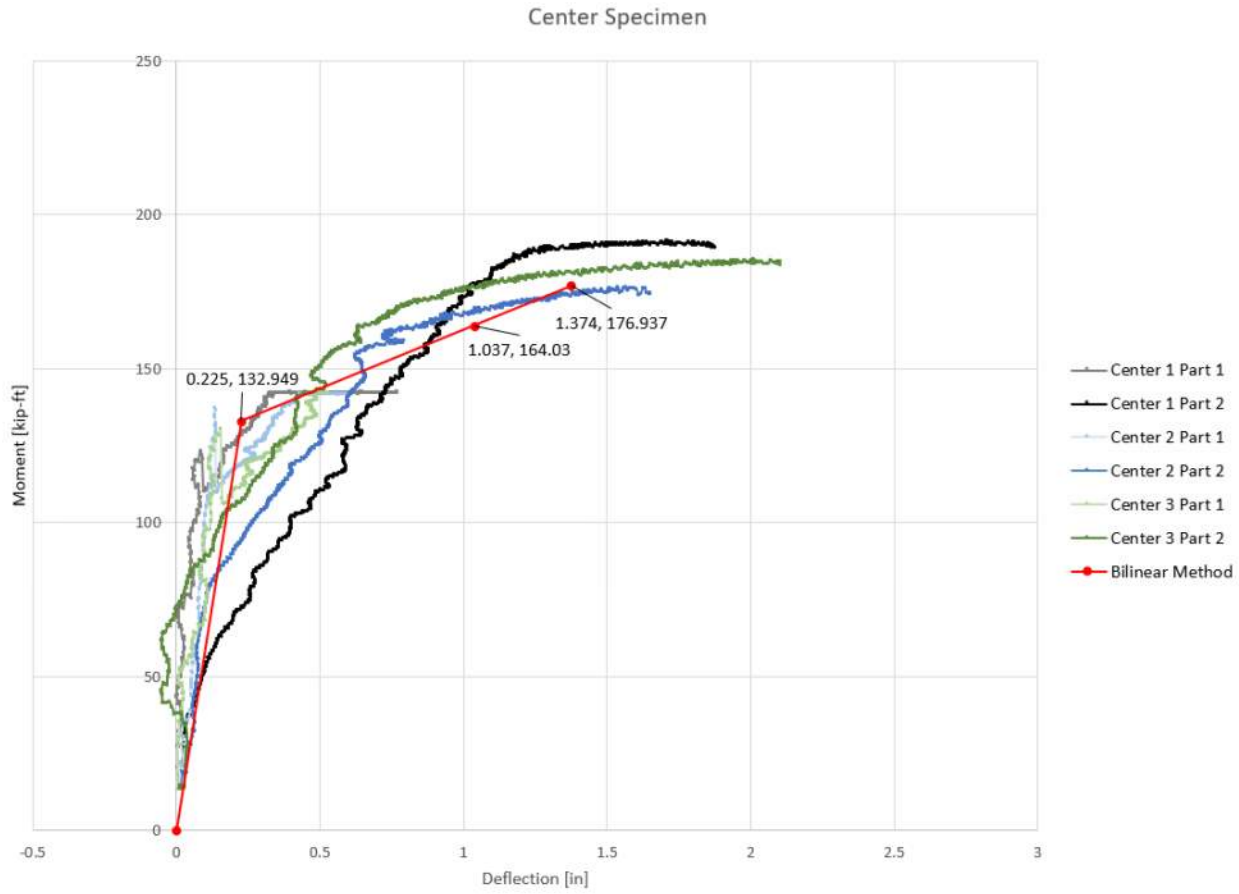

Figure 24. Moment versus displacement for center tests.

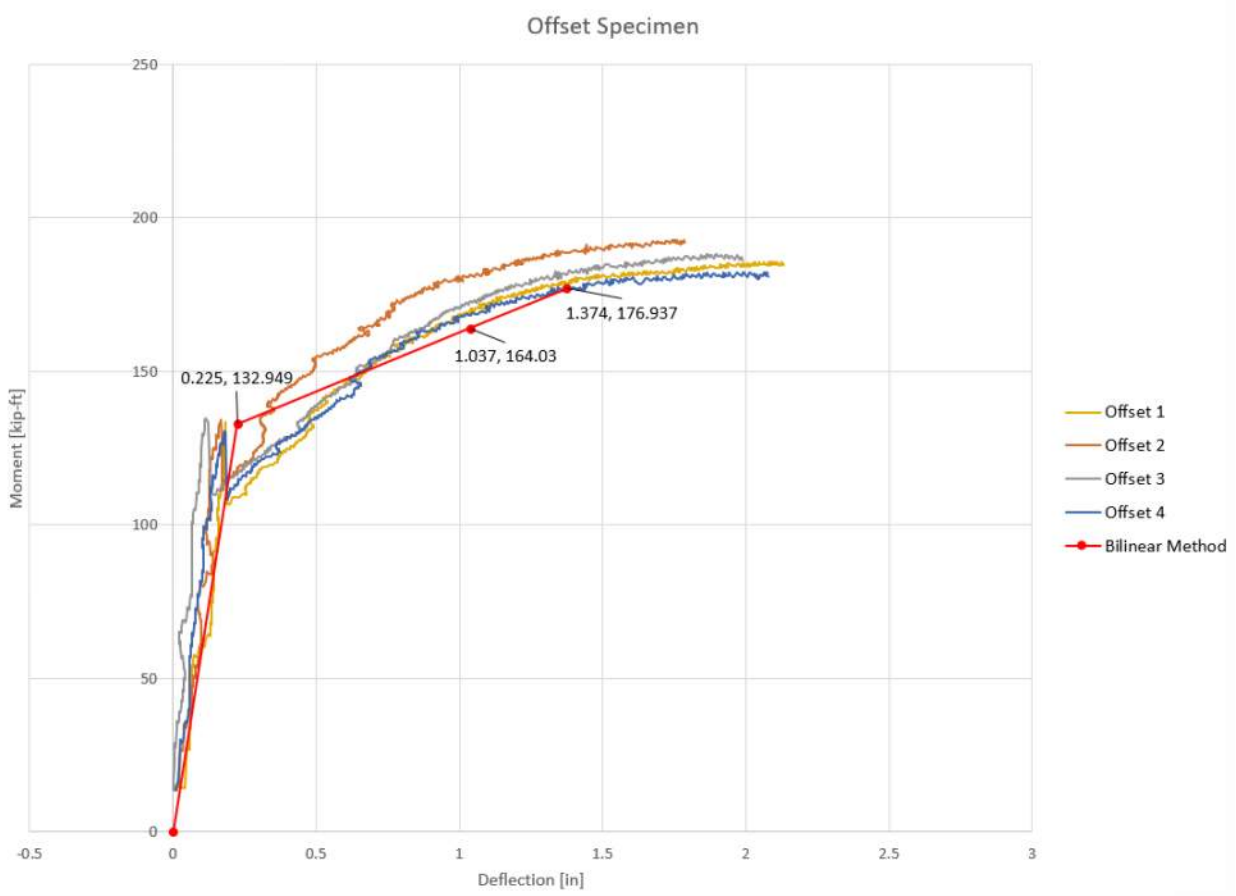

Figure 25. Moment versus displacement for offset tests.

Recommendations

The testing conducted in this project focused on a particular hollowcore configuration. Varying spans, concrete mixes, cross-sectional area, or stranding may result in different capacities, which could cause a different mode of failure. Testing a span that should govern in shear, rather than flexure, should be done in order to validate the shear calculations from ACI and PCI.

In regard to the observed crack patterns, the 12-inch hollowcore split in the transverse direction as opposed to the longitudinal cracks seen in the referenced 8-inch hollowcore tests. It is postulated that this difference is because of the flexural failure and punching shear failure,

respectively. Punching shear should be further researched to determine if this is the cause of the different crack patterns between the 12-inch and 8-inch hollowcore.

References

ACI Committee 318. (2014). *Building code requirements for structural concrete (ACI 318-14) [and] commentary on building code requirements for structural concrete (ACI 318R-14).* Farmington Hills, MI: American Concrete Institute.

American Institute of Steel Construction [AISC]. (2017). *Manual of Steel Construction 15th Edition.* Chicago: AISC.

Alameh, A. S., & Harajli, M. H. (1989). Deflection of progressively cracking partially prestressed concrete flexural members. *PCI Journal, 34*(3), 94-128.

Celal, M. S. (2012). *Shear behaviour of Precast/Prestressed hollow-core slabs* (Master's thesis). Retrieved from Proquest Dissertation & Theses Global Database, (Order No. MR84964).

Matthews, R. (2001). *Moment curvature* [PowersPoint slides]. StructSource. Retrieved from http://www.structsource.com/pdf/Momcurv_web.pdf

Mid-States Concrete Industries. (n.d.). Safe load table. Retrieved from https://static1.squarespace.com/static/59ee03b6017db2f97fb52c4f/t/5ba1340303ce64b9d5007457/1537291267660/12x48_NT2H.pdf

Mid-States Concrete Industries. (n.d.). Cross sections & strand configurations. Retrieved from https://www.msprecast.com/cross-sections-strand-patterns

Nawy, E. G. (2006). *Prestressed concrete: A fundamental approach*. United Kingdom: Pearson/Prentice Hall.

Parkhats V. (2018, May). Problem of cracks in prestressed hollow core slabs. Retrieved from https://www.researchgate.net/

Precast/Prestressed Concrete Institute [PCI]. (2015). *PCI manual for the design of hollow core slabs and walls (MNL-126-15E)*. Precast/Prestressed Concrete Institute.

Precast/Prestressed Concrete Institute [PCI]. (2017). *PCI design handbook: Precast and prestressed concrete (MNL-126-17)*. Precast/Prestressed Concrete Institute.

Spancrete. (n.d.). *Section 034XX: Precast, prestressed hollow core slabs.* Retrieved from Spancrete website: https://www.spancrete.com/resources/precast-design-and-engineering-handbook/hollowcore

Spancrete. (n.d.). Spancrete cross-sections. Retrieved from https://www.spancrete.com/application/files/1915/3013/0978/Hollowcore_Cross_Sections.pdf

Tawadrous, R., & Morcous, G. (2018, May). Shear strength of deep hollow-core slabs. *ACI Structural Journal, 115*(3), pp. 699-709. https://www.doi.org/10.14359/51701298

Wight, J. K. (2016). *Reinforced concrete mechanics and design.* Hoboken, New Jersey: Pearson Education.

Wu, Y. (2015). *Shear strengthening of single web prestressed hollow core slabs using externally bonded FRP sheets* (Master's thesis). Retrieved from Proquest Dissertation & Theses Global Database, (Order No. 1590790).

Appendix A: Calculations

- Test Frame Calculations
- Moment Curvature
- ACI Flexure, Shear, Cracking Moment, Nominal Moment, Maximum Probable Moment
- Deflection

Actuator

$P := 128kip$

Load Beam

W14x74 $F_y := 50ksi$

Stiffeners ensure that the flanges won't buckle. They don't add capacity.

$L := 4ft$

Flexure

$$M := \frac{P \cdot L}{4} = 128 \cdot kip \cdot ft$$

$S_x := 112in^3$ Manual Table 1-1 pg 1-25

$$P_u := \frac{4 \cdot S_x \cdot F_y}{L} = 466.667 \cdot kip$$

$Check_{Flexure} :=$	"Okay" if $P < P_u$ = "Okay" "Not Okay" otherwise

$$F_{O.S} := \frac{P_u}{P} = 3.646$$

Shear @ 2.5ft

This is to check maximum shear for an eccentric load of about 6"

$$R := \frac{P \cdot 2.5ft}{L} = 262.467 \frac{1}{m} \cdot kip \cdot ft$$

$t_w := \frac{7}{16}in$ Manual Table 1-1 pg 1-25

$d := 14.2in$ Manual Table 1-1 pg 1-25

$A_w := t_w \cdot d = 6.212 \cdot in^2$

$V_n := 0.6 \cdot F_y \cdot A_w = 186.375 \cdot kip$ Manual 16.1-350

$Check_{Shear} :=$	"Okay" if $R < V_n$ = "Okay" "Not Okay" otherwise

$$F_{O.S} := \frac{V_n}{P} = 1.456$$

Web Local Yielding

$F_{yw} := F_y = 50 \cdot ksi$

$k := 1.38in$ Manual Table 1-1 pg 1-25

$l_b := 5in$

$R_n := F_{yw} \cdot t_w \cdot (5k + l_b) = 260.313 \cdot kip$

$Check_{Yielding} :=$	"Okay" if $P < R_n$ = "Okay" "Not Okay" otherwise

$F_{O.S.} := \frac{R_n}{P} = 2.034$

Web Local Crippling

$t_f := 0.785in$ Manual Table 1-1 pg 1-25

$E := 29000ksi$

$Q_f := 1$

$R_n := 0.8 \cdot t_w^2 \cdot \left[1 + 3 \cdot \left(\frac{l_b}{d}\right)\left(\frac{t_w}{t_f}\right)^{1.5}\right] \cdot \sqrt{\frac{E \cdot F_{yw} \cdot t_f}{t_w}} \cdot Q_f = 355.541 \cdot kip$

$Check_{Yielding} :=$	"Okay" if $P < R_n$ = "Okay" "Not Okay" otherwise

$F_{O.S.} := \frac{R_n}{P} = 2.778$

Brackets

(12) 3/4" dia. A 325 N Bolts

$n := 12$

AISC Manual Table 7-1 pg 7-22

$r_{n/\Omega} := 11.9kip$

$\Omega := 2.00$

$r_n := r_{n/\Omega} \cdot \Omega = 23.8 \cdot kip$

$R_n := n \cdot r_n = 285.6 \cdot kip$

$Check :=$	"Okay" if $P < R_n$ = "Okay" "Not Okay" otherwise

$F_{O.S.} := \frac{R_n}{P} = 2.231$

Bolt Bearing

AISC Manual J3-6a pg 16.1-136

$D := 0.75in$

$t := 0.75in$

$F_u := 58ksi$

$R_n := 3.0 \cdot D \cdot t \cdot F_u = 97.875 \cdot kip$

Check :=	"Okay" if $P < R_n \cdot n$ = "Okay"
	"Not Okay" otherwise

$F_{O.S} := \frac{R_n \cdot n}{P} = 9.176$

Bolt Tearout

$l_c := 2.25in - .5 \cdot D = 1.875 \cdot in$

$R_n := 1.5 \cdot l_c \cdot t \cdot F_u = 122.344 \cdot kip$

Check :=	"Okay" if $P < R_n \cdot n$ = "Okay"
	"Not Okay" otherwise

$F_{O.S} := \frac{R_n \cdot n}{P} = 11.47$

Shear and Tension

$P_a := R = 80 \cdot kip$

$e := 5in$

$n' := 6$

$d_m := 9in$

$r_{at} := \frac{P_a \cdot e}{n' \cdot d_m} = 7.407 \cdot kip$ Manual E.q 7-14b pg 7-13 Tension

$R := n \cdot r_{at} = 88.889 \cdot kip$

Check :=	"Okay" if $P_a < R$ = "Okay"
	"Not Okay" otherwise

$F_{O.S} := \frac{R}{P_a} = 1.111$

Fastener Strength

$F_{nt} := 90ksi$ per bolt Manual Table J3.2

$F_{nv} := 54ksi$ per bolt Manual Table J3.2

$$F_{nt.D} := F_{nt}\cdot\left(\frac{\pi D^2}{4}\right) = 39.761\cdot kip$$

$$F_{nv.D} := F_{nv}\cdot\left(\frac{\pi D^2}{4}\right) = 23.856\cdot kip$$

$$A := 21.8in^2$$

$$f_{rv} := \frac{P_a}{\frac{\pi D^2}{4}\cdot n} = 15.09\cdot ksi$$

$$F'_{nt} := 1.3\cdot F_{nt} - \frac{F_{nt}}{F_{nv}}\cdot f_{rv} = 91.85\cdot ksi$$

$$Check := \begin{cases} F'_{nt} & \text{if } F'_{nt} < F_{nt} \\ F_{nt} & \text{otherwise} \end{cases} = 90\cdot ksi$$

$$F.O.S := \frac{Check\cdot\frac{\pi D^2}{4}}{r_{at}} = 5.368$$

Column

HP10x57

Pinned Connection

$$F_y := 36ksi$$

$$F_u := 58ksi$$

$Length := 10in$ Half of column + e

$$M := P_a\cdot Length = 66.667\cdot kip\cdot ft$$

Lateral Torsional Buckling

$L_b := 21.75in$ from brace to lowest bolt in bracket

$r_y := 2.45in$ Manual Table 1-4 pg 1-37

$$L_p := 1.76\cdot r_y\cdot\sqrt{\frac{E}{F_y}} = 10.199\cdot ft$$ Manual Eq F2-5 pg 16.1-48

$$Check_{LTB} := \begin{cases} \text{"Does Not Apply"} & \text{if } L_b \le L_p \\ \text{"Applies"} & \text{otherwise} \end{cases} = \text{"Does Not Apply"}$$

Tensile Yield Strength

$A_g := 16.7in^2$ Manual Table 1-4 pg 1-36

$P_n := F_y \cdot A_g = 601.2 \cdot kip$

$P_r := P_a = 80 \cdot kip$

$P_c := P_n = 601.2 \cdot kip$

$S_x := 58.8in^3$

$M_r := P_r \cdot 10in = 66.667 \cdot kip \cdot ft$ $M_c := S_x \cdot F_y = 176.4 \cdot kip \cdot ft$

$$\frac{P_r}{2 \cdot P_c} + \frac{M_r}{M_c} = 0.444$$

$$Check := \begin{cases} \frac{P_r}{2 \cdot P_c} + \frac{M_r}{M_c} & \text{if } \frac{P_r}{2 \cdot P_c} + \frac{M_r}{M_c} < 1 \\ 1 & \text{otherwise} \end{cases} = 0.444$$

$$Interaction_{Eq} := \frac{1}{\left(\frac{P_r}{2 \cdot P_c} + \frac{M_r}{M_c}\right)} = 2.25$$

Prying Action

Dimensional Constraints

$t_w := .565in$ $gage := 5.5in$ Manual Table 1-4 pg 1-36 $b_f := 12in$ plate width

$d_b := D$ 3/4" dia. A325 bolts

$$b := \frac{gage - t_w}{2} = 2.467 \cdot in$$

$$a := \frac{b_f - gage}{2} = 3.25 \cdot in$$

$$b' := b - \frac{d_b}{2} = 2.092 \cdot in$$

$$a' := \min\left(a + \frac{d_b}{2}, 1.25 \cdot b + \frac{d_b}{2}\right) = 3.459 \cdot in$$

$$\rho := \frac{b'}{a'} = 0.605$$

$$d' := d_b + \frac{1}{16}in = 0.812 \cdot in$$

$\delta := 1 - \frac{d'}{b} = 0.671$ Manual Eq. 9-20 pg 9-12

Plate Thickness Check $n := 8$ $p := 3in$ $F_u := 58ksi$

$r_n := 19.9 \cdot 2kip$ per bolt Manual Table 7-2

$B_c := r_n = 39.8 \cdot kip$ per bolt

$r_{at} := \frac{P_a}{n} = 10 \cdot kip$ per bolt

$T_u := r_{at} = 10 \cdot kip$ per bolt

$T_r := T_u$

$\beta := \frac{1}{\rho} \cdot \left(\frac{B_c}{T_r} - 1 \right) = 4.927$ Manual Eq 9-21 pg 9-13

$a' := \begin{cases} 1 & \text{if } \beta \geq 1 \\ \min\left[1, \frac{1}{\delta} \cdot \left(\frac{\beta}{1-\beta}\right)\right] & \text{otherwise} \end{cases} = 1$

$t_{min} := \sqrt{\frac{4 \cdot T_u \cdot b'}{p \cdot F_u \cdot (1 + \delta \cdot a')}} = 0.537 \cdot in$

$Check_{Flange} :=$	"Okay" if $t_{min} \leq b_f$ = "Okay" "Not Okay" otherwise

Bolt Capacity Check

$t_c := \sqrt{\frac{4 B_c \cdot b'}{p \cdot F_u}} = 1.384 \cdot in$ Manual Eq 9-26b pg 9-13

$\alpha := \frac{1}{\delta} \cdot \left[\frac{T_u}{B_c} \cdot \left(\frac{t_c}{t} \right)^2 - 1 \right] = -0.216$ Manual Eq 9-25 pg 9-13

$\alpha := 0$

Prying Force per Bolt

$q_u := B_c \cdot \left[\delta \cdot \alpha \cdot \rho \cdot \left(\frac{t}{t_c} \right)^2 \right] = 0 \cdot kip$ per bolt

Total Bolt Force including Prying Action

$T_u + q_u = 10 \cdot kip$ per bolt

Check :=	"Okay" if $T_u + q_u < B_c$ = "Okay"
	"Not Okay" otherwise

$$F_{O.S.} := \frac{B_c}{T_u + q_u} = 3.98$$

The test frame capacity exceeds expected demand from testing.

Concrete Plank Section Properties (from Mid-States Plank Section): 12" Hollowcore

Plank Width $b := 48in$

Plank Height $h := 12in$ $Weight := 150pcf$

Plank Area $A := 290.5478in^2$

Plank Perimeter $Perimeter := 238.1436in$

Plank Y Centroid $y_o := 6.1170in$ $y_{top} := y_o = 6.117 \cdot in$ $y_{bot} := h - y_o = 5.883 \cdot in$

Plank X Centroid $x_o := 23.9389in$

Plank Y MOI $I_y := 228996.4130in^4$

Plank X MOI $I_x := 5056.4914in^4$

Plank X Radius of Gyration $r_x := 7.4042in$

Plank Y Radius of Gyration $r_y := 28.0741in$

Overall Member Length $Length := 20ft$

Span Length $L := 19ft$

Concrete Properties (from Mid-States Plank Section)

Compressive Strength $f'_c := 11150psi$ $f'c := f'_c$

Ratio of effective compression block to neutral axis

$$\beta_1 := \begin{cases} 0.85 & \text{if } f'_c \le 4000psi \\ \left(1.05 - \frac{0.05 \cdot f'_c}{1000psi}\right) & \text{if } 4000psi < f'_c < 8000psi \\ 0.65 & \text{if } f'_c \ge 8000psi \end{cases} = 0.65$$

Concrete Modulus of Elasticity $E_c := 57000 \cdot \sqrt{f'_c \cdot psi} = 6018833 \cdot psi$

Concrete Modulus of Rupture $f_r := 7.5 \cdot \sqrt{f'_c \cdot psi} = 792 \cdot psi$

Concrete Strain at Peak Compressive Stress $\varepsilon_0 := 0.002$

Maximum Useable Concrete Strain $\varepsilon_{cu} := 0.003$

Slope of Descending Branch of Hognestad Parabola $Z := 150$

Hognestad Parabola of Concrete Stress with Descending Branch

$$f_c(\varepsilon_c) := \begin{cases} f'_c \cdot \left[2 \cdot \left(\frac{\varepsilon_c}{\varepsilon_0}\right) - \left(\frac{\varepsilon_c}{\varepsilon_0}\right)^2\right] & \text{if } \varepsilon_c \le \varepsilon_0 \\ f'_c \cdot \left[1 - \frac{Z}{1000} \cdot \left(\frac{\varepsilon_c - \varepsilon_0}{\varepsilon_0}\right)\right] & \text{otherwise} \end{cases}$$

Prestressing Steel

5-1/2in.-dia., 270 ksi, low-relaxation strands

Number of Strands	$n := 5$	
Area of Prestressed Steel	$A_{ps} := 0.1516 \cdot n\,in^2 = 0.758 \cdot in^2$	From Sumiden Wire
Depth to Steel	$d_{ps} := 10in$	From Mid-States
Specified Tensile Strength	$f_{pu} := 270ksi$	From Mid-States
Initial Prestress Force	$f_{pi} := 0.65 \cdot f_{pu} = 175.5 \cdot ksi$	From Mid-States
Steel Modulus of Elasticity	$E_{ps} := 28600000psi$	From Sumiden Wire
Prestressing Losses	$Losses := 0.7\%$	From Mid-States
Minimum Yield Strength at 1% Elongation	$f_{py} := 243ksi$	Design Aid 11.2.5
Effective Strain	$\varepsilon_{sy} := \frac{f_{pi} - f_{pu} \cdot Losses}{E_{ps}} = 6.07 \times 10^{-3}$	
	$\varepsilon_{py} := \frac{f_{py}}{E_{ps}} = 8.497 \times 10^{-3}$	
	$\varepsilon_{pu} := 0.014$	

Effective Stress in Reinforcement $f_{pe} := f_{pi} - f_{pi} \cdot \text{Losses} = 174.271 \cdot \text{ksi}$

Initial Prestressing Force $P_i := A_{ps} \cdot f_{pi} = 133.029 \cdot \text{kip}$

Effective Prestressing Force $P_e := A_{ps} \cdot f_{pe} = 132.098 \cdot \text{kip}$

Gross Transformed Section Analysis

Modular ratio

$$n := \frac{E_{ps}}{E_c} = 4.752$$

Centroid to Gross Transformed Section

$$y_{g.tr.top} := \frac{A \cdot y_o + (n-1) \cdot A_{ps} \cdot d_{ps}}{A + (n-1) \cdot A_{ps}} = 6.155 \cdot in$$

$$y_{g.tr.bot} := h - y_{g.tr.top} = 5.845 \cdot in$$

Gross Moment of Inertia of Transformed Section

$$I_{g.tr} := I_x + A \cdot \left(y_{g.tr.top} - y_o\right)^2 + 0 + (n-1) \cdot A_{ps} \cdot \left(d_{ps} - y_{g.tr.top}\right)^2$$

$$I_{g.tr} = 5099 \cdot in^4$$

Eccentricity of Strands to Centroid

$$e := d_{ps} - y_{g.tr.top} = 3.845 \cdot in$$

Section Modulus

$$S_t := \frac{I_{g.tr}}{y_{g.tr.top}} = 828.473 \cdot in^3$$

$$S_b := \frac{I_{g.tr}}{y_{g.tr.bot}} = 872.308 \cdot in^3$$

Cracked Moment of Inertia

$$\rho_p := \frac{A_{ps}}{A - b \cdot \left(h - d_{ps}\right)} = 3.896 \times 10^{-3}$$

ACI Eq. 5-110

$$I_{cr} := n \cdot A_{ps} \cdot d_{ps}^2 \cdot \left(1 - 1.6 \cdot \sqrt{n \cdot \rho_p}\right) = 281.769 \cdot in^4$$

Moment Curvature

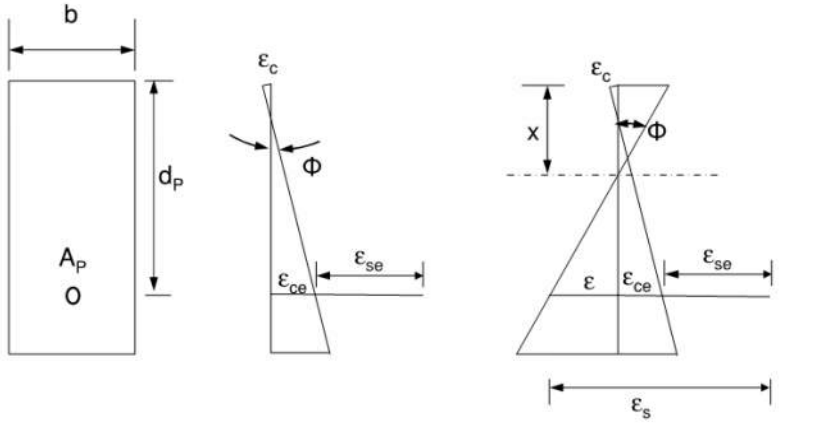

(a) Strain Distribution at Zero Moment

(a) Strain Distribution After Moment is Applied

Initial Stage - Zero Applied Moment (Gross Section Properties)

$$M_0 := 0\text{kip}\cdot\text{ft}$$

Stress at Bottom

$$\sigma_{bot} := \frac{-P_e}{A} - \frac{P_e\cdot e\cdot y_{g.tr.bot}}{I_{g.tr}} = -1.037\cdot\text{ksi}$$

Stress at Top

$$\sigma_{top} := \frac{-P_e}{A} + \frac{P_e\cdot e\cdot y_{g.tr.top}}{I_{g.tr}} = 0.158\cdot\text{ksi}$$

Strain at Bottom

$$\varepsilon_{bot} := \frac{\sigma_{bot}}{E_c} = -1.723\times 10^{-4}$$

Strain at Top

$$\varepsilon_{top} := \frac{\sigma_{top}}{E_c} = 2.633\times 10^{-5}$$

Curvature on Section

$$\Phi_0 := \frac{\varepsilon_{bot} - \varepsilon_{top}}{h} = -1.655\times 10^{-5}\cdot\frac{1}{\text{in}}$$

$$x := \frac{\varepsilon_{top}\cdot h}{\varepsilon_{top} - \varepsilon_{bot}} = 1.591\cdot\text{in}$$

Stress in Concrete

$$\sigma_{ce} := \frac{-P_e}{A} + \frac{-P_e\cdot e\cdot\left(d_{ps} - y_{g.tr.top}\right)}{\left(I_{g.tr}\right)} = -0.838\cdot\text{ksi}$$

Strain in Concrete

$$\varepsilon_{ce} := \frac{\sigma_{ce}}{E_c} = -1.392\times 10^{-4}$$

Strain in Steel After Prestress Losses

$$\varepsilon_{se} := -\frac{f_{pe}}{E_{ps}} = -6.093\times 10^{-3}$$

Only Self Weight

Effective Stress in Reinforcement

$$f_{pe} := f_{pi} - f_{pi} \cdot \text{Losses} = 174.271 \cdot \text{ksi}$$

Effective Prestressing Force

$$P_e := A_{ps} \cdot f_{pe} = 132.098 \cdot \text{kip}$$

Moment

$$M_{sw} := \frac{\text{Weight} \cdot A \cdot L^2}{8} = 13.657 \cdot \text{ft} \cdot \text{kip}$$

$$M_1 := M_{sw}$$

Stress at Bottom

$$\sigma_{bot} := \frac{-P_e}{A} - \frac{P_e \cdot e}{S_b} + \frac{M_{sw}}{S_b} = -0.849 \cdot \text{ksi}$$

Stress at Top

$$\sigma_{top} := \frac{-P_e}{A} + \frac{P_e \cdot e}{S_t} - \frac{M_{sw}}{S_t} = -0.039 \cdot \text{ksi}$$

Strain at Bottom

$$\varepsilon_{bot} := \frac{\sigma_{bot}}{E_c} = -1.411 \times 10^{-4}$$

Strain at Top

$$\varepsilon_{top} := \frac{\sigma_{top}}{E_c} = -6.536 \times 10^{-6}$$

Curvature

$$\Phi_1 := \frac{\varepsilon_{bot} - \varepsilon_{top}}{h} = -0.00001121 \cdot \frac{1}{\text{in}}$$

Zero Strain in Concrete at Level of Steel

Moment $M_{st} := \frac{-I_{g.tr} \cdot \sigma_{ce}}{e} = 92.569 \cdot ft \cdot kip$

$M_2 := M_{st}$

Stress at Bottom $\sigma_{bot} := \frac{-P_e}{A} - \frac{P_e \cdot e}{S_b} + \frac{M_{st}}{S_b} = 0.236 \cdot ksi$

Stress at Top $\sigma_{top} := \frac{-P_e}{A} + \frac{P_e \cdot e}{S_t} - \frac{M_{st}}{S_t} = -1.182 \cdot ksi$

Strain at Bottom $\varepsilon_{bot} := \frac{\sigma_{bot}}{E_c} = 3.929 \times 10^{-5}$

Strain at Top $\varepsilon_{top} := \frac{\sigma_{top}}{E_c} = -1.964 \times 10^{-4}$

Curvature $\Phi_2 := \frac{\varepsilon_{bot} - \varepsilon_{top}}{h} = 0.00001964 \cdot \frac{1}{in}$

Strain in concrete at lvl of steel $\varepsilon_{top} + d_{ps} \cdot \Phi_2 = 0$

First Cracking

Cacking Moment

$$M_{cr} := 7.5\sqrt{f'c \cdot psi} \cdot S_b + \frac{P_e \cdot S_b}{A} + P_e \cdot e = 132.949 \cdot ft \cdot kip$$

$$M_3 := M_{cr}$$

Stress at Bottom

$$\sigma_{bot} := \frac{-P_e}{A} - \frac{P_e \cdot e}{S_b} + \frac{M_3}{S_b} = 0.792 \cdot ksi$$

Stress at Top

$$\sigma_{top} := \frac{-P_e}{A} + \frac{P_e \cdot e}{S_t} - \frac{M_3}{S_t} = -1.767 \cdot ksi$$

Strain at Bottom

$$\varepsilon_{bot} := \frac{\sigma_{bot}}{E_c} = 1.316 \times 10^{-4}$$

Strain at Top

$$\varepsilon_{top} := \frac{\sigma_{top}}{E_c} = -2.936 \times 10^{-4}$$

Curvature

$$\Phi_3 := \frac{\varepsilon_{bot} - \varepsilon_{top}}{h} = 0.00003543 \cdot \frac{1}{in}$$

Cracked Section: Assume Strain in Concrete at the Top $\varepsilon_{cm} := 0.00075$

$$A_c(c) := \begin{cases} b \cdot c & \text{if } c \le 1.375\text{in} \\ b \cdot c + 0\text{in}^2 & \text{otherwise} \end{cases}$$

Strain in Strand

$$\varepsilon_p(c) := -\left(\varepsilon_{ce} + \varepsilon_{se}\right) + \varepsilon_{cm} \cdot \frac{d_{ps} - c}{c}$$

Stess in Strand

$$f_p(c) := \begin{cases} \left(\varepsilon_p(c) \cdot E_{ps}\right) & \text{if } \varepsilon_p(c) \le \varepsilon_{py} \\ f_{py} + \left(f_{pu} - f_{py}\right) \cdot \frac{\varepsilon_p(c) - \varepsilon_{py}}{\left(\varepsilon_{pu} - \varepsilon_{py}\right)} & \text{if } \varepsilon_{py} < \varepsilon_p(c) \le \varepsilon_{pu} \\ f_{pu} & \text{otherwise} \end{cases}$$

Concrete Force

$$F_c(c) := \frac{A_c(c)}{\varepsilon_{cm}} \int_0^{\varepsilon_{cm}} f_c\left(\varepsilon_c\right) d\varepsilon_c$$

Steel Force
assumes steel not yielded

$$F_s(c) := f_p(c) \cdot A_{ps}$$

Solve for Neutral Axis Depth...

$$c := \text{root}\left(F_c(c) - F_s(c), c, 0.05 \cdot d_{ps}, 0.6 d_{ps}\right)$$

$$c = 1.126 \cdot \text{in}$$

$$\text{Check}_{Voids} := \begin{cases} \text{"Okay"} & \text{if } c \le 1.375\text{in} \\ \text{"Redo Calcs for Voids"} & \text{otherwise} \end{cases} = \text{"Okay"}$$

Compute...

Moment of concrete stresses about the neutral axis

$$M_c := \frac{b \cdot c^2}{\varepsilon_{cm}^2} \int_0^{\varepsilon_{cm}} f_c\left(\varepsilon_c\right) \cdot \varepsilon_c \, d\varepsilon_c$$

Moment of steel stresses about the neutral axis

$$M_s := F_s(c) \cdot \left(d_{ps} - c\right)$$

Moment on section

$$M_4 := M_c + M_s = 158 \cdot \text{kip} \cdot \text{ft}$$

Compute Curvature...

Curvature on section

$$\Phi_4 := \frac{\varepsilon_{cm}}{c} = 0.00066603 \cdot \frac{1}{\text{in}}$$

Cracked Section: Assume Strain in Concrete at the Top $\varepsilon_{cm} := 0.001$

Strain in Strand

$$\varepsilon_p(c) := -\left(\varepsilon_{ce} + \varepsilon_{se}\right) + \varepsilon_{cm}\cdot\frac{d_{ps} - c}{c}$$

Stess in Strand

$$f_p(c) := \begin{cases} \left(\varepsilon_p(c)\cdot E_{ps}\right) & \text{if } \varepsilon_p(c) \le \varepsilon_{py} \\ f_{py} + \left(f_{pu} - f_{py}\right)\cdot\dfrac{\varepsilon_p(c) - \varepsilon_{py}}{\left(\varepsilon_{pu} - \varepsilon_{py}\right)} & \text{if } \varepsilon_{py} < \varepsilon_p(c) \le \varepsilon_{pu} \\ f_{pu} & \text{otherwise} \end{cases}$$

Concrete Force

$$F_c(c) := \frac{b\cdot c}{\varepsilon_{cm}}\int_0^{\varepsilon_{cm}} f_c\left(\varepsilon_c\right)\,d\varepsilon_c$$

Steel Force
assumes steel not yielded

$$F_s(c) := f_p(c)\cdot A_{ps}$$

Solve for Neutral Axis Depth...

$$c := \text{root}\left(F_c(c) - F_s(c), c, 0.05\cdot d_{ps}, 0.6 d_{ps}\right)$$

$$c = 0.918\cdot\text{in}$$

$$\text{Check}_{Voids} := \begin{cases} \text{"Okay"} & \text{if } c \le 1.375\text{in} \\ \text{"Redo Calcs for Voids"} & \text{otherwise} \end{cases} = \text{"Okay"}$$

Compute Moment...

Moment of concrete stresses about the neutral axis

$$M_c := \frac{b\cdot c^2}{\varepsilon_{cm}^2}\int_0^{\varepsilon_{cm}} f_c\left(\varepsilon_c\right)\cdot\varepsilon_c\,d\varepsilon_c = 10\cdot\text{kip}\cdot\text{ft}$$

Moment of steel stresses about the neutral axis

$$M_s := F_s(c)\cdot\left(d_{ps} - c\right)$$

Moment on section

$$M_5 := M_c + M_s = 165\cdot\text{kip}\cdot\text{ft}$$

Compute Curvature...

Curvature on section

$$\Phi_5 := \frac{\varepsilon_{cm}}{c} = 0.00108961\cdot\frac{1}{\text{in}}$$

Cracked Section: Assume Strain in Concrete at the Top $\varepsilon_{cm} := 0.002$

Strain in Strand

$$\varepsilon_p(c) := -\left(\varepsilon_{ce} + -\varepsilon_{se}\right) + \varepsilon_{cm}\cdot\frac{d_{ps} - c}{c}$$

Stess in Strand

$$f_p(c) := \begin{cases} \left(\varepsilon_p(c)\cdot E_{ps}\right) & \text{if } \varepsilon_p(c) \le \varepsilon_{py} \\ \left[f_{py} + \left(f_{pu} - f_{py}\right)\cdot\frac{\varepsilon_p(c) - \varepsilon_{py}}{\varepsilon_{pu} - \varepsilon_{py}}\right] & \text{if } \varepsilon_{py} < \varepsilon_p(c) < \varepsilon_{pu} \\ f_{pu} & \text{otherwise} \end{cases}$$

Concrete Force

$$F_c(c) := \frac{b\cdot c}{\varepsilon_{cm}}\int_0^{\varepsilon_{cm}} f_c\left(\varepsilon_c\right) d\varepsilon_c$$

Steel Force
assumes steel not yielded

$$F_s(c) := f_p(c)\cdot A_{ps}$$

Solve for Neutral Axis Depth...

$$c := \text{root}\left(F_c(c) - F_s(c), c, 0.05\cdot d_{ps}, 0.6 d_{ps}\right)$$

$$c = 0.574\cdot\text{in}$$

$$\text{Check}_{Voids} := \begin{cases} \text{"Okay"} & \text{if } c \le 1.375\text{in} \\ \text{"Redo Calcs for Voids"} & \text{otherwise} \end{cases} = \text{"Okay"}$$

Compute Moment...

Moment of concrete stresses about the neutral axis

$$M_c := \frac{b\cdot c^2}{\varepsilon_{cm}^2}\int_0^{\varepsilon_{cm}} f_c\left(\varepsilon_c\right)\cdot\varepsilon_c\, d\varepsilon_c$$

Moment of steel stresses about the neutral axis

$$M_s := F_s(c)\cdot\left(d_{ps} - c\right)$$

Moment on section

$$M_6 := M_c + M_s = 167\cdot\text{kip}\cdot\text{ft}$$

Compute Curvature...

Curvature on section

$$\Phi_6 := \frac{\varepsilon_{cm}}{c} = 0.00348676\cdot\frac{1}{\text{in}}$$

Cracked Section: Assume Strain in Concrete at the Top $\varepsilon_{cm} := 0.0029$

Strain in Strand

$$\varepsilon_p(c) := -\left(\varepsilon_{ce} + -\varepsilon_{se}\right) + \varepsilon_{cm}\cdot\frac{d_{ps} - c}{c}$$

Stess in Strand

$$f_p(c) := \begin{cases} \left(\varepsilon_p(c)\cdot E_{ps}\right) & \text{if } \varepsilon_p(c) \le \varepsilon_{py} \\ \left[f_{py} + \left(f_{pu} - f_{py}\right)\cdot\frac{\varepsilon_p(c) - \varepsilon_{py}}{\varepsilon_{pu} - \varepsilon_{py}}\right] & \text{if } \varepsilon_{py} < \varepsilon_p(c) < \varepsilon_{pu} \\ f_{pu} & \text{otherwise} \end{cases}$$

Concrete Force

$$F_c(c) := \frac{b\cdot c}{\varepsilon_{cm}}\int_0^{\varepsilon_{cm}} f_c\left(\varepsilon_c\right) d\varepsilon_c$$

Steel Force
assumes steel not yielded

$$F_s(c) := f_p(c)\cdot A_{ps}$$

Solve for Neutral Axis Depth...

$$c := \text{root}\left(F_c(c) - F_s(c), c, 0.05\cdot d_{ps}, 0.6 d_{ps}\right)$$

$$c = 0.503\cdot in$$

$$\text{Check}_{Voids} := \begin{cases} \text{"Okay"} & \text{if } c \le 1.375in \\ \text{"Redo Calcs for Voids"} & \text{otherwise} \end{cases} = \text{"Okay"}$$

Compute Moment...

Moment of concrete stresses about the neutral axis

$$M_c := \frac{b\cdot c^2}{\varepsilon_{cm}^2}\int_0^{\varepsilon_{cm}} f_c\left(\varepsilon_c\right)\cdot\varepsilon_c\, d\varepsilon_c$$

Moment of steel stresses about the neutral axis

$$M_s := F_s(c)\cdot\left(d_{ps} - c\right)$$

Moment on section

$$M_7 := M_c + M_s = 167\cdot kip\cdot ft$$

Compute Curvature...

Curvature on section

$$\Phi_7 := \frac{\varepsilon_{cm}}{c} = 0.00576087\cdot\frac{1}{in}$$

Load versus Displacement

$M_1 = 13.657 \cdot kip \cdot ft$ $M_3 = 132.949 \cdot kip \cdot ft$ $M_5 = 165.072 \cdot kip \cdot ft$ $M_7 = 167.061 \cdot kip \cdot ft$

$M_2 = 92.569 \cdot kip \cdot ft$ $M_4 = 158.388 \cdot kip \cdot ft$ $M_6 = 166.881 \cdot kip \cdot ft$ $M_{cr} = 132.949 \cdot kip \cdot ft$

$$M := \begin{pmatrix} M_0 \\ M_1 \\ M_2 \\ M_3 \\ M_4 \\ M_5 \\ M_6 \\ M_7 \end{pmatrix} = \begin{pmatrix} 0 \\ 13.657 \\ 92.569 \\ 132.949 \\ 158.388 \\ 165.072 \\ 166.881 \\ 167.061 \end{pmatrix} \cdot kip \cdot ft \qquad \Phi := \begin{pmatrix} \Phi_0 \\ \Phi_1 \\ \Phi_2 \\ \Phi_3 \\ \Phi_4 \\ \Phi_5 \\ \Phi_6 \\ \Phi_7 \end{pmatrix} = \begin{pmatrix} -1.655 \times 10^{-5} \\ -1.121 \times 10^{-5} \\ 1.964 \times 10^{-5} \\ 3.543 \times 10^{-5} \\ 6.66 \times 10^{-4} \\ 1.09 \times 10^{-3} \\ 3.487 \times 10^{-3} \\ 5.761 \times 10^{-3} \end{pmatrix} \cdot \frac{1}{in}$$

$$Load := (M - M_2) \cdot \frac{4}{L} = \begin{pmatrix} -2.875 \\ 0 \\ 16.613 \\ 25.114 \\ 30.47 \\ 31.877 \\ 32.258 \\ 32.296 \end{pmatrix} \cdot kip$$

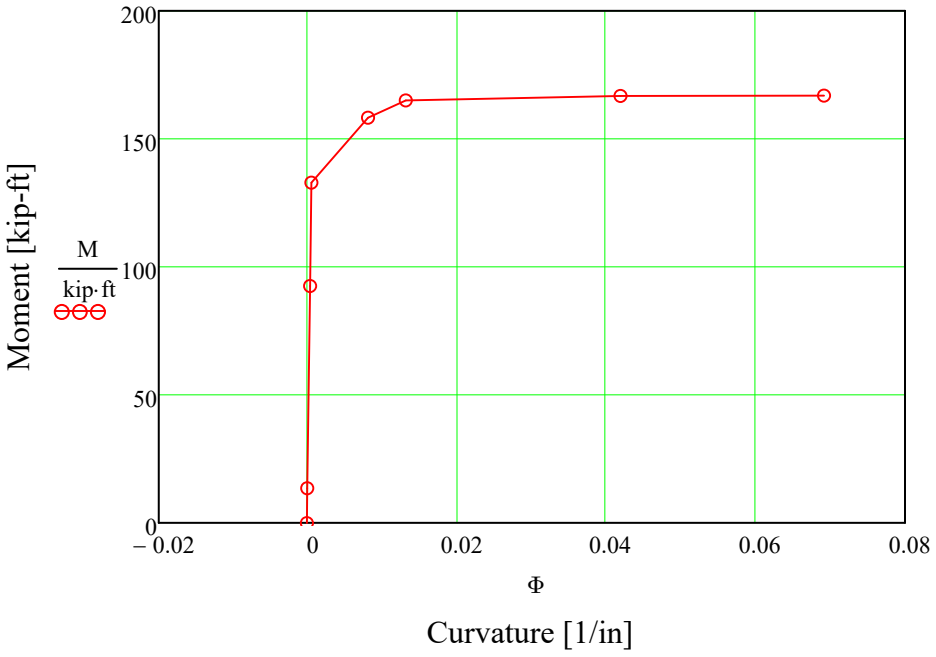

Shear

Maximum Load Expected from Moment Curvature Calculations

$Load_{sup} := 35kip$

$sw := A \cdot Weight \cdot Length = 6.053 \cdot kip$

$R := \frac{sw + Load_{sup}}{2} = 20.527 \cdot kip$

Shear Resistance Diagram

Web Thickness (Summation of web thicknesses at minimum width)

$b_w := 13.438in$

$\lambda := 1$

$V_{c.conc} := 2 \cdot \lambda \cdot \sqrt{f'c \cdot psi} \cdot b_w \cdot d_{ps} = 28.379 \cdot kip$

This creates the points of interest

$ORIGIN \equiv 1$

$i := 1, 2 .. 36$

$$x_i := i \cdot 0.25\,ft$$

$$i = \begin{pmatrix} 1 \\ 2 \\ 3 \\ 4 \\ 5 \\ 6 \\ 7 \\ 8 \\ 9 \\ 10 \\ 11 \\ 12 \\ 13 \\ 14 \\ 15 \\ 16 \\ 17 \\ 18 \\ 19 \\ 20 \\ 21 \\ 22 \\ 23 \\ 24 \\ 25 \\ 26 \\ 27 \\ 28 \\ 29 \\ 30 \\ 31 \\ 32 \\ 33 \\ 34 \\ 35 \\ 36 \end{pmatrix} \qquad x_i = \begin{pmatrix} 0.3 \\ 0.5 \\ 0.8 \\ 1.0 \\ 1.3 \\ 1.5 \\ 1.8 \\ 2.0 \\ 2.3 \\ 2.5 \\ 2.8 \\ 3.0 \\ 3.3 \\ 3.5 \\ 3.8 \\ 4.0 \\ 4.3 \\ 4.5 \\ 4.8 \\ 5.0 \\ 5.3 \\ 5.5 \\ 5.8 \\ 6.0 \\ 6.3 \\ 6.5 \\ 6.8 \\ 7.0 \\ 7.3 \\ 7.5 \\ 7.8 \\ 8.0 \\ 8.3 \\ 8.5 \\ 8.8 \\ 9.0 \end{pmatrix} ft$$

Shear along length of member

$$V_u := R - \frac{sw}{L} \cdot x = \cdot kip$$

	1
1	20.447
2	20.367
3	20.288
4	20.208
5	20.128
6	20.049
7	19.969
8	19.889
9	19.81
10	19.73
11	19.65
12	19.571
13	19.491
14	19.411
15	19.332
16	...

Moment along length of member

$$M_u := \overrightarrow{\left[\frac{\frac{sw}{Length} \cdot x}{2} \cdot (L - x)\right]} + \frac{Load_{sup} \cdot x}{2} = \cdot kip \cdot ft$$

	1
1	5.084
2	10.15
3	15.196
4	20.224
5	25.233
6	30.222
7	35.193
8	40.145
9	45.078
10	49.992
11	54.887
12	59.764
13	64.621
14	69.459
15	74.279
16	...

Flexure Shear Strength

Shear Force at Section due to Unfactored Load

$$V_d := \frac{Weight \cdot A \cdot Length}{2} - Weight \cdot A \cdot x = \begin{array}{|c|c|}\hline & 1 \\ \hline 1 & 2.951 \\ 2 & 2.875 \\ 3 & 2.8 \\ 4 & 2.724 \\ 5 & 2.648 \\ 6 & 2.573 \\ 7 & 2.497 \\ 8 & 2.421 \\ 9 & 2.346 \\ 10 & 2.27 \\ 11 & 2.194 \\ 12 & 2.119 \\ 13 & 2.043 \\ 14 & 1.967 \\ 15 & 1.892 \\ 16 & ... \\ \hline \end{array} \cdot kip$$

Factored Shear Force at Section due to Externally Applied Loads Occuring Simultaneously with Mmax

$$V_i := V_u - V_d = \begin{array}{|c|c|}\hline & 1 \\ \hline 1 & 17.496 \\ 2 & 17.492 \\ 3 & 17.488 \\ 4 & 17.484 \\ 5 & 17.48 \\ 6 & 17.476 \\ 7 & 17.472 \\ 8 & 17.468 \\ 9 & 17.464 \\ 10 & 17.46 \\ 11 & 17.456 \\ 12 & 17.452 \\ 13 & 17.448 \\ 14 & 17.444 \\ 15 & 17.44 \\ 16 & ... \\ \hline \end{array} \cdot kip$$

Stress due to Unfactored Dead Load @ Extreme Fiber of Section where Tensile Stress is caused by Externally Applied Loads

$$f_d := \frac{-P_e}{A} - \frac{P_e \cdot e}{S_b} + \frac{M_{sw}}{S_b} = -849.095 \cdot psi$$

Moment Causing Flexural Cracking at Section due to Externally Applied Loads

$$M_{cre} := M_{cr} = 132.949 \cdot kip \cdot ft$$

Moment due to Self Weight

$$M_d := \overrightarrow{\left[\frac{\frac{sw}{Length} \cdot x}{2} \cdot (L - x)\right]} = \cdot kip \cdot ft$$

	1
1	0.709
2	1.4
3	2.071
4	2.724
5	3.358
6	3.972
7	4.568
8	5.145
9	5.703
10	6.242
11	6.762
12	7.264
13	7.746
14	8.209
15	8.654
16	...

Maximum Factored Moment at Section due to Externally Applied Loads

$$M_{max} := M_u - M_d =$$

	1
1	4.375
2	8.75
3	13.125
4	17.5
5	21.875
6	26.25
7	30.625
8	35
9	39.375
10	43.75
11	48.125
12	52.5
13	56.875
14	61.25
15	65.625
16	...

$\cdot kip \cdot ft$

Operator to Choose the Max Value from Two Matrices

$$Max(V1, V2) := \left| \begin{array}{l} \text{for } i \in ORIGIN..\, last(V1) \\ \quad R_i \leftarrow \max\left(V1_i, V2_i\right) \\ \text{return } R \end{array} \right.$$

$$V_{ci} := Max\left(0.6 \cdot \lambda \cdot \sqrt{f'c \cdot psi} \cdot b_w \cdot d_{ps} + V_d + \frac{V_i \cdot M_{cre}}{M_{max}}, 1.7 \cdot \lambda \cdot \sqrt{f'c \cdot psi} \cdot b_w \cdot d_{ps} \cdot \frac{x}{x}\right) =$$

	1
1	543.139
2	277.165
3	188.457
4	144.065
5	117.4
6	99.598
7	86.86
8	77.288
9	69.827
10	63.842
11	58.932
12	54.828
13	51.343
14	48.345
15	45.737
16	...

$\cdot kip$

Web Shear Strength

Compressive Strength after Prestress Losses

$$f_{pc} := \sigma_{bot} - y_{g.tr.top} \cdot \frac{\sigma_{top} - \sigma_{bot}}{h} = 2.105 \cdot ksi$$

Strand Angle

$$\alpha := 0$$

Vertical Component of Effective Prestress Force

$$V_p := Load_{sup} \cdot \sin(\alpha) = 0 \cdot kip$$

$$V_{cw} := \left(3.5 \cdot \lambda \cdot \sqrt{f'c \cdot psi} + 0.3 \cdot f_{pc}\right) \cdot b_w \cdot d_{ps} + V_p = 134.505 \cdot kip$$

Predicted Failure Mode

Concrete Shear Strength

$$V_c := 2 \cdot \lambda \cdot \sqrt{f'c \cdot psi} \cdot b_w \cdot d_{ps} = 28.379 \cdot kip$$

Operator to Choose the Min Value from Two Matrices

$$\begin{aligned} &Min(V1, V2) := \\ &\quad \text{for } i \in ORIGIN .. last(V1) \\ &\quad\quad R_i \leftarrow \min\left(V1_i, V2_i\right) \\ &\quad \text{return } R \end{aligned}$$

Nominal Shear Strength (Considers Web Shear, Flexure Shear, and Concrete Shear)

$$V_n := \mathrm{Max}\left(\mathrm{Min}\left(V_{ci}, \begin{bmatrix} V_{cw} \\ V_{cw} \end{bmatrix}\right), \begin{bmatrix} V_c \\ V_c \end{bmatrix}\right) =$$

	1
1	134.505
2	134.505
3	134.505
4	134.505
5	117.4
6	99.598
7	86.86
8	77.288
9	69.827
10	63.842
11	58.932
12	54.828
13	51.343
14	48.345
15	45.737
16	...

$\cdot kip$

$$\left[\left[\begin{matrix} V_{cw} \\ V_{cw} \\ V_{cw} \\ V_{cw} \end{matrix}\right]\left[\begin{matrix} V_{c} \\ V_{c} \\ V_{c} \\ V_{c} \end{matrix}\right]\right]$$

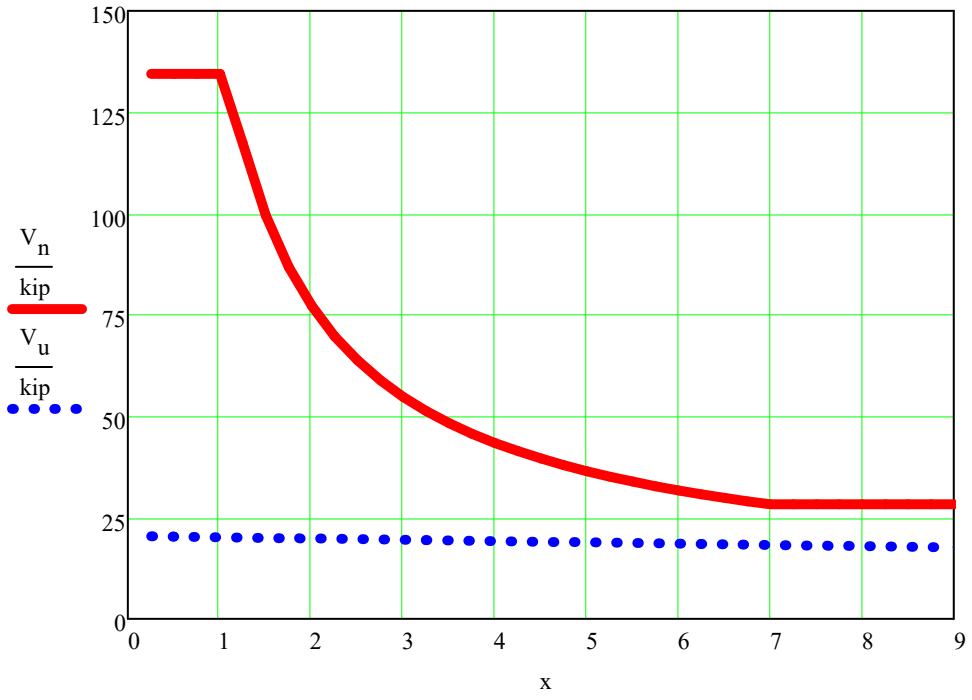
150
125
100
75
50
25
0
0
1
2
3
4
5
6
7
8
9
x
$\frac{V_n}{kip}$
$\frac{V_u}{kip}$

Punching Shear with Concentrated Load Centered Over Void

Distance from plate edge to void edge divided by 2

$d := 1.37in$

Plate Width

$c := 4in$

$t_{flange} := 1.37in$

Perimeter

$b_o := 4 \cdot (c + 2.2918in) = 25.167 \cdot in$

$\alpha_s := 40$

$$v_c := \min\left[3.5 \cdot \lambda \cdot \sqrt{f'c \cdot psi} + 0.3 \cdot \frac{f_{pc}}{2} + \frac{V_p}{b_o \cdot d}, \left(1.5 + \frac{\alpha_s \cdot d}{b_o}\right) \cdot \lambda \cdot \sqrt{f'c \cdot psi} + 0.3 \frac{f_{pc}}{2} + \frac{V_p}{b_o \cdot d}\right] = 685\,psi$$

Vertical Distance from Top to Void at Halfway Distance from Plate to Edge of Void

$vert := 2.5in$

$V_c := v_c \cdot b_o \cdot vert = 43.1 \cdot kip$

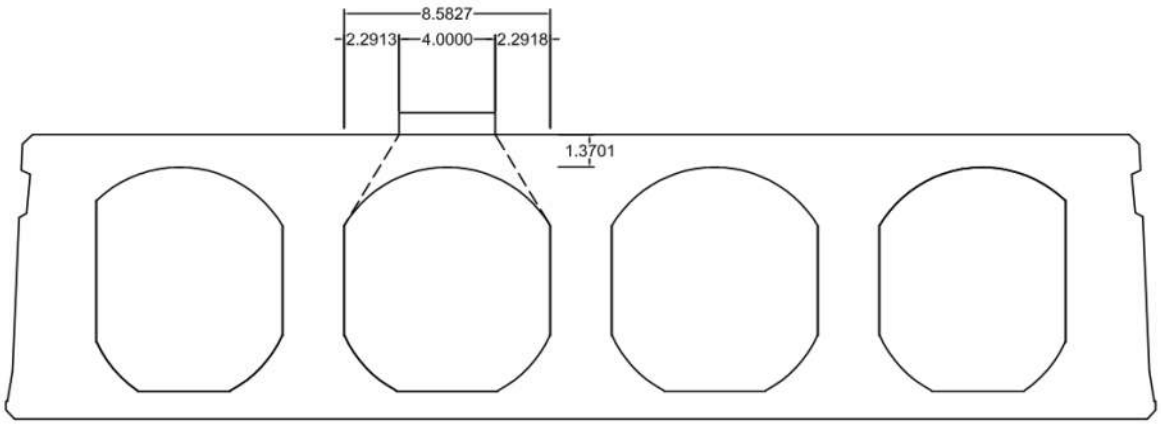

SUMMARY:

Load at Punching Shear	43.1 kips
Cracking Moment	133 kip-ft

ACI Nominal Moment

$$\frac{f_{py}}{f_{pu}} = 0.9$$

ACI 318-14 Table 20.3.2.3.1

$$\gamma_p := 0.28$$

$$\rho_p := \frac{A_{ps}}{b \cdot d_{ps}} = 1.579 \times 10^{-3}$$

$$f_{ps} := f_{pu} \cdot \left(1 - \frac{\gamma_p \cdot \rho_p \cdot f_{pu}}{\beta_1 \cdot f'_c} \right) = 265.552 \cdot ksi$$

$$a := \frac{A_{ps} \cdot f_{ps}}{.85 f'_c \cdot b} = 0.442 \cdot in$$

$$c := \frac{a}{\beta_1} = 0.681 \cdot in$$

$$M_n := A_{ps} \cdot f_{ps} \cdot \left(d_{ps} - \frac{a}{2} \right) = 164.0 \cdot kip \cdot ft$$

ACI Moment at Rupture

$$f_{rup} := \frac{43.505 kip}{0.1516 in^2} = 286.972 \cdot ksi$$

$$a := \frac{A_{ps} \cdot f_{rup}}{.85 f'_c \cdot b} = 0.478 \cdot in$$

$$c := \frac{a}{\beta_1} = 0.736 \cdot in$$

$$M_{rup} := A_{ps} \cdot f_{rup} \cdot \left(d_{ps} - \frac{a}{2} \right) = 176.9 \cdot kip \cdot ft$$

Deflection

Bilinear Method: Cracking

$$\Delta_{Bilinear.cr} := \frac{M_{cr}\cdot L^2}{12\cdot E_c\cdot I_{g.tr}} = 0.225\cdot in$$

Bilinear Method: Nominal

$$P_n := \frac{4\cdot M_n}{L} = 34.533\cdot kip \qquad P_{rup} := \frac{4M_{rup}}{L} = 37.25\cdot kip$$

$$P_{cr} := \frac{4M_{cr}}{L} = 27.989\cdot kip$$

$$\rho := \frac{A_{ps}}{A - b\cdot\left(h - d_{ps}\right)} = 3.896\times 10^{-3}$$

$$k := \sqrt{2\cdot n\cdot\rho + (n\cdot\rho)^2} - n\cdot\rho = 0.175$$

$$I_{cr} := \frac{1}{3}\cdot b\cdot\left(k\cdot d_{ps}\right)^3 + n\cdot A_{ps}\cdot\left(d_{ps} - k\cdot d_{ps}\right)^2 = 330.725\cdot in^4$$

$$\Delta_{Bilinear.nom} := \frac{P_{cr}\cdot L^3}{48\cdot E_c\cdot I_{g.tr}} + \frac{\left(P_n - P_{cr}\right)\cdot L^3}{48\cdot E_c\cdot I_{cr}} = 1.037\cdot in$$

Bilinear Method: Rupture

$$P_{rup} := \frac{4\cdot M_{rup}}{L} = 37.25\cdot kip$$

$$P_{cr} := \frac{4M_{cr}}{L} = 27.989\cdot kip$$

$$\rho := \frac{A_{ps}}{A - b\cdot\left(h - d_{ps}\right)} = 3.896\times 10^{-3}$$

$$k := \sqrt{2\cdot n\cdot\rho + (n\cdot\rho)^2} - n\cdot\rho = 0.175$$

$$I_{cr} := \frac{1}{3}\cdot b\cdot\left(k\cdot d_{ps}\right)^3 + n\cdot A_{ps}\cdot\left(d_{ps} - k\cdot d_{ps}\right)^2 = 330.725\cdot in^4$$

$$\Delta_{Bilinear.rup} := \frac{P_{cr}\cdot L^3}{48\cdot E_c\cdot I_{g.tr}} + \frac{\left(P_n - P_{cr}\right)\cdot L^3}{48\cdot E_c\cdot I_{cr}} = 1.374\cdot in$$

Ie* Method: Cracking

$$\Delta_{Ie*.cr} := \frac{5\cdot M_2\cdot L^2}{48\cdot E_c\cdot I_{g.tr}} + \frac{\left(M_{cr} - M_2\right)\cdot L^2}{12\cdot E_c\cdot I_{g.tr}} = 0.23\cdot in$$

Ie* Method: Nominal

$$I_{e*.nom} := \frac{I_{cr}}{1 - \frac{M_{cr}}{M_n}\left(1 - \frac{I_{cr}}{I_{g.tr}}\right)} = 1.366 \times 10^3\cdot in^4$$

$$\Delta_{Ie*.nom} := \frac{5\cdot M_2\cdot L^2}{48\cdot E_c\cdot I_{e*.nom}} + \frac{\left(M_n - M_2\right)\cdot L^2}{12\cdot E_c\cdot I_{e*.nom}} = 1.06\cdot in$$

Ie* Method: Rupture

$$I_{e*.rup} := \frac{I_{cr}}{1 - \frac{M_{cr}}{M_{rup}}\left(1 - \frac{I_{cr}}{I_{g.tr}}\right)} = 1.112 \times 10^3\cdot in^4$$

$$\Delta_{Ie*.rup} := \frac{5\cdot M_2\cdot L^2}{48\cdot E_c\cdot I_{e*.rup}} + \frac{\left(M_{rup} - M_2\right)\cdot L^2}{12\cdot E_c\cdot I_{e*.rup}} = 1.40\cdot in$$

Summary

$\Delta_{Ie*.cr} = 0.231\cdot in$ $\Delta_{Bilinear.cr} = 0.225\cdot in$

$\Delta_{Ie*.nom} = 1.058\cdot in$ $\Delta_{Bilinear.nom} = 1.037\cdot in$

$\Delta_{Ie*.rup} = 1.4\cdot in$ $\Delta_{Bilinear.rup} = 1.374\cdot in$

Concrete Plank Section Properties (from Mid-States Plank Section): 8" Hollowcore

Plank Width $b := 48in$

Plank Height $h := 8in$ $Weight := 150pcf$

Plank Area $A := 216.5334in^2$

Plank Perimeter $Perimeter := 221.2139in$

Plank Y Centroid $y_o := 4.0674in$ $y_{top} := y_o = 4.067 \cdot in$ $y_{bot} := h - y_o = 3.933 \cdot in$

Plank X Centroid $x_o := 23.9973in$

Plank Y MOI $I_y := 167089.3228in^4$

Plank X MOI $I_x := 1666.6523in^4$

Plank X Radius of Gyration $r_x := 4.9235in$

Plank Y Radius of Gyration $r_y := 27.7787in$

Overall Member Length $Length := 20ft$

Span Length $L := 18ft$

Concrete Properties (from Mid-States Plank Section)

Compressive Strength $f'_c := 11150psi$ $f'c := f'_c$

Ratio of effective compression block to neutral axis

$$\beta_1 := \begin{cases} 0.85 & \text{if } f'_c \le 4000psi \\ \left(1.05 - \frac{0.05 \cdot f'_c}{1000psi}\right) & \text{if } 4000psi < f'_c < 8000psi \\ 0.65 & \text{if } f'_c \ge 8000psi \end{cases} = 0.65$$

Concrete Modulus of Elasticity $E_c := 57000 \cdot \sqrt{f'_c \cdot psi} = 6018833 \cdot psi$

Concrete Modulus of Rupture $f_r := 7.5 \cdot \sqrt{f'_c \cdot psi} = 792 \cdot psi$

Concrete Strain at Peak Compressive Stress $\varepsilon_0 := 0.002$

Maximum Useable Concrete Strain $\varepsilon_{cu} := 0.003$

Slope of Descending Branch of Hognestad Parabola $Z := 150$

Hognestad Parabola of Concrete Stress with Descending Branch

$$f_c(\varepsilon_c) := \begin{cases} f'_c \cdot \left[2 \cdot \left(\frac{\varepsilon_c}{\varepsilon_0}\right) - \left(\frac{\varepsilon_c}{\varepsilon_0}\right)^2\right] & \text{if } \varepsilon_c \le \varepsilon_0 \\ f'_c \cdot \left[1 - \frac{Z}{1000} \cdot \left(\frac{\varepsilon_c - \varepsilon_0}{\varepsilon_0}\right)\right] & \text{otherwise} \end{cases}$$

Prestressing Steel

5-1/2in.-dia., 270 ksi, low-relaxation strands

Number of Strands	$n := 7$	
Area of Prestressed Steel	$A_{ps} := 0.1516 \cdot n\,in^2 = 1.061 \cdot in^2$	From Sumiden Wire
Depth to Steel	$d_{ps} := 6in$	From Mid-States
Specified Tensile Strength	$f_{pu} := 270ksi$	From Mid-States
Initial Prestress Force	$f_{pi} := 0.65 \cdot f_{pu} = 175.5 \cdot ksi$	From Mid-States
Steel Modulus of Elasticity	$E_{ps} := 28600000psi$	From Sumiden Wire
Prestressing Losses	$Losses := 0.7\%$	From Mid-States
Minimum Yield Strength at 1% Elongation	$f_{py} := 243ksi$	Design Aid 11.2.5
Effective Strain	$\varepsilon_{sy} := \frac{f_{pi} - f_{pu} \cdot Losses}{E_{ps}} = 6.07 \times 10^{-3}$	
	$\varepsilon_{py} := \frac{f_{py}}{E_{ps}} = 8.497 \times 10^{-3}$	
	$\varepsilon_{pu} := 0.014$	

Effective Stress in Reinforcement $f_{pe} := f_{pi} - f_{pi} \cdot \text{Losses} = 174.271 \cdot \text{ksi}$

Initial Prestressing Force $P_i := A_{ps} \cdot f_{pi} = 186.241 \cdot \text{kip}$

Effective Prestressing Force $P_e := A_{ps} \cdot f_{pe} = 184.937 \cdot \text{kip}$

Gross Transformed Section Analysis

Modular ratio

$$n := \frac{E_{ps}}{E_c} = 4.752$$

Centroid to Gross Transformed Section

$$y_{g.tr.top} := \frac{A \cdot y_o + (n-1) \cdot A_{ps} \cdot d_{ps}}{A + (n-1) \cdot A_{ps}} = 4.102 \cdot in$$

$$y_{g.tr.bot} := h - y_{g.tr.top} = 3.898 \cdot in$$

Gross Moment of Inertia of Transformed Section

$$I_{g.tr} := I_x + A \cdot \left(y_{g.tr.top} - y_o\right)^2 + 0 + (n-1) \cdot A_{ps} \cdot \left(d_{ps} - y_{g.tr.top}\right)^2$$

$$I_{g.tr} = 1681 \cdot in^4$$

Eccentricity of Strands to Centroid

$$e := d_{ps} - y_{g.tr.top} = 1.898 \cdot in$$

Section Modulus

$$S_t := \frac{I_{g.tr}}{y_{g.tr.top}} = 409.833 \cdot in^3$$

$$S_b := \frac{I_{g.tr}}{y_{g.tr.bot}} = 431.344 \cdot in^3$$

Cracked Moment of Inertia

$$\rho_p := \frac{A_{ps}}{A - b \cdot \left(h - d_{ps}\right)} = 8.804 \times 10^{-3}$$

ACI Eq. 5-110

$$I_{cr} := n \cdot A_{ps} \cdot d_{ps}^2 \cdot \left(1 - 1.6 \cdot \sqrt{n \cdot \rho_p}\right) = 122.124 \cdot in^4$$

Moment Curvature

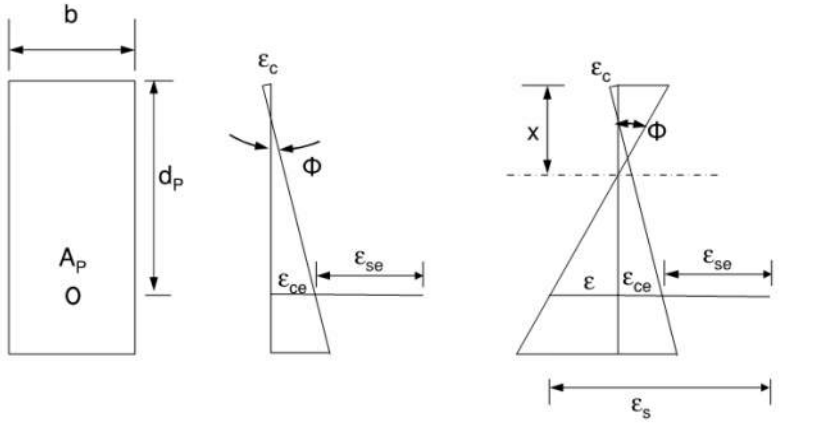

(a) Strain Distribution at Zero Moment

(a) Strain Distribution After Moment is Applied

Initial Stage - Zero Applied Moment (Gross Section Properties)

$$M_0 := 0\text{kip}\cdot\text{ft}$$

Stress at Bottom

$$\sigma_{bot} := \frac{-P_e}{A} - \frac{P_e\cdot e\cdot y_{g.tr.bot}}{I_{g.tr}} = -1.668\cdot\text{ksi}$$

Stress at Top

$$\sigma_{top} := \frac{-P_e}{A} + \frac{P_e\cdot e\cdot y_{g.tr.top}}{I_{g.tr}} = 2.26\times 10^{-3}\cdot\text{ksi}$$

Strain at Bottom

$$\varepsilon_{bot} := \frac{\sigma_{bot}}{E_c} = -2.771\times 10^{-4}$$

Strain at Top

$$\varepsilon_{top} := \frac{\sigma_{top}}{E_c} = 3.754\times 10^{-7}$$

Curvature on Section

$$\Phi_0 := \frac{\varepsilon_{bot}-\varepsilon_{top}}{h} = -3.468\times 10^{-5}\cdot\frac{1}{\text{in}}$$

$$x := \frac{\varepsilon_{top}\cdot h}{\varepsilon_{top}-\varepsilon_{bot}} = 0.011\cdot\text{in}$$

Stress in Concrete

$$\sigma_{ce} := \frac{-P_e}{A} + \frac{-P_e\cdot e\cdot\left(d_{ps}-y_{g.tr.top}\right)}{\left(I_{g.tr}\right)} = -1.25\cdot\text{ksi}$$

Strain in Concrete

$$\varepsilon_{ce} := \frac{\sigma_{ce}}{E_c} = -2.077\times 10^{-4}$$

Strain in Steel After Prestress Losses

$$\varepsilon_{se} := -\frac{f_{pe}}{E_{ps}} = -6.093\times 10^{-3}$$

Only Self Weight

Effective Stress in Reinforcement

$$f_{pe} := f_{pi} - f_{pi} \cdot Losses = 174.271 \cdot ksi$$

Effective Prestressing Force

$$P_e := A_{ps} \cdot f_{pe} = 184.937 \cdot kip$$

Moment

$$M_{sw} := \frac{Weight \cdot A \cdot L^2}{8} = 9.135 \cdot ft \cdot kip$$

$$M_1 := M_{sw}$$

Stress at Bottom

$$\sigma_{bot} := \frac{-P_e}{A} - \frac{P_e \cdot e}{S_b} + \frac{M_{sw}}{S_b} = -1.414 \cdot ksi$$

Stress at Top

$$\sigma_{top} := \frac{-P_e}{A} + \frac{P_e \cdot e}{S_t} - \frac{M_{sw}}{S_t} = -0.265 \cdot ksi$$

Strain at Bottom

$$\varepsilon_{bot} := \frac{\sigma_{bot}}{E_c} = -2.349 \times 10^{-4}$$

Strain at Top

$$\varepsilon_{top} := \frac{\sigma_{top}}{E_c} = -4.406 \times 10^{-5}$$

Curvature

$$\Phi_1 := \frac{\varepsilon_{bot} - \varepsilon_{top}}{h} = -0.00002385 \cdot \frac{1}{in}$$

Zero Strain in Concrete at Level of Steel

Moment $M_{st} := \frac{-I_{g.tr} \cdot \sigma_{ce}}{e} = 92.302 \cdot ft \cdot kip$

$M_2 := M_{st}$

Stress at Bottom $\sigma_{bot} := \frac{-P_e}{A} - \frac{P_e \cdot e}{S_b} + \frac{M_{st}}{S_b} = 0.9 \cdot ksi$

Stress at Top $\sigma_{top} := \frac{-P_e}{A} + \frac{P_e \cdot e}{S_t} - \frac{M_{st}}{S_t} = -2.7 \cdot ksi$

Strain at Bottom $\varepsilon_{bot} := \frac{\sigma_{bot}}{E_c} = 1.496 \times 10^{-4}$

Strain at Top $\varepsilon_{top} := \frac{\sigma_{top}}{E_c} = -4.487 \times 10^{-4}$

Curvature $\Phi_2 := \frac{\varepsilon_{bot} - \varepsilon_{top}}{h} = 0.00007478 \cdot \frac{1}{in}$

Strain in concrete at lvl of steel $\varepsilon_{top} + d_{ps} \cdot \Phi_2 = 0$

First Cracking

Cacking Moment

$$M_{cr} := 7.5\sqrt{f'c \cdot psi} \cdot S_b + \frac{P_e \cdot S_b}{A} + P_e \cdot e = 88.414 \cdot ft \cdot kip$$

$$M_3 := M_{cr}$$

Stress at Bottom

$$\sigma_{bot} := \frac{-P_e}{A} - \frac{P_e \cdot e}{S_b} + \frac{M_3}{S_b} = 0.792 \cdot ksi$$

Stress at Top

$$\sigma_{top} := \frac{-P_e}{A} + \frac{P_e \cdot e}{S_t} - \frac{M_3}{S_t} = -2.587 \cdot ksi$$

Strain at Bottom

$$\varepsilon_{bot} := \frac{\sigma_{bot}}{E_c} = 1.316 \times 10^{-4}$$

Strain at Top

$$\varepsilon_{top} := \frac{\sigma_{top}}{E_c} = -4.297 \times 10^{-4}$$

Curvature

$$\Phi_3 := \frac{\varepsilon_{bot} - \varepsilon_{top}}{h} = 0.00007016 \cdot \frac{1}{in}$$

Cracked Section: Assume Strain in Concrete at the Top $\varepsilon_{cm} := 0.0004$

$$A_c(c) := \begin{cases} b \cdot c & \text{if } c \le 1.375\text{in} \\ b \cdot c + 0\text{in}^2 & \text{otherwise} \end{cases}$$

Strain in Strand

$$\varepsilon_p(c) := -\left(\varepsilon_{ce} + \varepsilon_{se}\right) + \varepsilon_{cm} \cdot \frac{d_{ps} - c}{c}$$

Stess in Strand

$$f_p(c) := \begin{cases} \left(\varepsilon_p(c) \cdot E_{ps}\right) & \text{if } \varepsilon_p(c) \le \varepsilon_{py} \\ f_{py} + \left(f_{pu} - f_{py}\right) \cdot \frac{\varepsilon_p(c) - \varepsilon_{py}}{\left(\varepsilon_{pu} - \varepsilon_{py}\right)} & \text{if } \varepsilon_{py} < \varepsilon_p(c) \le \varepsilon_{pu} \\ f_{pu} & \text{otherwise} \end{cases}$$

Concrete Force

$$F_c(c) := \frac{A_c(c)}{\varepsilon_{cm}} \int_0^{\varepsilon_{cm}} f_c\left(\varepsilon_c\right) d\varepsilon_c$$

Steel Force
assumes steel not yielded

$$F_s(c) := f_p(c) \cdot A_{ps}$$

Solve for Neutral Axis Depth...

$$c := \text{root}\left(F_c(c) - F_s(c), c, 0.05 \cdot d_{ps}, 0.6 d_{ps}\right)$$

$$c = 2.134 \cdot \text{in}$$

Compute...

Moment of concrete stresses about the neutral axis

$$M_c := \frac{b \cdot c^2}{\varepsilon_{cm}^2} \int_0^{\varepsilon_{cm}} f_c\left(\varepsilon_c\right) \cdot \varepsilon_c \, d\varepsilon_c$$

Moment of steel stresses about the neutral axis

$$M_s := F_s(c) \cdot \left(d_{ps} - c\right)$$

Moment on section

$$M_4 := M_c + M_s = 94 \cdot \text{kip} \cdot \text{ft}$$

Compute Curvature...

Curvature on section

$$\Phi_4 := \frac{\varepsilon_{cm}}{c} = 0.00018741 \cdot \frac{1}{\text{in}}$$

Cracked Section: Assume Strain in Concrete at the Top $\varepsilon_{cm} := 0.001$

Strain in Strand

$$\varepsilon_p(c) := -\left(\varepsilon_{ce} + \varepsilon_{se}\right) + \varepsilon_{cm}\cdot\frac{d_{ps} - c}{c}$$

Stess in Strand

$$f_p(c) := \begin{cases} \left(\varepsilon_p(c)\cdot E_{ps}\right) & \text{if } \varepsilon_p(c) \le \varepsilon_{py} \\ f_{py} + \left(f_{pu} - f_{py}\right)\cdot\dfrac{\varepsilon_p(c) - \varepsilon_{py}}{\left(\varepsilon_{pu} - \varepsilon_{py}\right)} & \text{if } \varepsilon_{py} < \varepsilon_p(c) \le \varepsilon_{pu} \\ f_{pu} & \text{otherwise} \end{cases}$$

Concrete Force

$$F_c(c) := \frac{b\cdot c}{\varepsilon_{cm}}\int_0^{\varepsilon_{cm}} f_c\left(\varepsilon_c\right)\,d\varepsilon_c$$

Steel Force
assumes steel not yielded

$$F_s(c) := f_p(c)\cdot A_{ps}$$

Solve for Neutral Axis Depth...

$$c := \text{root}\left(F_c(c) - F_s(c), c, 0.05\cdot d_{ps}, 0.6 d_{ps}\right)$$

$$c = 1.199\cdot\text{in}$$

$$\text{Check}_{Voids} := \begin{cases} \text{"Okay"} & \text{if } c \le 1.375\text{in} \\ \text{"Redo Calcs for Voids"} & \text{otherwise} \end{cases} = \text{"Okay"}$$

Compute Moment...

Moment of concrete stresses about the neutral axis

$$M_c := \frac{b\cdot c^2}{\varepsilon_{cm}^2}\int_0^{\varepsilon_{cm}} f_c\left(\varepsilon_c\right)\cdot\varepsilon_c\,d\varepsilon_c = 17\cdot\text{kip}\cdot\text{ft}$$

Moment of steel stresses about the neutral axis

$$M_s := F_s(c)\cdot\left(d_{ps} - c\right)$$

Moment on section

$$M_5 := M_c + M_s = 124\cdot\text{kip}\cdot\text{ft}$$

Compute Curvature...

Curvature on section

$$\Phi_5 := \frac{\varepsilon_{cm}}{c} = 0.00083428\cdot\frac{1}{\text{in}}$$

Cracked Section: Assume Strain in Concrete at the Top $\varepsilon_{cm} := 0.0025$

Strain in Strand

$$\varepsilon_p(c) := -\left(\varepsilon_{ce} + -\varepsilon_{se}\right) + \varepsilon_{cm}\cdot\frac{d_{ps} - c}{c}$$

Stess in Strand

$$f_p(c) := \begin{cases} \left(\varepsilon_p(c)\cdot E_{ps}\right) & \text{if } \varepsilon_p(c) \le \varepsilon_{py} \\ \left[f_{py} + \left(f_{pu} - f_{py}\right)\cdot\frac{\varepsilon_p(c) - \varepsilon_{py}}{\varepsilon_{pu} - \varepsilon_{py}}\right] & \text{if } \varepsilon_{py} < \varepsilon_p(c) < \varepsilon_{pu} \\ f_{pu} & \text{otherwise} \end{cases}$$

Concrete Force

$$F_c(c) := \frac{b\cdot c}{\varepsilon_{cm}}\int_0^{\varepsilon_{cm}} f_c\left(\varepsilon_c\right) d\varepsilon_c$$

Steel Force
assumes steel not yielded

$$F_s(c) := f_p(c)\cdot A_{ps}$$

Solve for Neutral Axis Depth...

$$c := \text{root}\left(F_c(c) - F_s(c), c, 0.05\cdot d_{ps}, 0.6 d_{ps}\right)$$

$$c = 0.715\cdot\text{in}$$

$$\text{Check}_{Voids} := \begin{cases} \text{"Okay"} & \text{if } c \le 1.375\text{in} \\ \text{"Redo Calcs for Voids"} & \text{otherwise} \end{cases} = \text{"Okay"}$$

Compute Moment...

Moment of concrete stresses about the neutral axis

$$M_c := \frac{b\cdot c^2}{\varepsilon_{cm}^2}\int_0^{\varepsilon_{cm}} f_c\left(\varepsilon_c\right)\cdot\varepsilon_c\, d\varepsilon_c$$

Moment of steel stresses about the neutral axis

$$M_s := F_s(c)\cdot\left(d_{ps} - c\right)$$

Moment on section

$$M_6 := M_c + M_s = 133\cdot\text{kip}\cdot\text{ft}$$

Compute Curvature...

Curvature on section

$$\Phi_6 := \frac{\varepsilon_{cm}}{c} = 0.00349639\cdot\frac{1}{\text{in}}$$

Cracked Section: Assume Strain in Concrete at the Top $\varepsilon_{cm} := 0.003$

Strain in Strand

$$\varepsilon_p(c) := -\left(\varepsilon_{ce} + -\varepsilon_{se}\right) + \varepsilon_{cm}\cdot\frac{d_{ps} - c}{c}$$

Stess in Strand

$$f_p(c) := \begin{cases} \left(\varepsilon_p(c)\cdot E_{ps}\right) & \text{if } \varepsilon_p(c) \le \varepsilon_{py} \\ \left[f_{py} + \left(f_{pu} - f_{py}\right)\cdot\frac{\varepsilon_p(c) - \varepsilon_{py}}{\varepsilon_{pu} - \varepsilon_{py}}\right] & \text{if } \varepsilon_{py} < \varepsilon_p(c) < \varepsilon_{pu} \\ f_{pu} & \text{otherwise} \end{cases}$$

Concrete Force

$$F_c(c) := \frac{b\cdot c}{\varepsilon_{cm}}\int_0^{\varepsilon_{cm}} f_c\left(\varepsilon_c\right) d\varepsilon_c$$

Steel Force
assumes steel not yielded

$$F_s(c) := f_p(c)\cdot A_{ps}$$

Solve for Neutral Axis Depth...

$$c := \text{root}\left(F_c(c) - F_s(c), c, 0.05\cdot d_{ps}, 0.6 d_{ps}\right)$$

$$c = 0.7\cdot in$$

$$\text{Check}_{Voids} := \begin{cases} \text{"Okay"} & \text{if } c \le 1.375in \\ \text{"Redo Calcs for Voids"} & \text{otherwise} \end{cases} = \text{"Okay"}$$

Compute Moment...

Moment of concrete stresses about the neutral axis

$$M_c := \frac{b\cdot c^2}{\varepsilon_{cm}^2}\int_0^{\varepsilon_{cm}} f_c\left(\varepsilon_c\right)\cdot\varepsilon_c\, d\varepsilon_c$$

Moment of steel stresses about the neutral axis

$$M_s := F_s(c)\cdot\left(d_{ps} - c\right)$$

Moment on section

$$M_7 := M_c + M_s = 136\cdot kip\cdot ft$$

Compute Curvature...

Curvature on section

$$\Phi_7 := \frac{\varepsilon_{cm}}{c} = 0.0042884\cdot\frac{1}{in}$$

Load versus Displacement

$M_1 = 9.135 \cdot kip \cdot ft$ $M_3 = 88.414 \cdot kip \cdot ft$ $M_5 = 124.303 \cdot kip \cdot ft$ $M_7 = 136.421 \cdot kip \cdot ft$

$M_2 = 92.302 \cdot kip \cdot ft$ $M_4 = 93.747 \cdot kip \cdot ft$ $M_6 = 133.068 \cdot kip \cdot ft$ $M_{cr} = 88.414 \cdot kip \cdot ft$

$$M := \begin{pmatrix} M_0 \\ M_1 \\ M_2 \\ M_3 \\ M_4 \\ M_5 \\ M_6 \\ M_7 \end{pmatrix} = \begin{pmatrix} 0 \\ 9.135 \\ 92.302 \\ 88.414 \\ 93.747 \\ 124.303 \\ 133.068 \\ 136.421 \end{pmatrix} \cdot kip \cdot ft \qquad \Phi := \begin{pmatrix} \Phi_0 \\ \Phi_1 \\ \Phi_2 \\ \Phi_3 \\ \Phi_4 \\ \Phi_5 \\ \Phi_6 \\ \Phi_7 \end{pmatrix} = \begin{pmatrix} -3.468 \times 10^{-5} \\ -2.385 \times 10^{-5} \\ 7.478 \times 10^{-5} \\ 7.016 \times 10^{-5} \\ 1.874 \times 10^{-4} \\ 8.343 \times 10^{-4} \\ 3.496 \times 10^{-3} \\ 4.288 \times 10^{-3} \end{pmatrix} \cdot \frac{1}{in}$$

$$Load := \left(M - M_2\right) \cdot \frac{4}{L} = \begin{pmatrix} -2.03 \\ 0 \\ 18.481 \\ 17.617 \\ 18.803 \\ 25.593 \\ 27.541 \\ 28.286 \end{pmatrix} \cdot kip$$

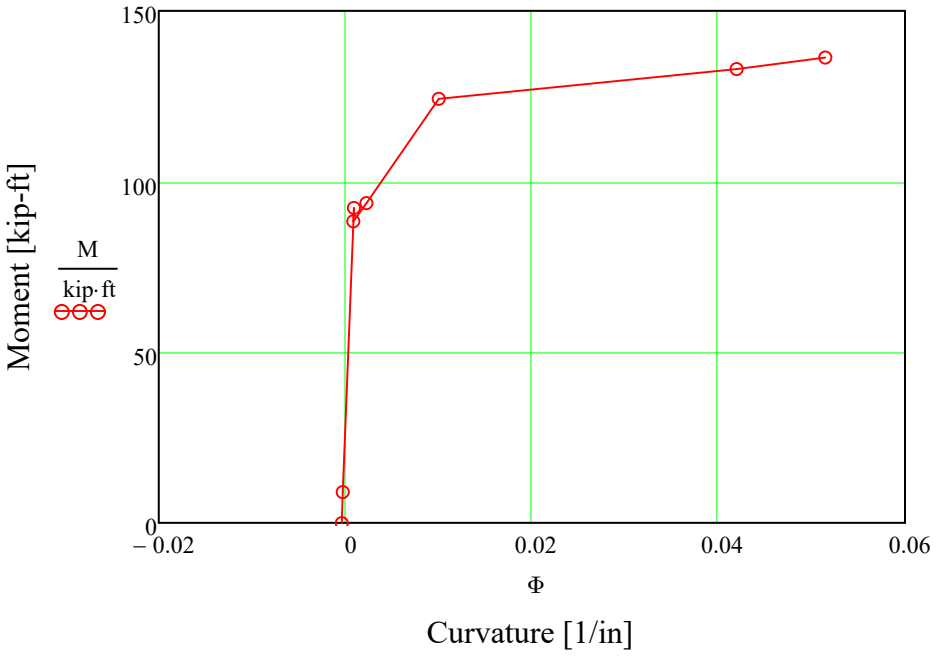

Shear

Maximum Load Expected from Moment Curvature Calculations

$Load_{sup} := 30kip$

$sw := A \cdot Weight \cdot Length = 4.511 \cdot kip$

$R := \frac{sw + Load_{sup}}{2} = 17.256 \cdot kip$

Shear Resistance Diagram

Web Thickness (Summation of web thicknesses at minimum width)

$b_w := 13.438in$

$\lambda := 1$

$V_{c.conc} := 2 \cdot \lambda \cdot \sqrt{f'c \cdot psi} \cdot b_w \cdot d_{ps} = 17.028 \cdot kip$

This creates the points of interest

$ORIGIN \equiv 1$

$i := 1, 2 .. 36$

$$x_i := i \cdot 0.25\,ft$$

$$i = \begin{pmatrix} 1 \\ 2 \\ 3 \\ 4 \\ 5 \\ 6 \\ 7 \\ 8 \\ 9 \\ 10 \\ 11 \\ 12 \\ 13 \\ 14 \\ 15 \\ 16 \\ 17 \\ 18 \\ 19 \\ 20 \\ 21 \\ 22 \\ 23 \\ 24 \\ 25 \\ 26 \\ 27 \\ 28 \\ 29 \\ 30 \\ 31 \\ 32 \\ 33 \\ 34 \\ 35 \\ 36 \end{pmatrix} \qquad x_i = \begin{pmatrix} 0.3 \\ 0.5 \\ 0.8 \\ 1.0 \\ 1.3 \\ 1.5 \\ 1.8 \\ 2.0 \\ 2.3 \\ 2.5 \\ 2.8 \\ 3.0 \\ 3.3 \\ 3.5 \\ 3.8 \\ 4.0 \\ 4.3 \\ 4.5 \\ 4.8 \\ 5.0 \\ 5.3 \\ 5.5 \\ 5.8 \\ 6.0 \\ 6.3 \\ 6.5 \\ 6.8 \\ 7.0 \\ 7.3 \\ 7.5 \\ 7.8 \\ 8.0 \\ 8.3 \\ 8.5 \\ 8.8 \\ 9.0 \end{pmatrix} ft$$

Shear along length of member

$$V_u := R - \frac{sw}{L}\cdot x = \cdot kip$$

	1
1	17.193
2	17.13
3	17.068
4	17.005
5	16.942
6	16.88
7	16.817
8	16.754
9	16.692
10	16.629
11	16.566
12	16.504
13	16.441
14	16.378
15	16.316
16	...

Moment along length of member

$$M_u := \overrightarrow{\left[\frac{\frac{sw}{Length}\cdot x}{2}\cdot(L - x)\right]} + \frac{Load_{sup}\cdot x}{2} = \cdot kip\cdot ft$$

	1
1	4.25
2	8.487
3	12.709
4	16.917
5	21.111
6	25.291
7	29.457
8	33.609
9	37.747
10	41.87
11	45.98
12	50.075
13	54.156
14	58.223
15	62.277
16	...

Flexure Shear Strength

Shear Force at Section due to Unfactored Load

$$V_d := \frac{Weight \cdot A \cdot Length}{2} - Weight \cdot A \cdot x = \begin{array}{|c|c|}\hline & 1 \\ \hline 1 & 2.199 \\ 2 & 2.143 \\ 3 & 2.086 \\ 4 & 2.03 \\ 5 & 1.974 \\ 6 & 1.917 \\ 7 & 1.861 \\ 8 & 1.804 \\ 9 & 1.748 \\ 10 & 1.692 \\ 11 & 1.635 \\ 12 & 1.579 \\ 13 & 1.523 \\ 14 & 1.466 \\ 15 & 1.41 \\ 16 & ... \\ \hline \end{array} \cdot kip$$

Factored Shear Force at Section due to Externally Applied Loads Occuring Simultaneously with Mmax

$$V_i := V_u - V_d = \begin{array}{|c|c|}\hline & 1 \\ \hline 1 & 14.994 \\ 2 & 14.987 \\ 3 & 14.981 \\ 4 & 14.975 \\ 5 & 14.969 \\ 6 & 14.962 \\ 7 & 14.956 \\ 8 & 14.95 \\ 9 & 14.944 \\ 10 & 14.937 \\ 11 & 14.931 \\ 12 & 14.925 \\ 13 & 14.919 \\ 14 & 14.912 \\ 15 & 14.906 \\ 16 & ... \\ \hline \end{array} \cdot kip$$

Stress due to Unfactored Dead Load @ Extreme Fiber of Section where Tensile Stress is caused by Externally Applied Loads

$$f_d := \frac{-P_e}{A} - \frac{P_e \cdot e}{S_b} + \frac{M_{sw}}{S_b} = -1.414 \times 10^3 \cdot psi$$

Moment Causing Flexural Cracking at Section due to Externally Applied Loads

$$M_{cre} := M_{cr} = 88.414 \cdot kip \cdot ft$$

Moment due to Self Weight

$$M_d := \left[\frac{\frac{sw}{Length} \cdot x}{2} \cdot (L - x)\right] \rightarrow =$$

	1
1	0.5
2	0.987
3	1.459
4	1.917
5	2.361
6	2.791
7	3.207
8	3.609
9	3.997
10	4.37
11	4.73
12	5.075
13	5.406
14	5.723
15	6.027
16	...

$\cdot kip \cdot ft$

Maximum Factored Moment at Section due to Externally Applied Loads

$$M_{max} := M_u - M_d =$$

	1
1	3.75
2	7.5
3	11.25
4	15
5	18.75
6	22.5
7	26.25
8	30
9	33.75
10	37.5
11	41.25
12	45
13	48.75
14	52.5
15	56.25
16	...

$\cdot kip \cdot ft$

Operator to Choose the Max Value from Two Matrices

$$Max(V1, V2) := \left| \begin{array}{l} \text{for } i \in ORIGIN..\, last(V1) \\ \quad R_i \leftarrow \max\left(V1_i, V2_i\right) \\ \text{return } R \end{array} \right.$$

$$V_{ci} := Max\left(0.6 \cdot \lambda \cdot \sqrt{f'c \cdot psi} \cdot b_w \cdot d_{ps} + V_d + \frac{V_i \cdot M_{cre}}{M_{max}}, 1.7 \cdot \lambda \cdot \sqrt{f'c \cdot psi} \cdot b_w \cdot d_{ps} \cdot \frac{x}{x}\right) =$$

	1
1	360.814
2	183.93
3	124.932
4	95.404
5	77.665
6	65.82
7	57.343
8	50.972
9	46.004
10	42.018
11	38.746
12	36.011
13	33.687
14	31.688
15	29.947
16	...

$\cdot kip$

Web Shear Strength

Compressive Strength after Prestress Losses

$$f_{pc} := \sigma_{bot} - y_{g.tr.top} \cdot \frac{\sigma_{top} - \sigma_{bot}}{h} = 2.524 \cdot ksi$$

Strand Angle

$$\alpha := 0$$

Vertical Component of Effective Prestress Force

$$V_p := Load_{sup} \cdot \sin(\alpha) = 0 \cdot kip$$

$$V_{cw} := \left(3.5 \cdot \lambda \cdot \sqrt{f'c \cdot psi} + 0.3 \cdot f_{pc}\right) \cdot b_w \cdot d_{ps} + V_p = 90.859 \cdot kip$$

Predicted Failure Mode

Concrete Shear Strength

$$V_c := 2 \cdot \lambda \cdot \sqrt{f'c \cdot psi} \cdot b_w \cdot d_{ps} = 17.028 \cdot kip$$

Operator to Choose the Min Value from Two Matrices

$$\begin{aligned} &Min(V1, V2) := \\ &\quad \text{for } i \in ORIGIN .. last(V1) \\ &\quad\quad R_i \leftarrow \min\left(V1_i, V2_i\right) \\ &\quad \text{return } R \end{aligned}$$

Nominal Shear Strength (Considers Web Shear, Flexure Shear, and Concrete Shear)

$$V_n := \mathrm{Max}\left(\mathrm{Min}\left(V_{ci}, \begin{pmatrix} V_{cw} \\ V_{cw} \end{pmatrix}\right), \begin{pmatrix} V_c \\ V_c \end{pmatrix}\right) = \begin{array}{|c|r|} \hline & 1 \\ \hline 1 & 90.859 \\ 2 & 90.859 \\ 3 & 90.859 \\ 4 & 90.859 \\ 5 & 77.665 \\ 6 & 65.82 \\ 7 & 57.343 \\ 8 & 50.972 \\ 9 & 46.004 \\ 10 & 42.018 \\ 11 & 38.746 \\ 12 & 36.011 \\ 13 & 33.687 \\ 14 & 31.688 \\ 15 & 29.947 \\ 16 & \ldots \\ \hline \end{array} \cdot \mathrm{kip}$$

$$\left[\left[\begin{pmatrix} V_{cw} \\ V_{cw} \\ V_{cw} \\ V_{cw} \end{pmatrix}\right]\left[\begin{pmatrix} V_{c} \\ V_{c} \\ V_{c} \\ V_{c} \end{pmatrix}\right]\right]$$

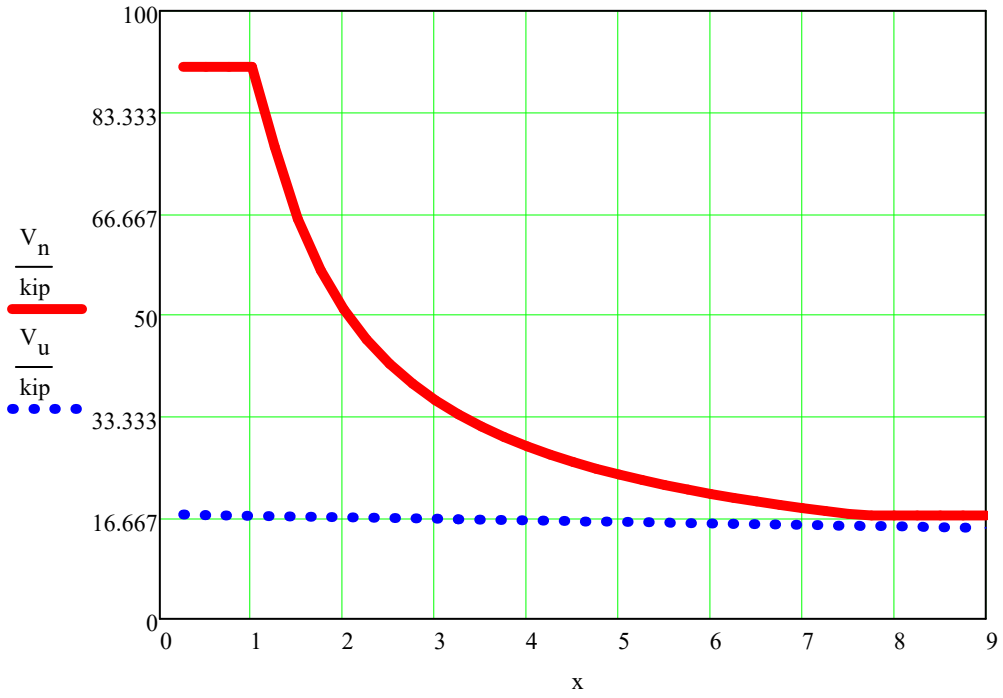
100
83.333
66.667
50
33.333
16.667
0
0
1
2
3
4
5
6
7
8
9
x
Vn / kip
Vu / kip

Punching Shear with Concentrated Load Centered Over Void

Distance from plate edge to void edge divided by 2

$d := 0.375in$

Plate Width

$c := 4in$

$t_{flange} := 1.375in$

Perimeter

$b_o := 4 \cdot (c + 0.75in) = 19 \cdot in$

$\alpha_s := 40$

$$v_c := \min\left[3.5 \cdot \lambda \cdot \sqrt{f'c \cdot psi} + 0.3 \cdot \frac{f_{pc}}{2} + \frac{V_p}{b_o \cdot d}, \left(1.5 + \frac{\alpha_s \cdot d}{b_o}\right) \cdot \lambda \cdot \sqrt{f'c \cdot psi} + 0.3 \frac{f_{pc}}{2} + \frac{V_p}{b_o \cdot d}\right] = 620\,psi$$

Vertical Distance from Top to Void at Halfway Distance from Plate to Edge of Void

$vert := 2in + \frac{5}{16}in$

$V_c := v_c \cdot b_o \cdot vert = 27.3 \cdot kip$

ACI Nominal Moment

$$\frac{f_{py}}{f_{pu}} = 0.9$$

ACI 318-14 Table 20.3.2.3.1

$$\gamma_p := 0.28$$

$$\rho_p := \frac{A_{ps}}{b \cdot d_{ps}} = 3.685 \times 10^{-3}$$

$$f_{ps} := f_{pu} \cdot \left(1 - \frac{\gamma_p \cdot \rho_p \cdot f_{pu}}{\beta_1 \cdot f'_c} \right) = 259.622 \cdot ksi$$

$$a := \frac{A_{ps} \cdot f_{ps}}{.85 f'_c \cdot b} = 0.606 \cdot in$$

$$c := \frac{a}{\beta_1} = 0.932 \cdot in$$

$$M_n := A_{ps} \cdot f_{ps} \cdot \left(d_{ps} - \frac{a}{2} \right) = 130.8 \cdot kip \cdot ft$$

ACI Moment at Rupture

$$f_{rup} := \frac{43.505 kip}{0.1516 in^2} = 286.972 \cdot ksi$$

$$a := \frac{A_{ps} \cdot f_{rup}}{.85 f'_c \cdot b} = 0.669 \cdot in$$

$$c := \frac{a}{\beta_1} = 1.030 \cdot in$$

$$M_{rup} := A_{ps} \cdot f_{rup} \cdot \left(d_{ps} - \frac{a}{2} \right) = 143.8 \cdot kip \cdot ft$$

Deflection

Bilinear Method: Cracking

$$\Delta_{Bilinear.cr} := \frac{M_{cr}\cdot L^2}{12\cdot E_c\cdot I_{g.tr}} = 0.408\cdot in$$

Bilinear Method: Nominal

$$P_n := \frac{4\cdot M_n}{L} = 29.067\cdot kip$$

$$P_{cr} := \frac{4M_{cr}}{L} = 19.647\cdot kip$$

$$\rho := \frac{A_{ps}}{A - b\cdot\left(h - d_{ps}\right)} = 8.804\times 10^{-3}$$

$$k := \sqrt{2\cdot n\cdot\rho + (n\cdot\rho)^2} - n\cdot\rho = 0.25$$

$$I_{cr} := \frac{1}{3}\cdot b\cdot\left(k\cdot d_{ps}\right)^3 + n\cdot A_{ps}\cdot\left(d_{ps} - k\cdot d_{ps}\right)^2 = 156.275\cdot in^4$$

$$\Delta_{Bilinear.nom} := \frac{P_{cr}\cdot L^3}{48\cdot E_c\cdot I_{g.tr}} + \frac{\left(P_n - P_{cr}\right)\cdot L^3}{48\cdot E_c\cdot I_{cr}} = 2.51\cdot in$$

Bilinear Method: Rupture

$$P_n := \frac{4\cdot M_{rup}}{L} = 31.95\cdot kip$$

$$P_{cr} := \frac{4M_{cr}}{L} = 19.647\cdot kip$$

$$\rho := \frac{A_{ps}}{A - b\cdot\left(h - d_{ps}\right)} = 8.804\times 10^{-3}$$

$$k := \sqrt{2\cdot n\cdot\rho + (n\cdot\rho)^2} - n\cdot\rho = 0.25$$

$$I_{cr} := \frac{1}{3}\cdot b\cdot\left(k\cdot d_{ps}\right)^3 + n\cdot A_{ps}\cdot\left(d_{ps} - k\cdot d_{ps}\right)^2 = 156.275\cdot in^4$$

$$\Delta_{Bilinear.rup} := \frac{P_{cr}\cdot L^3}{48\cdot E_c\cdot I_{g.tr}} + \frac{\left(P_n - P_{cr}\right)\cdot L^3}{48\cdot E_c\cdot I_{cr}} = 3.154\cdot in$$

Ie* Method: Cracking

$$\Delta_{Ie*.cr} := \frac{5\cdot M_2\cdot L^2}{48\cdot E_c\cdot I_{g.tr}} + \frac{\left(M_{cr} - M_2\right)\cdot L^2}{12\cdot E_c\cdot I_{g.tr}} = 0.42\cdot in$$

Ie* Method: Nominal

$$I_{e*.nom} := \frac{I_{cr}}{1 - \frac{M_{cr}}{M_n}\left(1 - \frac{I_{cr}}{I_{g.tr}}\right)} = 403.915\cdot in^4$$

$$\Delta_{Ie*.nom} := \frac{5\cdot M_2\cdot L^2}{48\cdot E_c\cdot I_{e*.nom}} + \frac{\left(M_n - M_2\right)\cdot L^2}{12\cdot E_c\cdot I_{e*.nom}} = 2.55\cdot in$$

Ie* Method: Rupture

$$I_{e*.rup} := \frac{I_{cr}}{1 - \frac{M_{cr}}{M_{rup}}\left(1 - \frac{I_{cr}}{I_{g.tr}}\right)} = 353.396\cdot in^4$$

$$\Delta_{Ie*.rup} := \frac{5\cdot M_2\cdot L^2}{48\cdot E_c\cdot I_{e*.rup}} + \frac{\left(M_{rup} - M_2\right)\cdot L^2}{12\cdot E_c\cdot I_{e*.rup}} = 3.20\cdot in$$

Summary

$\Delta_{Ie*.cr} = 0.418\cdot in$ $\Delta_{Bilinear.cr} = 0.408\cdot in$

$\Delta_{Ie*.nom} = 2.554\cdot in$ $\Delta_{Bilinear.nom} = 2.51\cdot in$

$\Delta_{Ie*.rup} = 3.204\cdot in$ $\Delta_{Bilinear.rup} = 3.154\cdot in$

Appendix B: Drawings

Appendix B contains drawings of each of the individual test frame members, as well as the frame configuration. These were produced by measuring the members in the lab and recreating them in AutoCAD. Appendix B also contains the crack patterns and strand slip for each of the test specimens. The cross-sectional area and length of the test specimen created a template for each test. Once cracking and strand slip were observed and recorded in the lab, they were documented in the AutoCAD template.

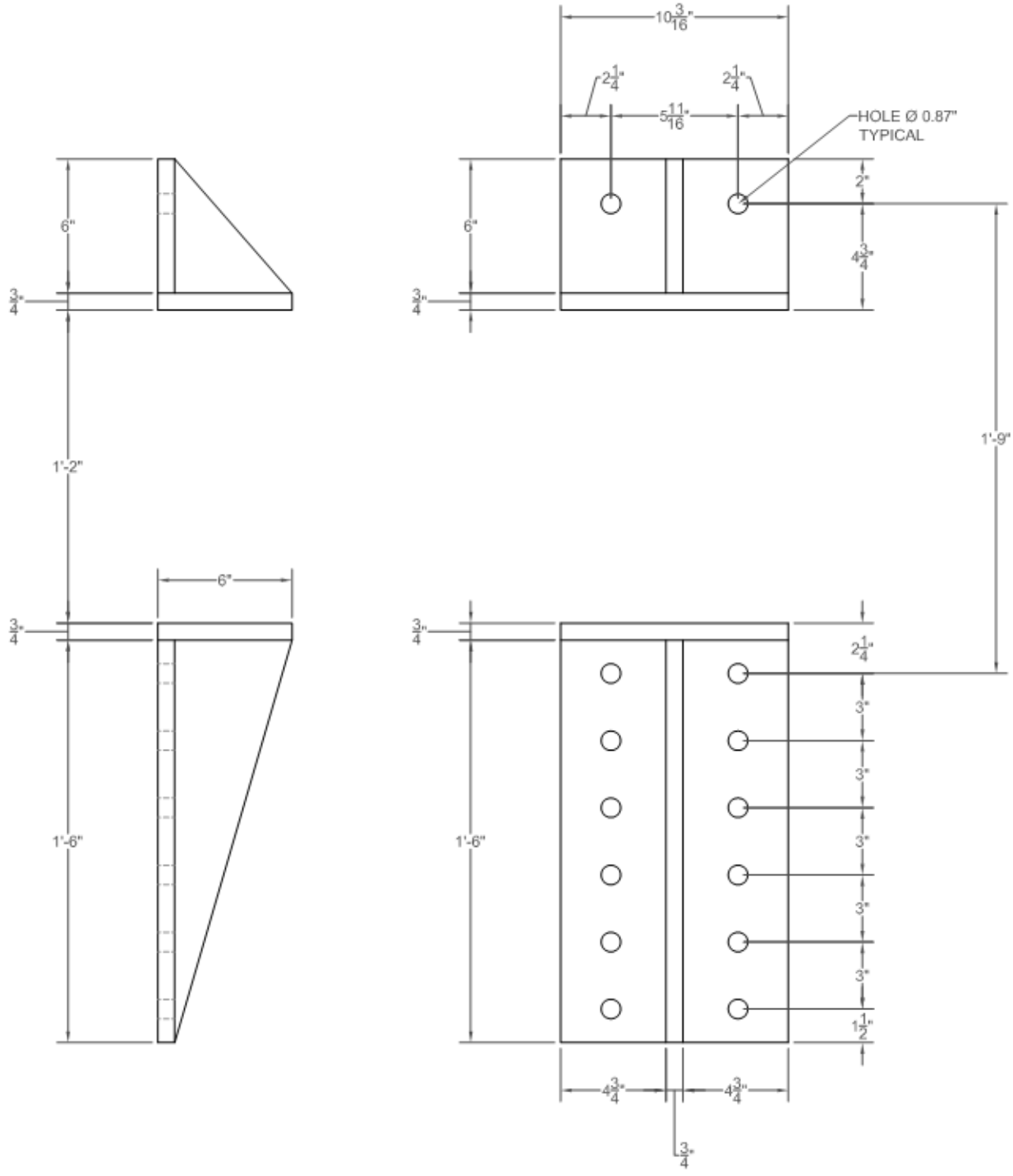

Figure B- 1. Test frame brackets.

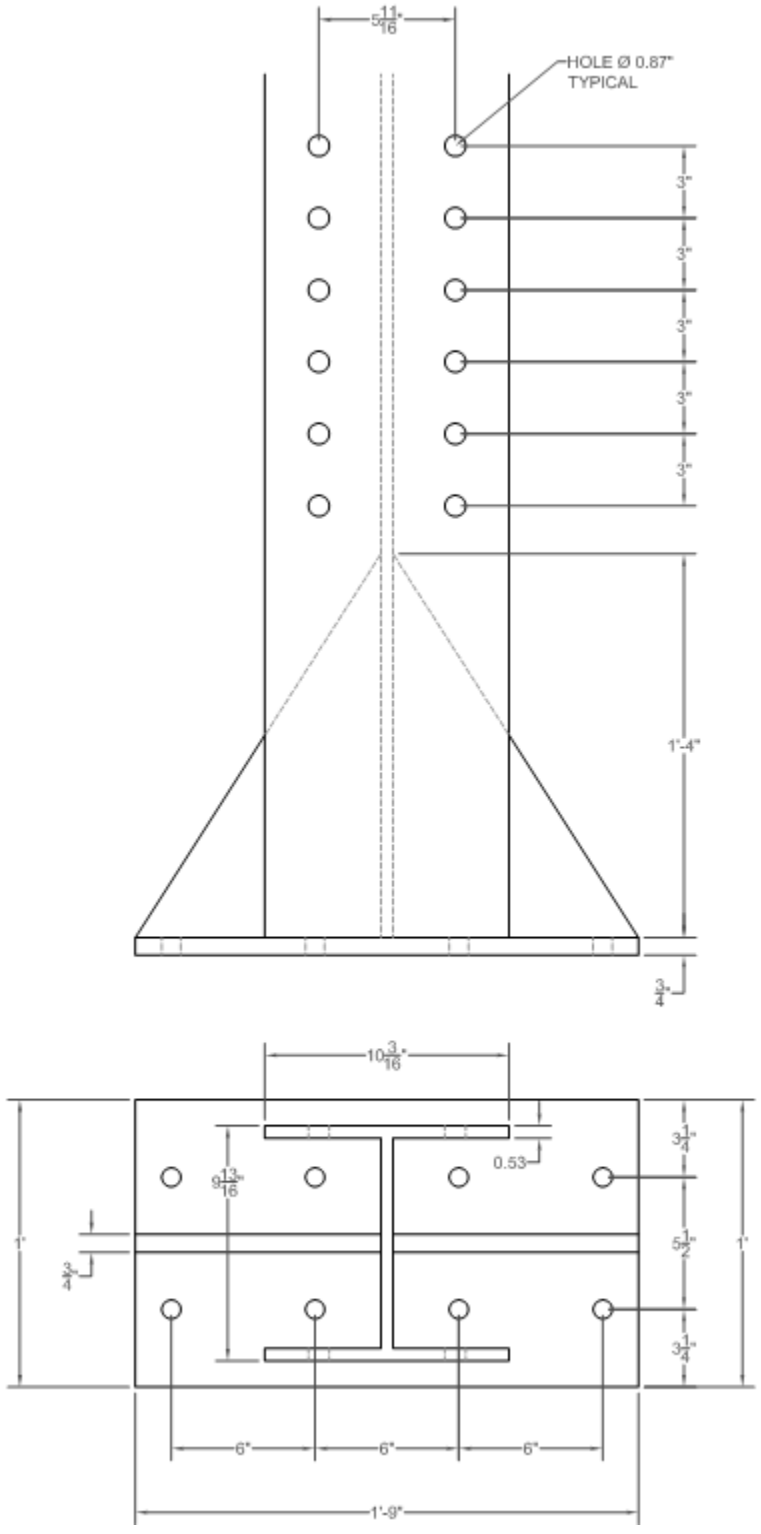

Figure B- 2. Test frame columns.

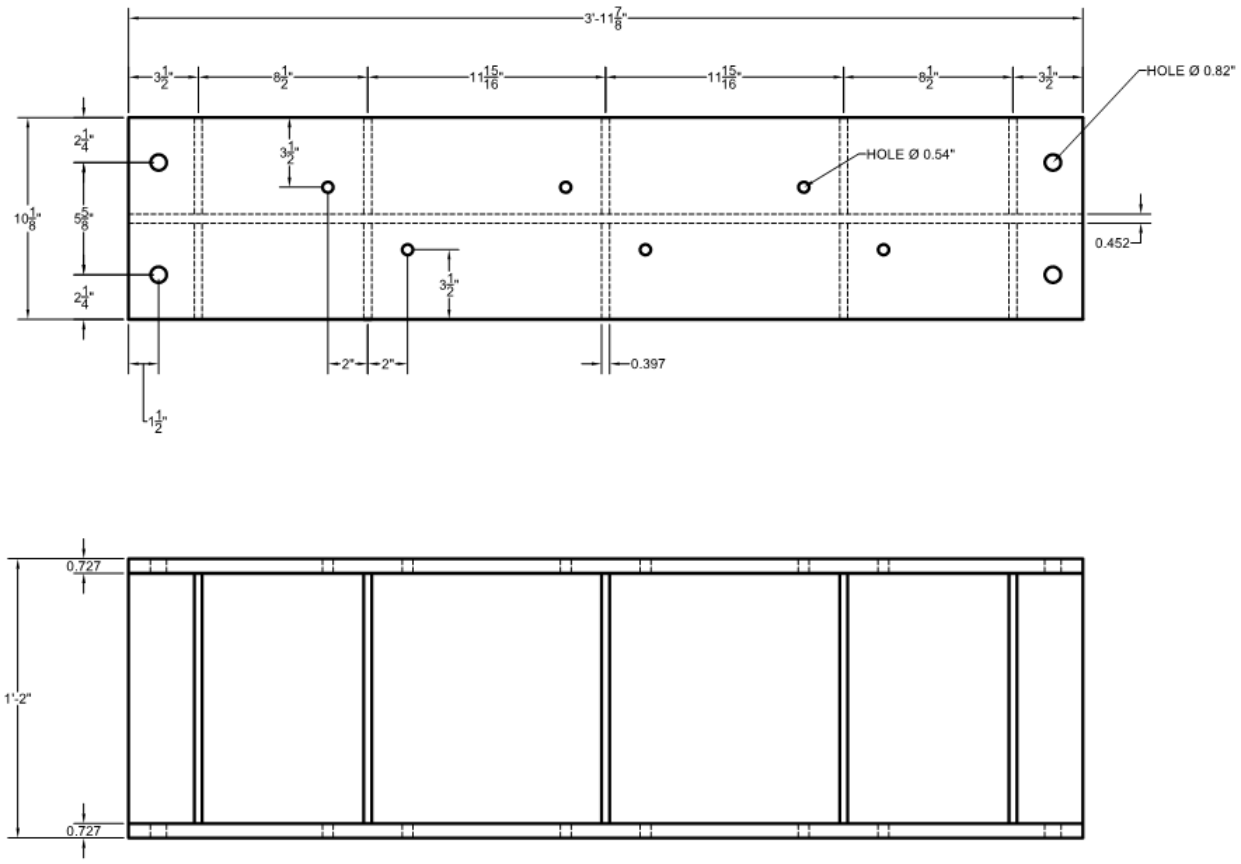

Figure B- 3. Test frame beam for Center tests.

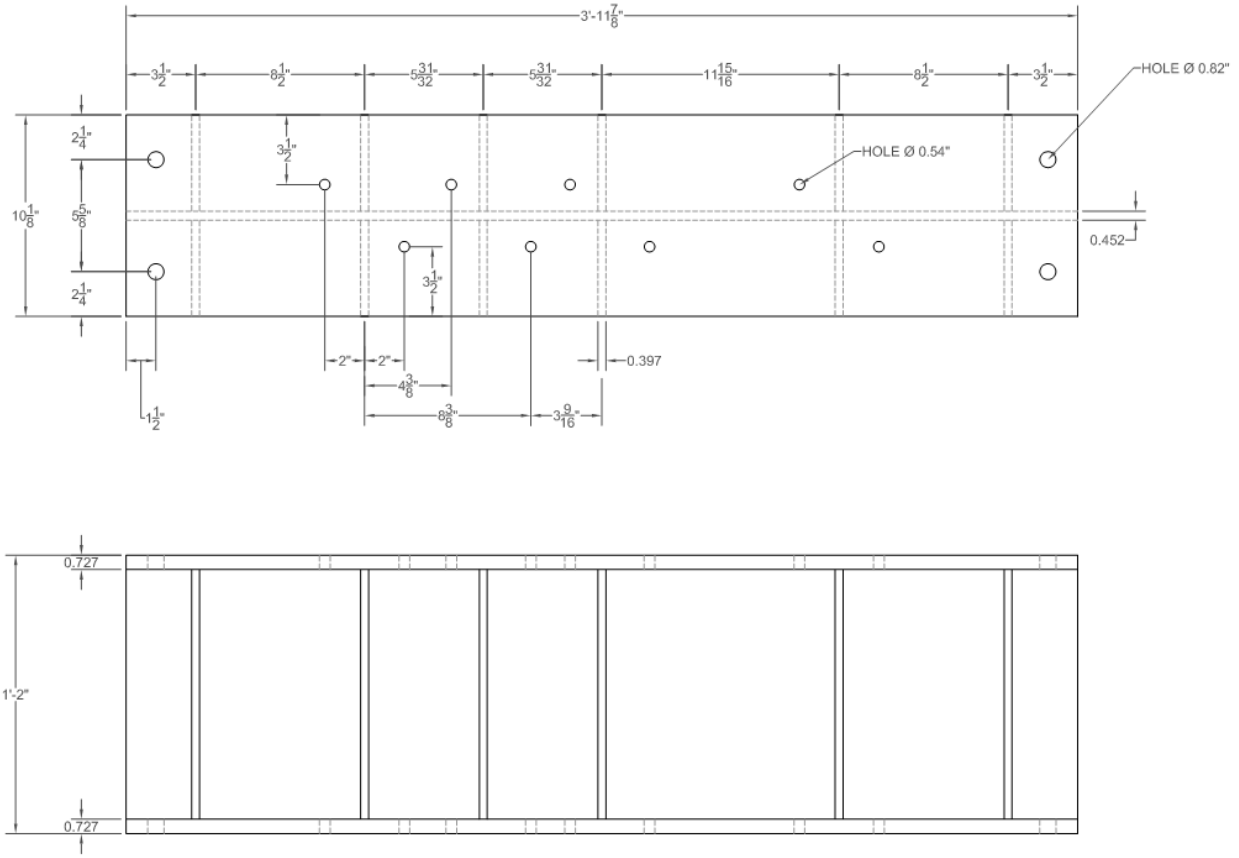

Figure B- 4. Test frame beam for Offset tests.

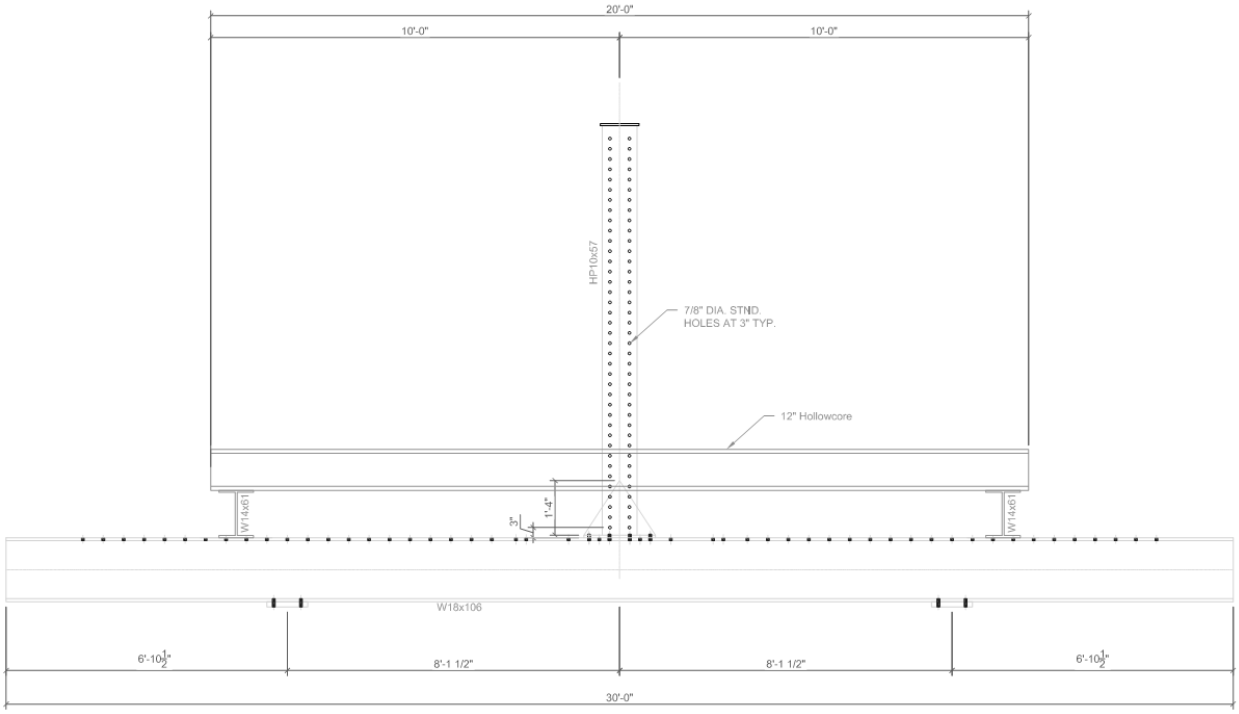

Figure B- 5. Test frame configuration.

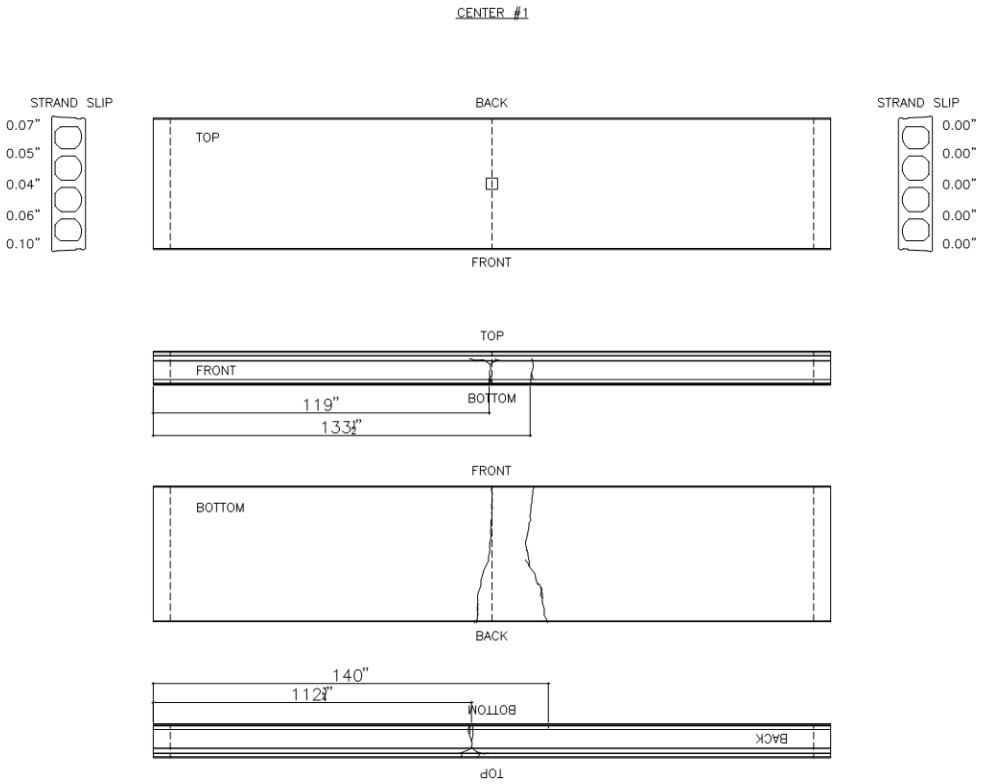

Figure B- 6. Center #1 crack patterns and strand slip.

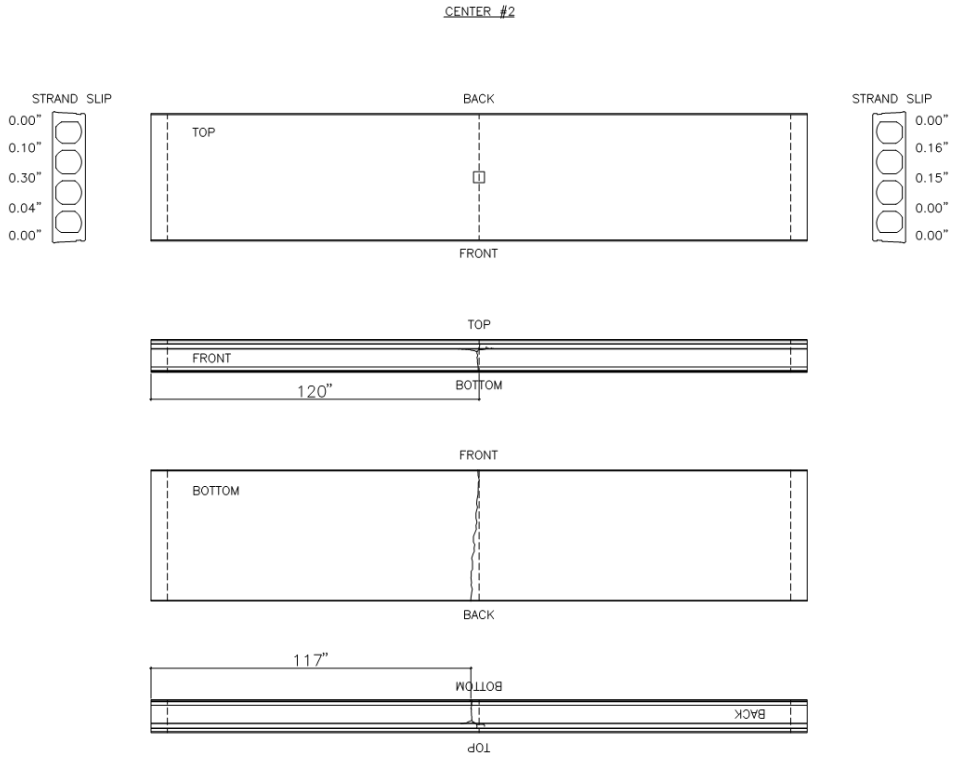

Figure B- 7. Center #2 crack patterns and strand slip.

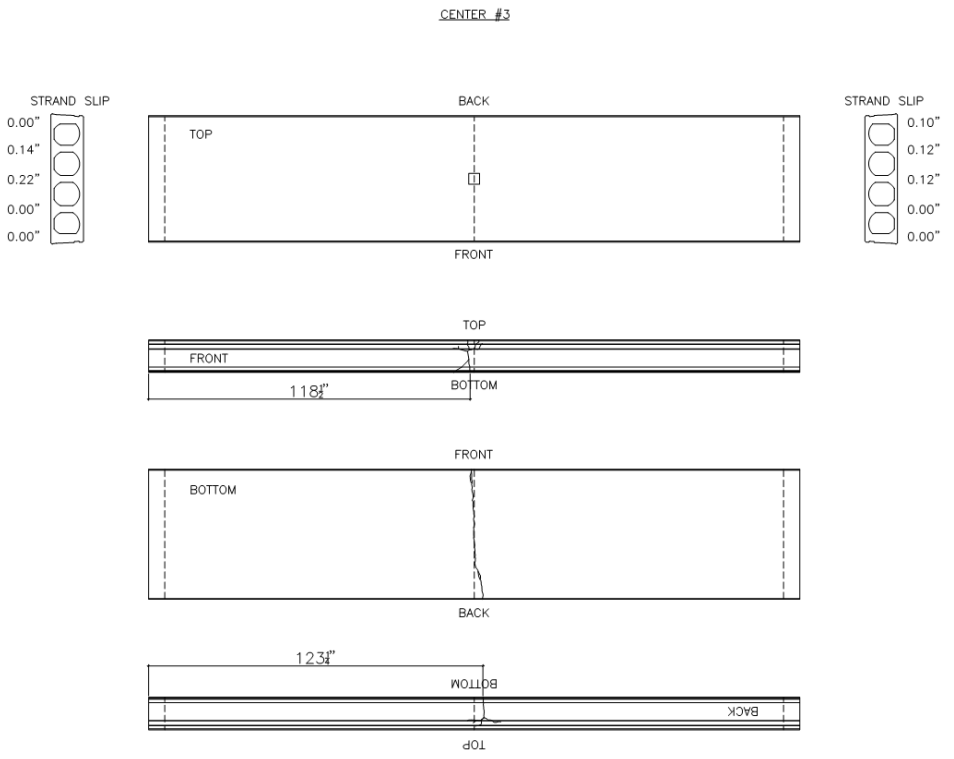

Figure B- 8. Center #3 crack patterns and strand slip.

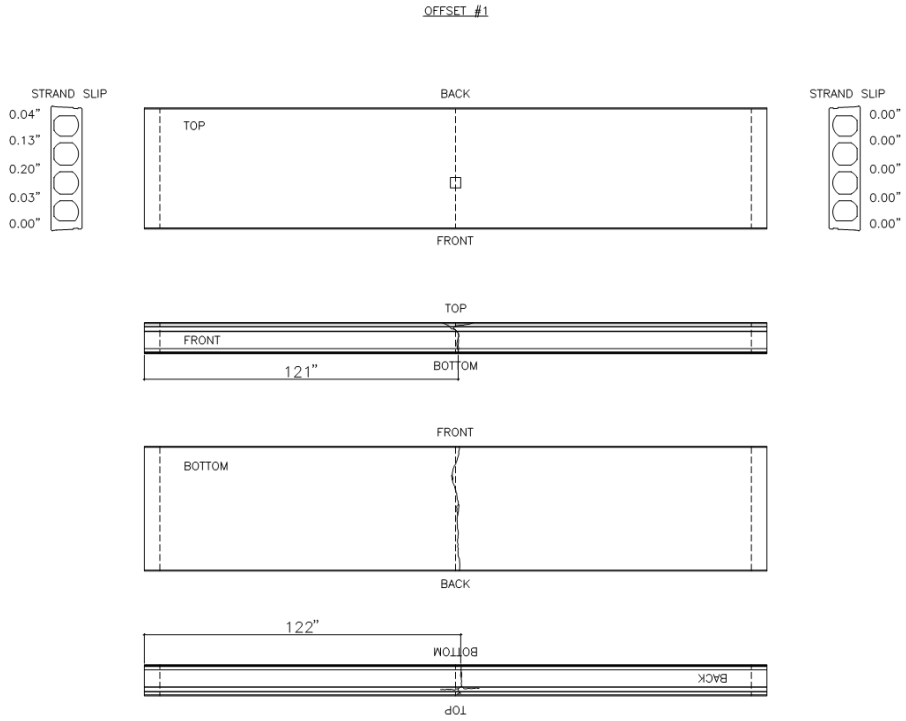

Figure B- 9. Offset #1 crack patterns and strand slip.

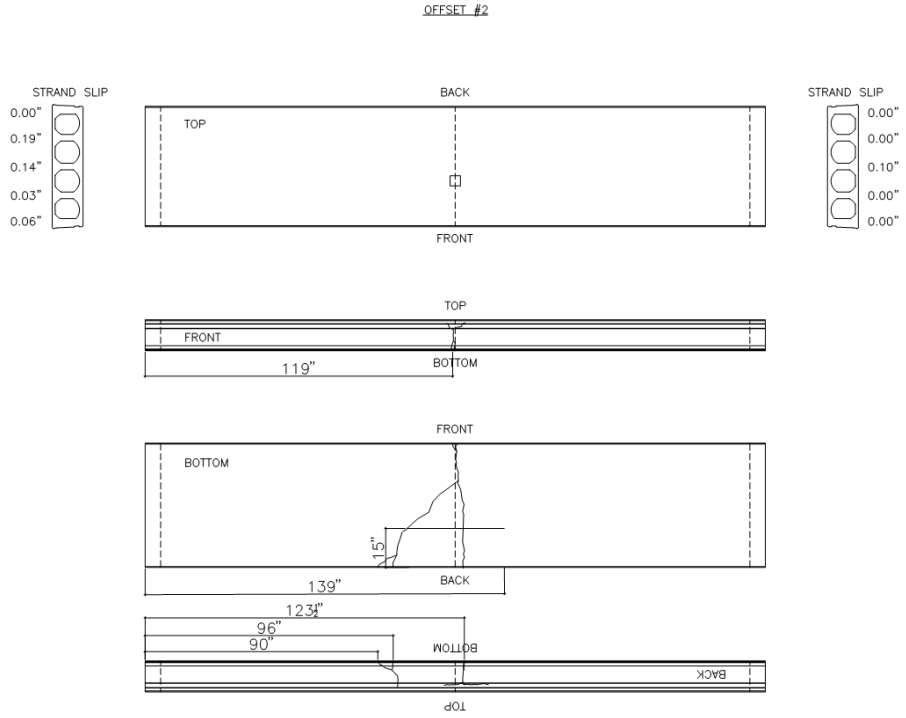

Figure B- 10. Offset #2 crack patterns and strand slip.

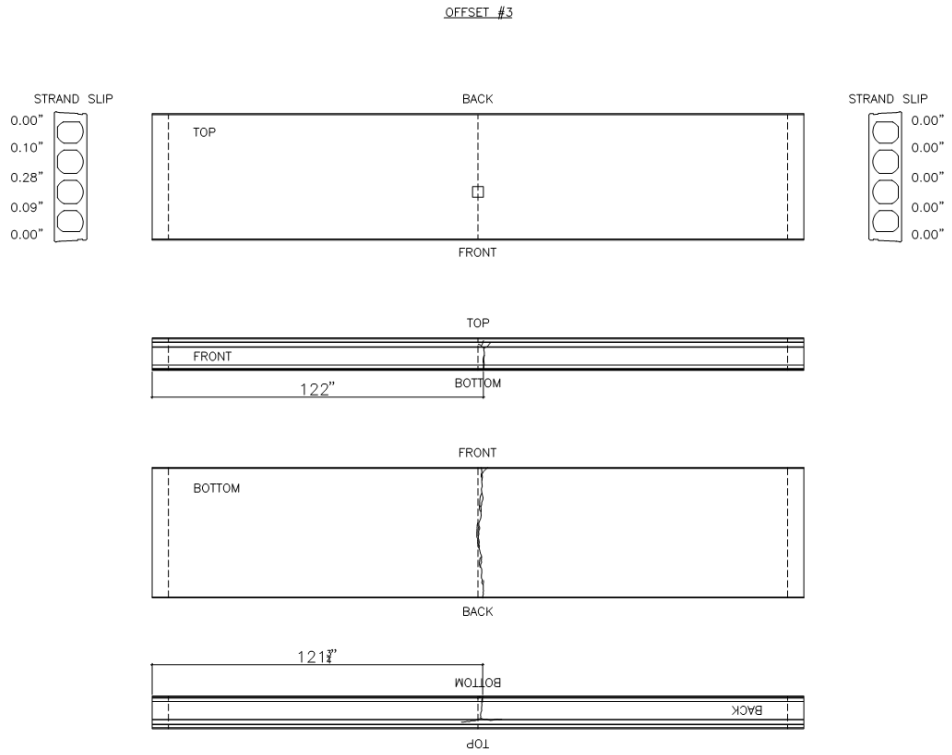

Figure B- 11. Offset #3 crack patterns and strand slip.

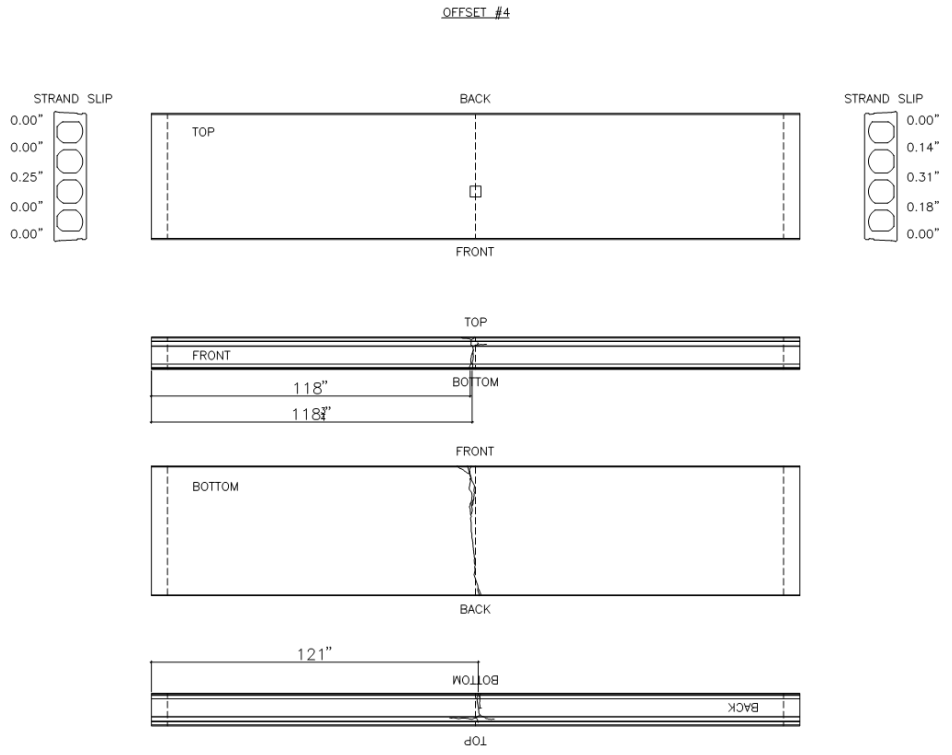

Figure B- 12. Offset #4 crack patterns and strand slip.

Appendix C: Graphs

Appendix C contains load versus displacement graphs for the center and offset tests. For the center tests, the graphs are broken into parts to more easily see each of the test's behavior. There are graphs for part 1, part 2, parts 1 and 2 for all of the tests, and parts 1 and 2 for the individual tests.

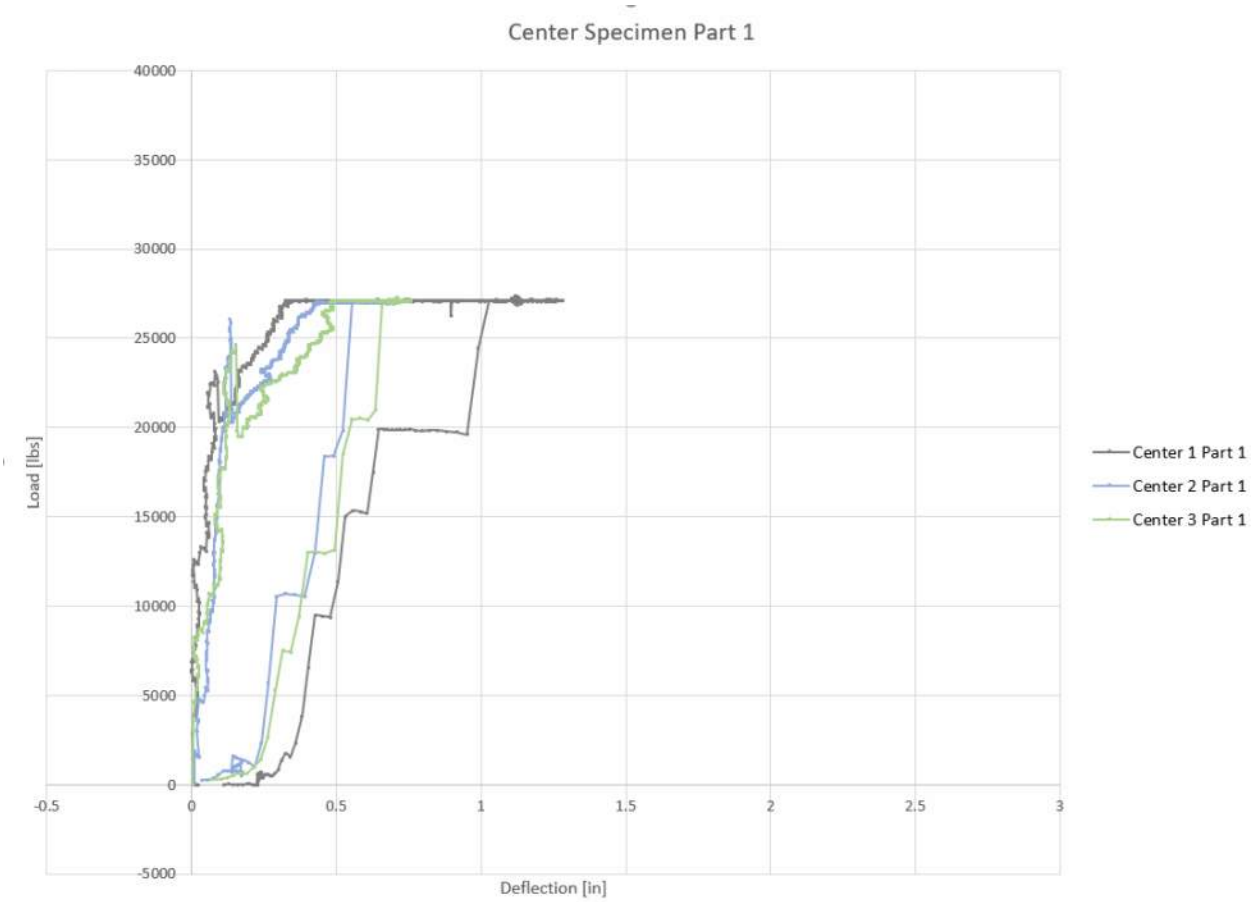

Figure C- 1. Load versus displacement: Center specimens part 1.

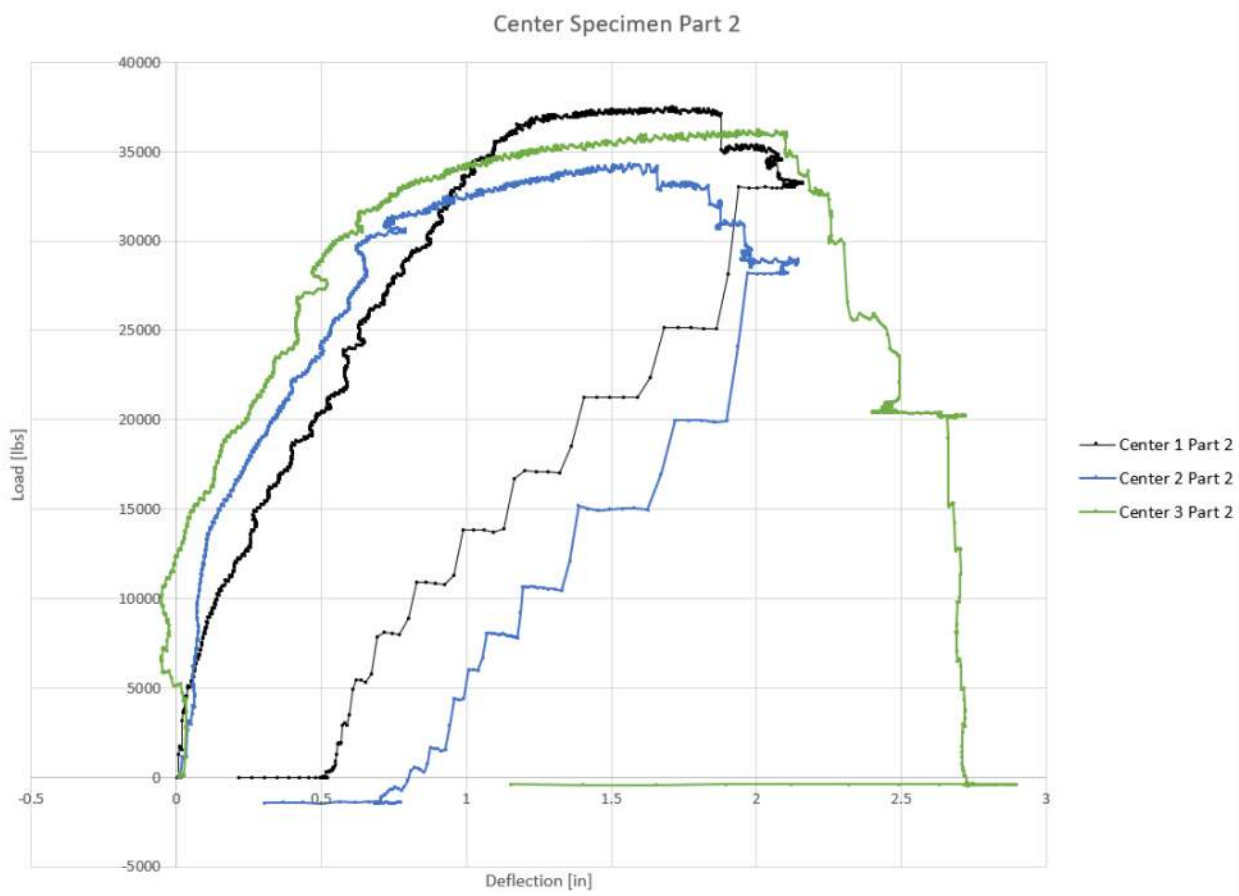

Figure C- 2. Load versus displacement: Center specimens part 2.

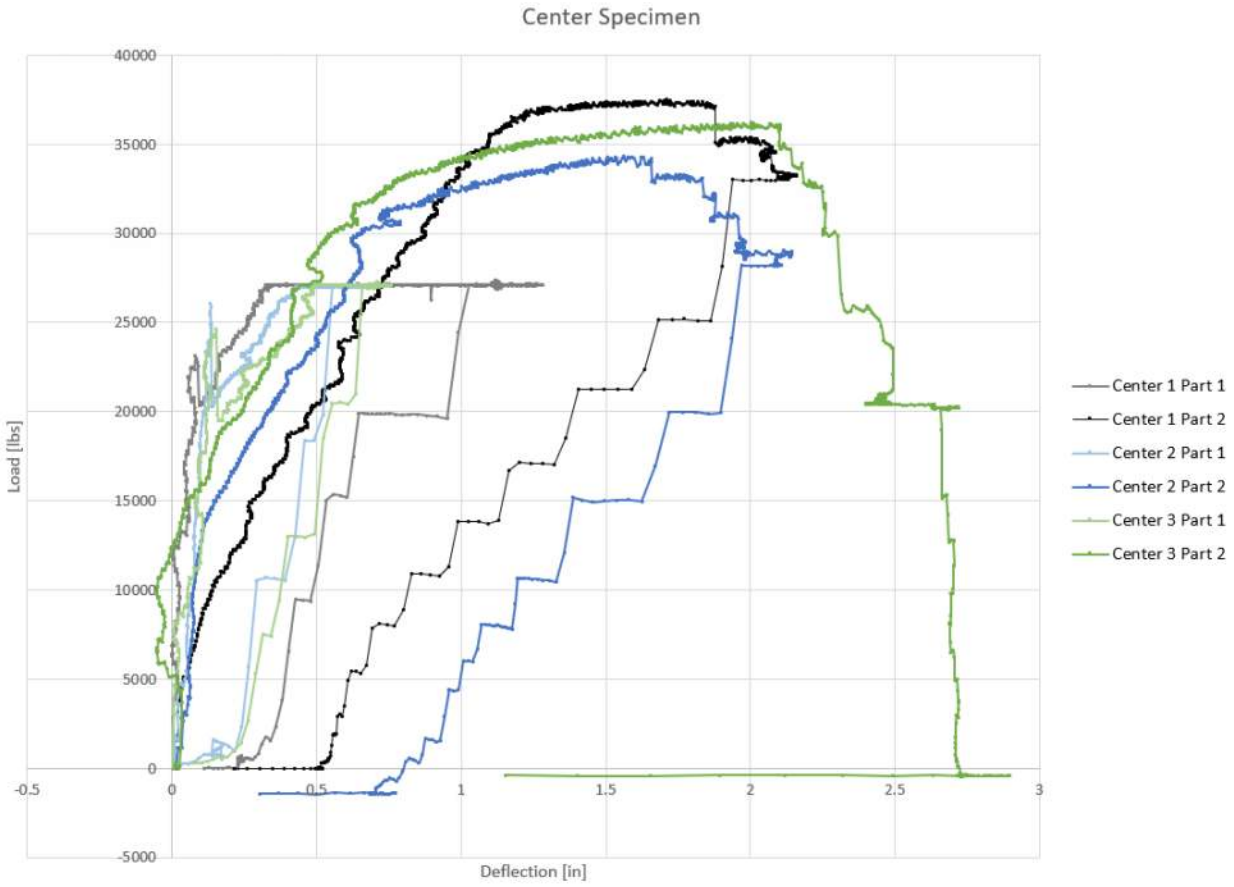

Figure C- 3. Load versus displacement: Center specimen.

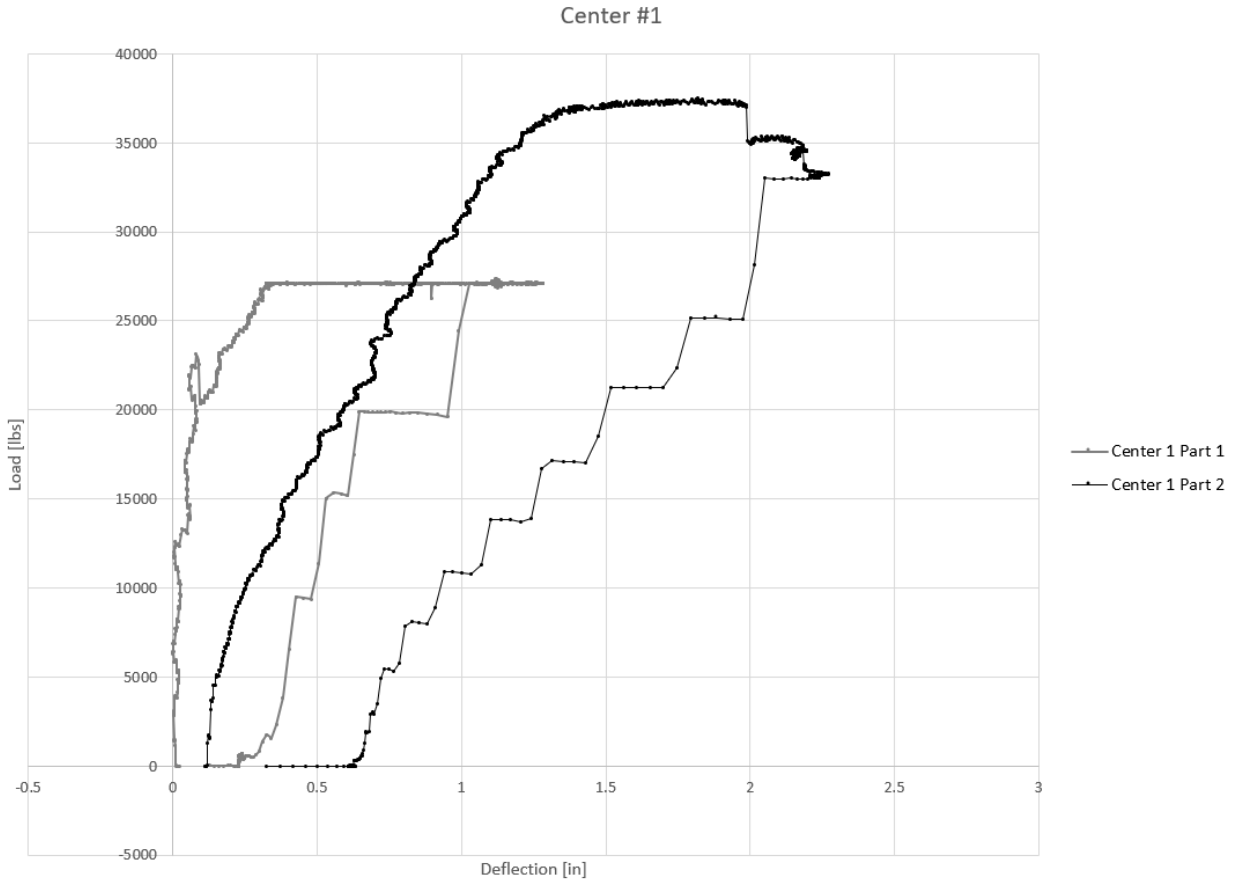

Figure C- 4. Load versus displacement: Center #1.

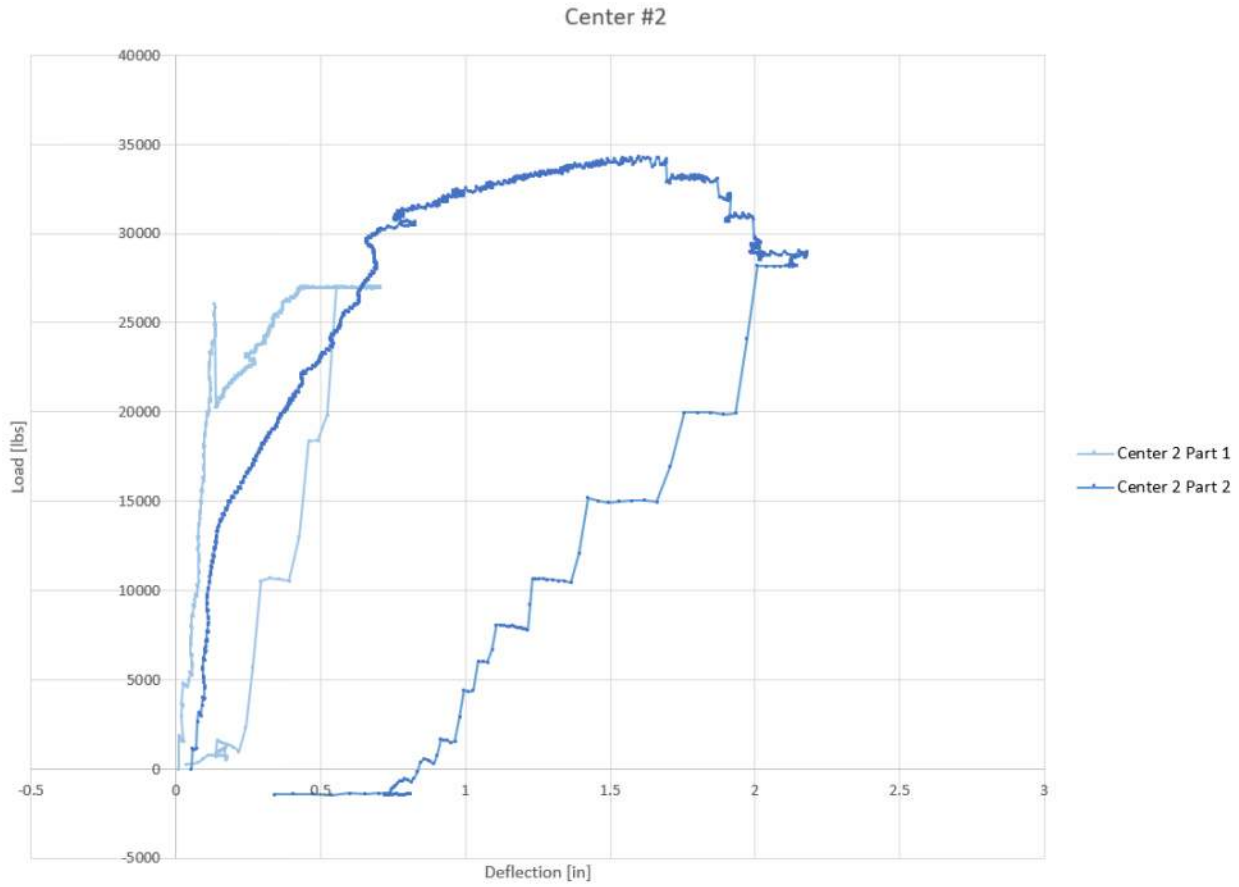

Figure C- 5. Load versus displacement: Center #2.

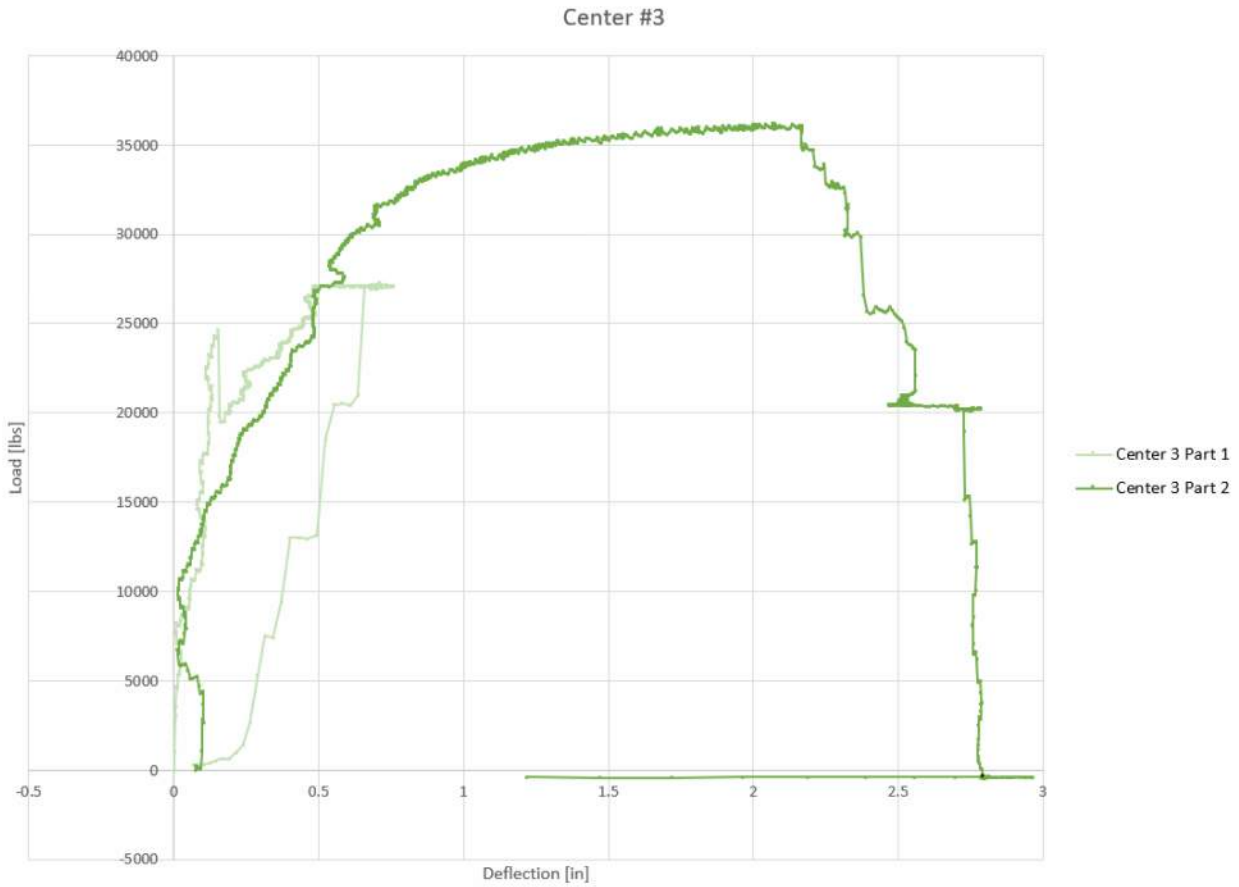

Figure C- 6. Load versus displacement: Center #3.

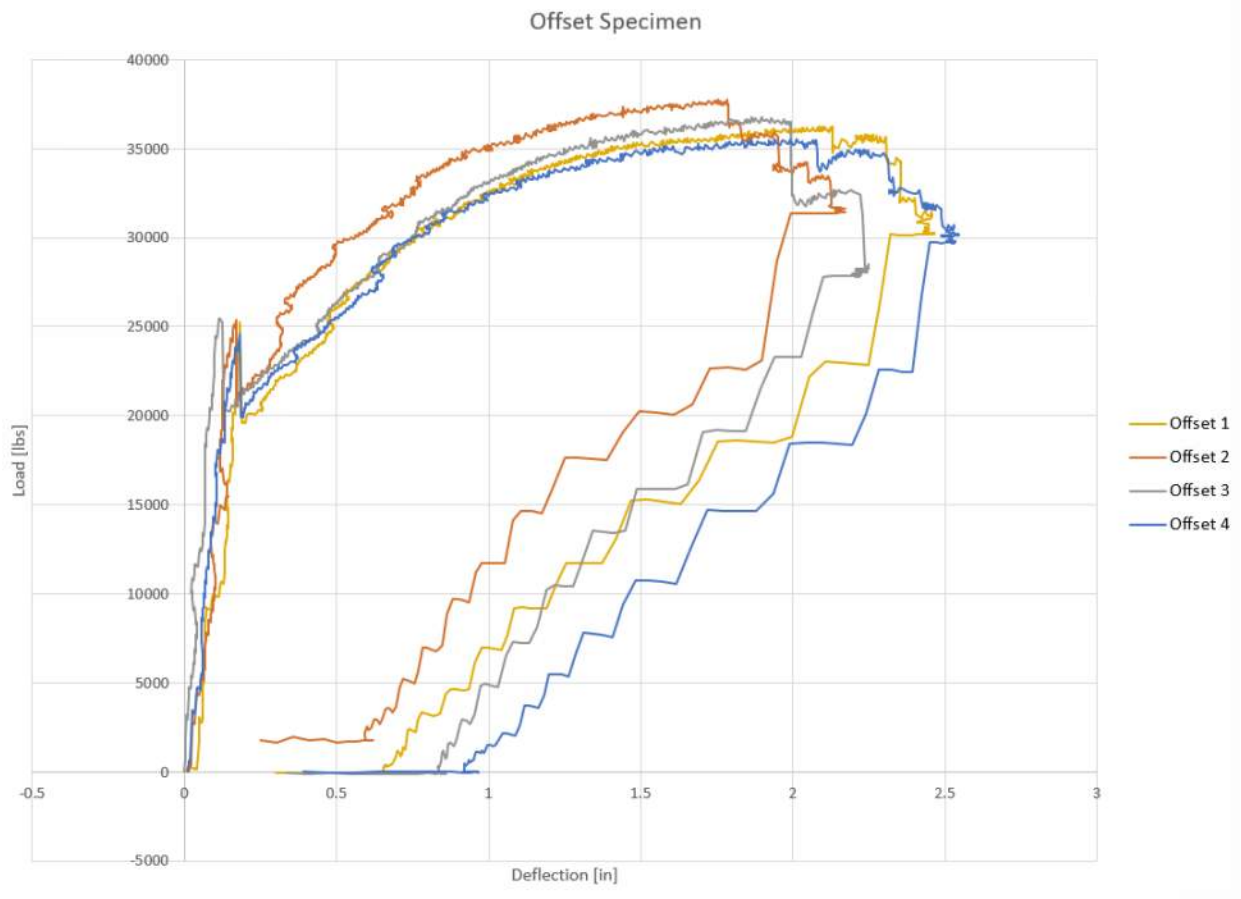

Figure C- 7. Load versus displacement: Offset specimen.

Appendix D: Specifications

Appendix D contains the cut sheets for the following:

- LVDT
- Load Cell
- Actuator
- Concrete Mix
- Strand Inspection

Model VL7A AC-AC

Long Stroke Displacement Transducer

DESCRIPTION

Model VL7A (spring return armature) ac-ac long stroke displacement transducer is designed for measuring static and dynamic displacements from ±0.5 in to ±3.0 in. This model achieve impressive 0.25 % full scale non-linearities. Displacement transducer bodies and probes are constructed of stainless steel for durability in harsh, industrial environments.

FEATURES

- 0.25 % non-linearity
- Stainless steel construction
- 12,7 mm to 76,2 mm [0.5 in to 3.0 in] range
- Enhanced immunity to electrical noise
- Infinite resolution
- -58 °F to 257 °F operating range (standard)
- Spring return armature
- Not RoHS compliant

Model VL7A AC-AC

PERFORMANCE SPECIFICATIONS

Characteristic	Measure
Stroke range	±12,7 mm to 76,2 mm [±0.5 in to 3.0 in]
Non-linearity (max.)	±0.25 % full scale
Non-repeatability (max.)	<20 microinches
Output sensitivity	See table
Resolution	Infinite

ENVIRONMENTAL SPECIFICATIONS

Characteristic	Measure
Temperature, operating	-50 °C to 125 °C [-58 °F to 257 °F]
Temperature effect, zero (max.)	0.006 % full scale/°F
Temperature effect, span (max.)	0.006 % full scale/°F

ELECTRICAL SPECIFICATIONS

Characteristic	Measure
Element type	ac-ac displacement transducer
Input supply (calibrated)	5 V RMS @ 5 kHz
Input supply (acceptable)	1 V to 7 V RMS @ 2 kHz to 10 kHz
Electrical termination	Multiconductor shielded cable

MECHANICAL SPECIFICATIONS

Characteristic	Measure
Case material	Stainless steel
Probe material	Stainless steel
Armature type	Captive guided spring return
Probe thread	Not applicable
Weight	See table
Spring force (max.)	4 oz/in

RANGE CODES

Range Code	Available ranges
HP	±12,7 mm [±0.5 in]
HQ	±25,4 mm [±1.0 in]
HR	±50,8 mm [±2.0 in]
HS	±76,2 mm [±3.0 in]

OPTION CODES

Range Code	**Many range/option combinations are available in our quick-ship and fast-track manufacture programs. Please see http://sensing.honeywell.com/TMsensor-ship for updated listings.**
Stroke ranges	±12,7 mm to ±50,8 mm [±0.5 in to ±2.0 in]; 76,2 mm [±3.0 in]
Electrical termination	Multiconductor shielded cable (1,83 m [6 ft]) TM405. Axial Bendix connector on body radial (side) TM406. Bendix connector on body
Electrical cable orientation	TM49. Axial cable exit
Mounting threads	TM511. 13/16-32 UNF
Improved linearity	L10. ±0.1 % max. linearity (less than or equal to 101,6 mm [±4.0 in]
Higher temperature	TM315. 204 °C [400 °F] up to 101,6 mm [±4.0 in]

MOUNTING DIMENSIONS

Range code	Available stroke range	L	X	Approx. unit weight	Typical full scale output at 3 V RMS
HP	±12,7 mm [±0.5 in]	135,89 mm [5.35 in]	38,1 mm [1.5 in]	184,27 g [6.5 oz]	2.4 V RMS
HQ	±25,4 mm [±1.0 in]	161,29 mm [6.35 in]	63,5 mm [2.5 in]	226,8 g [8.0 oz]	3.0 V RMS
HR	±50,8 mm [±2.0 in]	279,4 mm [11.0 in]	76,2 mm [3.0 in]	396,89 g [14 oz]	4.8 V RMS
HS	±76,2 mm [±3.0 in]	389,89 mm [15.35 in]	114,3 mm [4.5 in]	481,94 g [17 oz]	4.5 V RMS

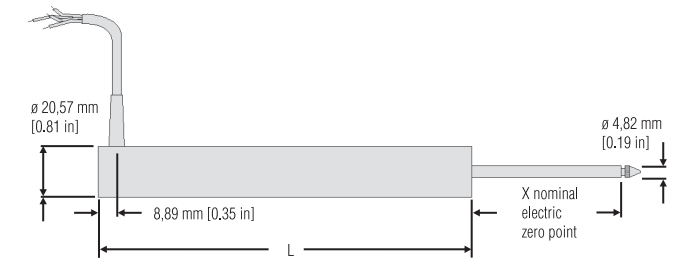

For reference only

WIRING CODES

Wire color	Supply
Red	(+) supply (calibrated @ 3 V RMS, 5 kHz)
Yellow	Supply return
Blue	Output
Green	Output return
Black	Secondary center tap (normally not connected)

TYPICAL SYSTEM DIAGRAM

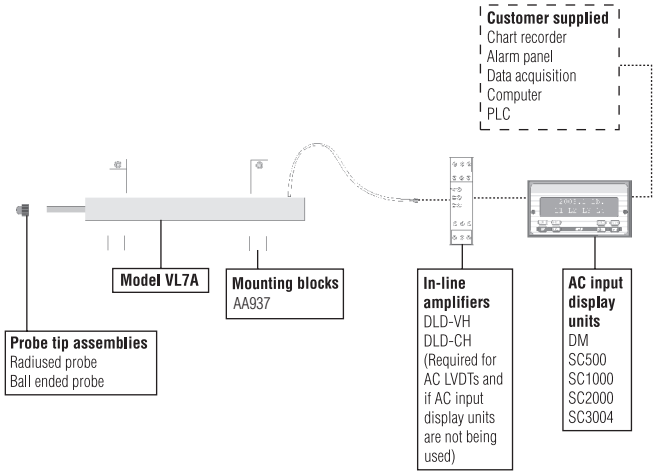

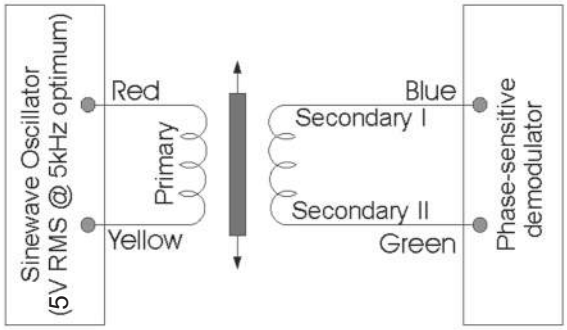

Warranty. Honeywell warrants goods of its manufacture as being free of defective materials and faulty workmanship. Honeywell's standard product warranty applies unless agreed to otherwise by Honeywell in writing; please refer to your order acknowledgement or consult your local sales office for specific warranty details. If warranted goods are returned to Honeywell during the period of coverage, Honeywell will repair or replace, at its option, without charge those items it finds defective. **The foregoing is buyer's sole remedy and is in lieu of all warranties, expressed or implied, including those of merchantability and fitness for a particular purpose. In no event shall Honeywell be liable for consequential, special, or indirect damages.**

While we provide application assistance personally, through our literature and the Honeywell web site, it is up to the customer to determine the suitability of the product in the application.

Specifications may change without notice. The information we supply is believed to be accurate and reliable as of this printing. However, we assume no responsibility for its use.

For more information about Sensing and Control products, visit www.honeywell.com/sensing or call +1-815-235-6847
Email inquiries to info.sc@honeywell.com

⚠ WARNING
PERSONAL INJURY

- DO NOT USE these products as safety or emergency stop devices or in any other application where failure of the product could result in personal injury.

Failure to comply with these instructions could result in death or serious injury.

⚠ WARNING
MISUSE OF DOCUMENTATION

- The information presented in this catalogue is for reference only. DO NOT USE this document as product installation information.
- Complete installation, operation and maintenance information is provided in the instructions supplied with each product.

Failure to comply with these instructions could result in death or serious injury.

Sensing and Control
Automation and Control Solutions
Honeywell
1985 Douglas Drive North
Golden Valley, MN 55422 USA
+1-815-235-6847
www.honeywell.com/sensing

Honeywell

008751-1-EN IL50 GLO
May 2008

AVAILABLE with Signature Calibration
SEE PG. IN-5

Precision Pancake Load Cells

Models 41 and 43

HERMETIC, STAINLESS

5 to 500,000 lbs.

CSA APPROVED · CE CENELEC APPROVED · FM APPROVED INTRINSICALLY SAFE AMP

Model 41
Tension/Compression

Model 43
Compression Only

Models 41 and 43 are low profile "pancake" type load cells. These bonded foil, strain gage load cells are engineered to measure loads from 5 to 500,000 lbs. The tension/ compression Model 41 is designed with the threaded hole running completely through the center of the cell. Model 41 utilizes two stabilizing diaphragms, which are welded to the sensing member to reduce off-center and side-loading effects. The compression-only Model 43 has a load button which is fixed as an integral part of the load cell and cannot be removed or changed. Both models achieve impressive non-linearity, hysteresis, and repeatability specifications for such applications as tube mills, extruding processes and weighing. Each unit has a welded construction and can be hermetically sealed for added durability. **Models 41 and 43 are available with optional 0-5VDC or 4-20mA output.**

Dimensions

Model 41 (Order Code AL111)

Available Ranges*	D"	H"	F#	G" Dia. B.C.	K" Dia. Thru	T	A"	B"	C"
5; 10; 25 lbs.	2.50	.80	6	2.000	.19	1/4-28UNF	.82	.75	1.25
50; 100; 250; **500; 1000** lbs.	3.00	1.00	6	2.250	.28	3/8-24UNF	.82	.75	1.25
2000; 3000; 4000; **5000** lbs.	3.50	1.00	6	2.625	.34	1/2-20UNF	.82	.75	1.25
7500; **10,000;** 15,000 lbs.	5.50	1.80	8	4.500	.40	1-14UNS	1.25	1.50	2.00
20,000; 30,000; **50,000** lbs.	6.00	1.80	8	4.875	.53	1-1/2-12UNF	1.25	1.50	2.00
75,000; 100,000 lbs.	9.00	2.50	12	7.750	.66	2-12UN	1.25	1.50	2.00
150,000; 200,000 lbs.	11.00	2.50	12	9.500	.78	2-1/2-12UN	1.25	1.50	2.00
300,000; 400,000; 500,000 lbs.	14.00	4.25	12	11.750	1.03	3-1/2-8UN	1.25	1.50	**

NOTES: * Stocked ranges are in bold.
** "C" dimension varies on high ranges. Consult SENSOTEC.
Bolt holes (K) are counter-bored for ranges 15,000 lbs. and below.
Models 41 and 43 load cells ≤ 25 lbs do not have overload stops. Consult SENSOTEC for custom cells with overload stops.

Model 41 (Tension/Compression)

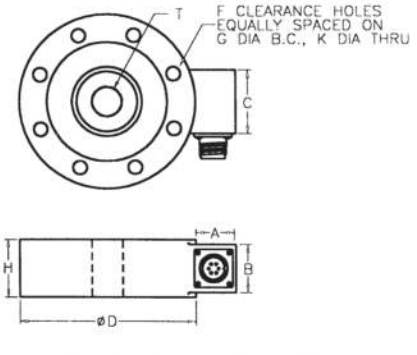

Model 43 (Compression Only)

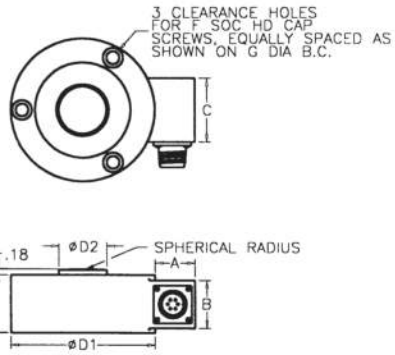

Model 43 (Order Code AL112)

Available Ranges	D1" Dia.	D2" Dia.	H"	F Typ. Dia.	G" B.C.	A"	B"	C"
5; 10; 25 lbs.	2.50	.37	.98	#8	2.000	.82	.75	1.25
50; 100; 250; 500; 1000 lbs.	3.00*	.56	1.18	1/4	2.250	.82	.75	1.25
2000; 3000; 4000; 5000 lbs.	3.50	.69	1.18	5/16	2.625	.82	.75	1.25
7500; 10,000; 15,000; 20,000; 30,000 lbs.	4.50	1.50	2.00	3/8	3.790	1.25	1.50	2.00
50,000; 75,000; 100,000 lbs.	4.50	1.50	2.00	3/8	3.790	1.25	1.50	2.00
150,000; 200,000 lbs.	5.50	2.00	2.18	3/8	4.812	1.25	1.50	2.00
300,000 lbs.	7.00	2.50	2.68	3/8	6.000	1.25	1.50	2.00
400,000 lbs.	7.50	2.50	2.68	3/8	6.750	1.25	1.50	2.00
500,000 lbs.	11.00	4.75	4.50	3/4	9.500	1.25	1.50	2.00

* 3" diameter has six mounting holes.

Options (See Appendix)

Temperature compensated 1b, 1c, 1d, 1e, 1f; Int. shunt cal 8a; Special calibration (Model 41) 30a, 30b; Signature calibration 53e

Premium Options: 1i; 2a (Model 43≥50 lbs.), 2b (Model 41≥50 lbs.), 2j, 2N, 2q; 3a, 6a (≥5000 lbs.), 6e, 6f, 6g, 6h, 6i, 6j (≥7500 lbs.); 9a, 9b; Intrinsically safe amp 2n.

Accessories: Mating connectors and connector/cable assemblies; Pull plates; Load buttons.

		Model 41 (Tension/Compression) Order Code AL111	Model 43 (Compression only) Order code AL112
PERFORMANCE	Load Ranges	5 to 500,000 lbs.	5 to 500,000 lbs.
	Non-Linearity (max)		
	5 to 25 lbs.	±0.2% F.S.	±0.2% F.S.
	50 to 500,000 lbs.	±0.1% F.S.	±0.1% F.S.
	Hysteresis (max)		
	5 to 25 lbs.	±0.1% F.S.	±0.1% F.S.
	50 to 500,000 lbs.	±0.08% F.S.	±0.08% F.S.
	Non-Repeatability (max)		
	5 to 25 lbs.	±0.1% F.S.	±0.1% F.S.
	50 to 500,000 lbs.	±0.03% F.S.	±0.03% F.S.
	Output (standard)		
	5 to 25 lbs.	2mV/V	2mV/V
	50 to 500,000 lbs.	3mV/V	3mV/V
	Resolution	Infinite	Infinite
ENVIRONMENTAL	Temperature, Operating	-65° F to 250° F	-65° F to 250° F
	Temperature, Compensated	60° F to 160° F	60° F to 160° F
	Temperature Effect		
	- Zero (max)	.002% F.S./° F	.002% F.S./° F
	- Span (max)	.002% Rdg./° F	.002% Rdg./° F
ELECTRICAL	Strain Gage Type	Bonded foil	Bonded foil
	Excitation (calibration)	10VDC	10VDC
	Excitation (acceptable)	Up to 15VDC or AC	Up to 15VDC or AC
	Insulation Resistance	5000 megohms @ 50VDC	5000 megohms @ 50VDC
	Bridge Resistance	350 ohms	350 ohms
	Shunt Calibration Data	Included	Included
	Wiring Code (std)	#2 (See P. AP-8)	#2 (See Pg. AP-8)
	Electrical Termination (std)		
	5 to 5000 lbs	PTIH-10-6P or equiv. (Hermetic stainless)	PTIH-10-6P or equiv. (Hermetic stainless)
	7500 to 500,000 lbs	MS3102E-14S-6P or equiv.	MS3102E-14S-6P or equiv.
	Mating Connector (not incl.)		
	5 to 5000 lbs	PT06A-10-6S or equiv.	PT06A-10-6S or equiv.
	7500 to 500,000 lbs	MS3106A-14S-6S or equiv.	MS3106A-14S-6S or equiv.
MECHANICAL	Static Overload Capacity	50% over capacity	50% over capacity
	Thread Size	See "T" Dimension Info	N/A
	Maximum Extraneous Forces without damage	See table below	See table below
	Deflection—Full Scale	.003"	.003"
	Casing Material		
	5 to 200,000 lbs	17-4PH Stainless	17-4PH Stainless
	300,000 to 500,000 lbs	4340 Painted	17-4PH Stainless
INTERNALLY AMPLIFIED UNITS* (Optional)	Outputs Available	±5VDC, 4-20mA	0-5VDC, 4-20mA

NOTES: *Standard calibration for tension/compression load cells is in tension only. Internal amplifiers are available for all ranges. Internal amplification for ranges <5,000 lbs. ("H" dimension <1.80") may increase height. Using an in-line amplifier will avoid this height increase.

ALLOWABLE EXTRANEOUS FORCE WITHOUT DAMAGE (% of load capacity)

Ranges	Side Load (lbs.)	Bending (lb-in)	Torque (lb-in)	Total Extraneous Force
5; 10; 25; 50; 100; 250; 500 lbs.	50%	40%	25%	100%
1000; 2000; 3000; 4000; 5000 lbs.	30%	25%	25%	100%
10,000; 15,000; 20,000; 30,000; 50,000 lbs.	20%	20%	15%	100%
100,000; 150,000; 200,000; 300,000; 400,000; 500,000 lbs.	20%	20%	10%	100%

General Information

How to order (See Pg. AP-19)
Load cell selection flow chart (see Pg. LO-1)

▼ Shown from left to right: **RRH-3010, RRH-1001, RRH-6010**

Versatility in Testing, Maintenance and Tensioning Applications

- **Relief valves prevent damage in case of over-pressurization**
- **Baked enamel finish for increased corrosion resistance**
- **Collar threads enable easy fixturing (except RRH-1001 and RRH-1508)**
- **Double-acting operation for fast retraction**
- **Nickel-plated, floating center tube increases product life**
- **Hollow plunger allows for both pull and push forces**
- **CR-400 couplers and dust caps included on all models**
- **Plunger wiper reduces contamination, extending cylinder life**

Gauges

Minimize the risk of overloading and ensure long, dependable service from your equipment. Refer to the System Components section for a full range of gauges.

Page: 122

Saddles

All RRH-Series cylinders are equipped with smooth saddles. See table on next page for optional threaded saddles and all dimensional information.

Page: 29

▼ *Double-acting hollow plunger cylinders are applied for bridge launching systems.*

Cylinder Capacity (tons)	Stroke (in)	Model Number	Max. Cylinder Capacity (tons)		Cylinder Effective Area (in^2)		Oil Capacity (in^3)	
			Advance	Retract	Advance	Retract	Advance	Retract
30	7.00	RRH-307	36	24	7.22	4.71	50.55	32.99
	10.13	RRH-3010	36	24	7.22	4.71	73.12	47.71
60	3.50	RRH-603	64	42	12.73	8.37	44.57	29.21
	6.50	RRH-606	64	42	12.73	8.37	82.77	54.24
	10.12	RRH-6010	64	42	12.73	8.37	128.94	84.49
100	1.50	RRH-1001	103	68	20.63	13.54	30.94	20.32
	3.00	RRH-1003	103	68	20.63	13.54	61.88	40.64
	6.00	RRH-1006	103	68	20.63	13.54	123.76	81.29
	10.13	RRH-10010	103	68	20.63	13.54	208.84	137.17
150	8.00	RRH-1508	158	80	31.62	15.91	252.97	127.23

Optional Heat Treated Saddles						
Saddle Type	Cylinder Model Number	Saddle Model No.	Saddle Dimensions (in) A	B	C	
Threaded Hollow	RRH-307, 3010	HP-3015	2.49	1¼"-7	.38	
	RRH-603, 606, 6010	HP-5016	3.61	1⅝"-5½	.50	
	RRH-1001, 1003, RRH-1006, 10010	HP-10016	4.97	2½"-8	.51	

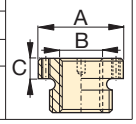

Smooth hollow saddles are standard on all RRH-models.

RRH Series

Capacity:
30-150 tons

Stroke:
1.50-10.13 inches

Center Hole Diameter:
1.31-3.13 inches

Maximum Operating Pressure:
10,000 psi

Hoses

Enerpac offers a complete line of high quality hydraulic hoses. To ensure the integrity of your system, specify only Enerpac hydraulic hoses.

Page: 116

Pump Selection

A double-acting cylinder must be powered by a pump with a 4-way valve.

Page: 109

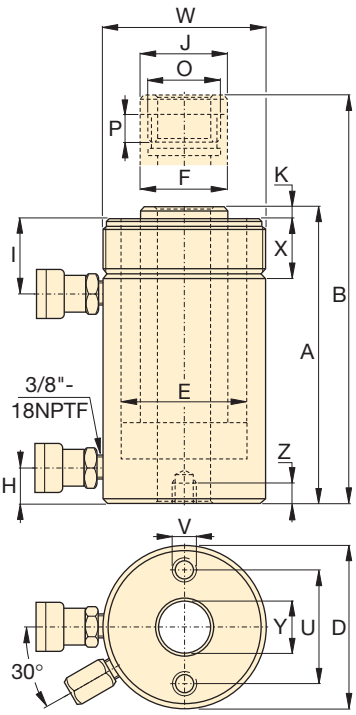

Base Mounting Hole Dimensions (in)			
Model Number	Bolt Circle U	Thread V	Thread Depth Z
RRH-307	3.63	⅜"- 16	.62
RRH-3010	3.63	⅜"- 16	.62
RRH-603	5.12	½"- 13	.55
RRH-606	5.12	½"- 13	.55
RRH-6010	5.12	½"- 13	.55
RRH-1001	7.00	⅝"- 11	.75
RRH-1003	7.00	⅝"- 11	.75
RRH-1006	7.00	⅝"- 11	.75
RRH-10010	7.00	⅝"- 11	.75
RRH-1508	–	–	–

	Collap. Height A (in)	Ext. Height B (in)	Out. Diam. D (in)	Cyl. Bore Diam. E (in)	Plngr. Diam. F (in)	Cyl. Base to Adv. Port H (in)	Cyl. Top to Return Port I (in)	Saddle Diam. J (in)	Saddle Protrusion from Plngr. K (in)	Thread O (in)	Plunger Thread Length P (in)	Collar Thread W (in)	Collar Thread Length X (in)	Center Hole Diam. Y (in)	Weight (lbs)	Model Number
	13.00	20.00	4.50	3.50	2.50	1.00	2.38	2.50	.38	1 13/16"-16	.88	4½"-12	1.66	1.31	48	RRH-307
	17.00	27.13	4.50	3.50	2.50	1.00	2.38	2.50	.38	1 13/16"-16	.88	4½"-12	1.66	1.31	60	RRH-3010
	9.75	13.25	6.25	4.88	3.63	1.25	2.63	3.61	.50	2¾"-16	.75	6¼"-12	1.91	2.13	62	RRH-603
	12.75	19.25	6.25	4.88	3.63	1.25	2.63	3.61	.50	2¾"-16	.75	6¼"-12	1.91	2.13	78	RRH-606
	17.25	27.38	6.25	4.88	3.63	1.25	2.63	3.61	.50	2¾"-16	.75	6¼"-12	1.91	2.13	101	RRH-6010
	6.50	8.00	8.38	6.50	5.00	1.50	1.75	4.97	.50	4"-16	1.00	–	–	3.13	85	RRH-1001
	10.00	13.00	8.38	6.50	5.00	1.50	3.38	4.97	.50	4"-16	1.00	8⅜"-12	2.38	3.13	135	RRH-1003
	13.50	19.50	8.38	6.50	5.00	1.50	3.38	4.97	.50	4"-16	1.00	8⅜"-12	2.38	3.13	175	RRH-1006
	18.13	28.25	8.38	6.50	5.00	1.50	3.38	4.97	.50	4"-16	1.00	8⅜"-12	2.38	3.13	235	RRH-10010
	13.75	21.75	9.75	7.50	6.00	1.50	2.38	5.00	.19	4¼"-12	1.00	–	–	3.13	245	RRH-1508

Form: MCP-EWCO-01

Elematic ELiMIX for Windows

Page: 1

PCE Engineering

ELEMATIC

BATCH REPORT

Printed: 5/26/2020
Day: 5/26/2020 Time: 18:52
Bed # 5

Recipe	Station/Mixer	Quantity [yd3]	Work number	Sample	Water corr. mode
5	11 / 1	2	00123456	Yes	Silo probes/in batcher

Material	Moist./Abs.[%]	Target [lbs]	Actual [lbs]	Difference [lbs]	Water [lbs]
Fly Ash		352	332	-20	
Type 3 Cement		908	915	7	
3/4 N-Trak (1)	3.30/2.20	2937	2930	-7	32
3/8 N-Trak (4)	3.75/2.90	499	490	-9	4
Sand 1 (5)	5.06/1.20	3613	3610	-3	139
Cold water		280	275	-5	275
Total water		**456**	**451**	**-5**	**451**

W/C ratio	0.362	0.358	-0.004
Water Correction	3.00		
Temperature [°F]	70	~~32~~ 78.3°	
Mixing time [sec]		36	
Mixer current reading		1108	
Mixer probe reading		0	
Air temperature	72.1°		

Slump/Spread _____ VSI _____
Casting Program 20052605 12" on bed 5
Casting Program _____ on bed _____

Bed/ Form Number	Release/ Design Strength (psi)	Date Broken	Time Broken	Age	Pounds Loading	PSI
5	3500 / 9000	5-27	300	8	414390	3532
|	|	6/23		28	140060	11146
		|		|	140180	11155
					140200	11159

SUMIDEN WIRE
PRODUCTS CORPORATION

Prestressed Concrete Strand Division
EAST: 710 MARSHALL STUART DR • DICKSON, TN 37055 • (866) 491-5020
TEXAS: 1800 HIGHWAY 146 • DAYTON, TX 77535 • (866) 811-1120
WEST: 1412 EL PINAL DR • STOCKTON, CA 95205 • (866) 246-3758

MILL CERTIFICATE OF INSPECTION

Order Number: SLPC200585-1 Page No : 1 OF 1
B/L No: SIPC201304 Issue Date : 04/02/2020

Commodity: Steel Strand, Uncoated Seven Wire for Prestressed Concrete
Size & Grade: 1/2" x 270 KSI
Specification: ASTM A416 - Latest 1/2" - Low Relaxation
Customer Name: MID-STATES CONCRETE INDUSTRIES
Customer P.O.: L2673
Destination: MIDCON-IL
State Job No:

No	Pack #	Heat #	B.S.	Elong.	Y.P.	Area	-REPRESENTATIVE- E-Modulus	-REPRESENTATIVE- CURVE#
		Min:	41,300 (LB)	3.5 (%)	37,170 (LB)	(IN2)	(MPSI)	
1	D135321-1	D6640780	43,505	5.4	40,633	0.1518	28.6	100002R
2	D135321-2	D6640780	43,505	5.4	40,633	0.1518	28.6	100002R
3	D135321-3	D6640780	43,505	5.4	40,633	0.1518	28.6	100002R
4	D135321-4	D6640780	43,505	5.4	40,633	0.1518	28.6	100002R
5	D135321-5	D6640780	43,505	5.4	40,633	0.1518	28.6	100002R
6	D135321-6	D6640780	43,505	5.4	40,633	0.1518	28.6	100002R
7	D135321-7	D6640780	43,505	5.4	40,633	0.1518	28.6	100002R

We hereby certify that:
* We have accurately carried out the inspection of COMMODITY and met the requirements in accordance with the applicable SPECIFICATION, both listed above.
* The raw material, and all manufacturing processes used in the production of the COMMODITY described above occurred in the USA, in compliance with the Buy America requirements of 23 CFR 635.410. The steel was melted and manufactured in the USA.
* The material described above will bond to concrete of a normal strength and consistency in conformance with the prediction equations for transfer and development length given in the ACI/AASHTO specifications.
* The individual below has the authority to make this certificate legally binding for SWPC.

Quality Assurance Section

Load - Elongation Curve

For Uncoated Seven Wire Steel Strand for Prestressed Concrete

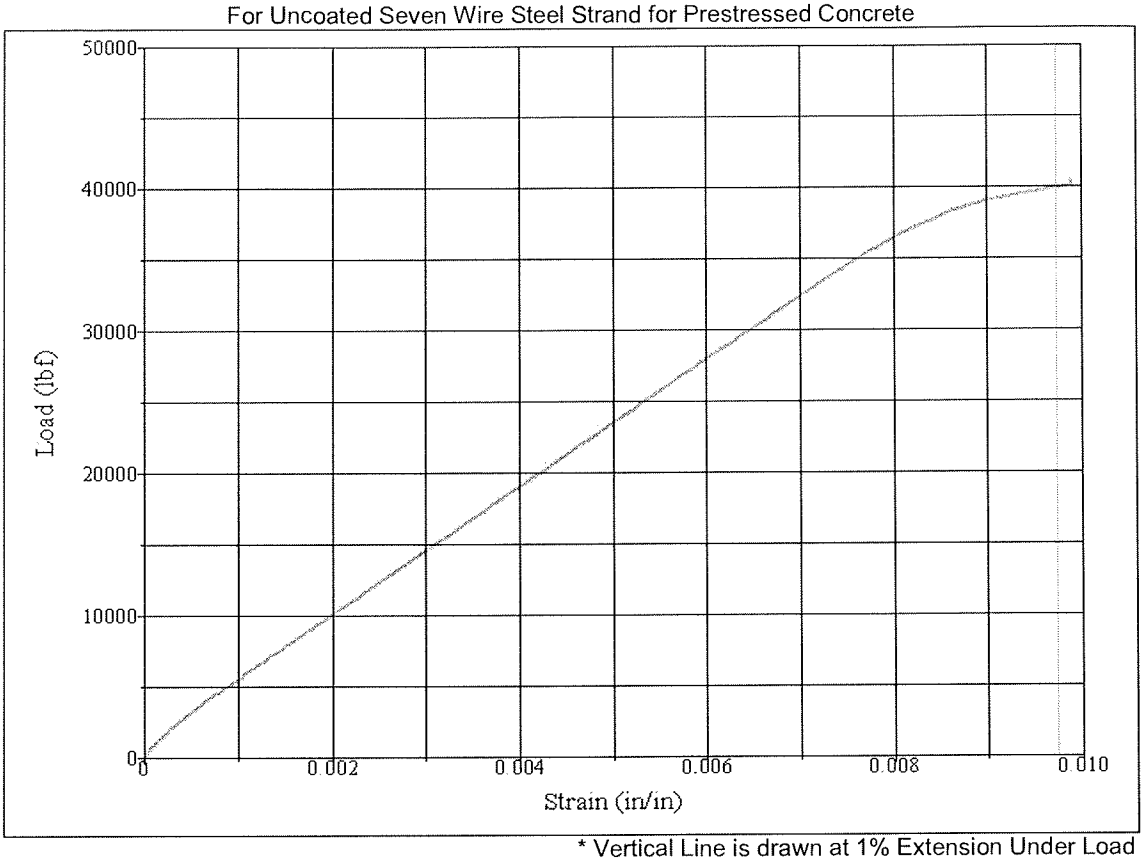

* Vertical Line is drawn at 1% Extension Under Load
* Tested to ASTM A1061 Standards

Curve Number	**D100002R**	
Size	**1/2"**	
Grade	**270K**	
Area	**0.1516**	**in²**
Modulus	**28.6**	**Msi**

SWPC

Approval

Curve D100002R

Sumiden Wire Products Corporation - PC Strand Division - 710 Marshall Stuart Drive, Dickson, TN 37055 - Phone - (615) 446-3199

Sumiden Wire Products Corporation

Relaxation Curve of PC Strand

Strand Size	0.50" x 270K	Initial Load	80% GUTS = 33,040lbf
Pack Number	D 134837	Area in^2	0.1512
Heat Number	D06-16580	Relax % @ 1000hrs Extrapolated from 200 hrs.	0.70%
Specification	ASTM A416	Tested by	Don Hiranaga
Test Method	ASTM E328	04/23/19-05/02/19	

Matt Badman PC Engineer

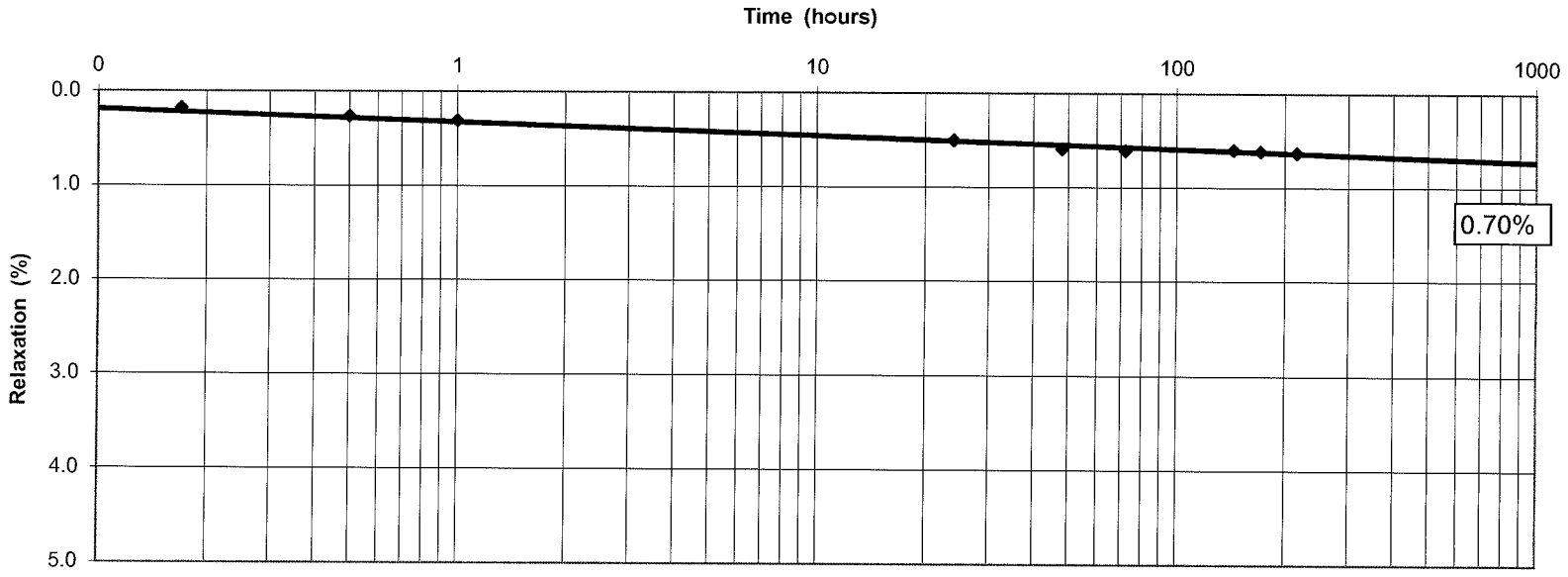

Tested at:
Sumiden Wire Products Corp
1412 El Pinal Drive
Stockton, CA 95205

SUMIDEN WIRE PRODUCTS CORP

Appendix E: Images

Appendix E contains images of the test operation. The first few images show the standard setup of the hollowcore. The remaining images are the observations of cracking and deflections of each of the specimen.

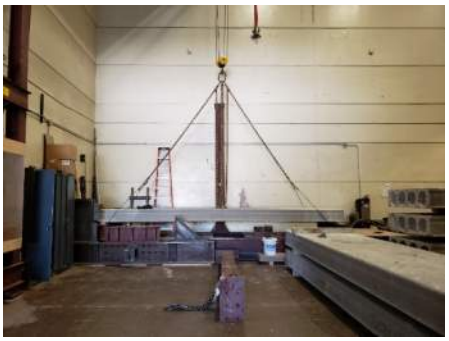

Figure E- 1. Center #1 test frame setup.

Figure E- 2. Center #1 cross-section.

Figure E- 3. Center #1 concentrated load location.

Figure E- 4. Center #1 tension cracks.

Figure E- 5. Center #1 side cracks.

Figure E- 6. Center #1 side cracks.

Figure E- 7. Center #1 exposed strand in crack.

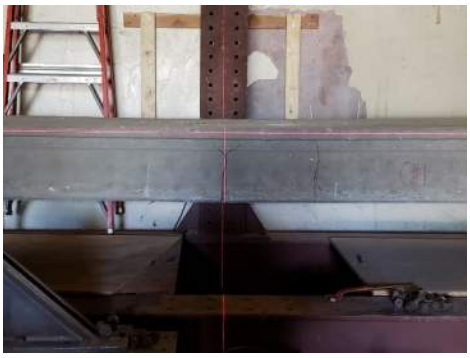

Figure E- 8. Center #1 side deflection.

Figure E- 9. Center #1 left end deflection.

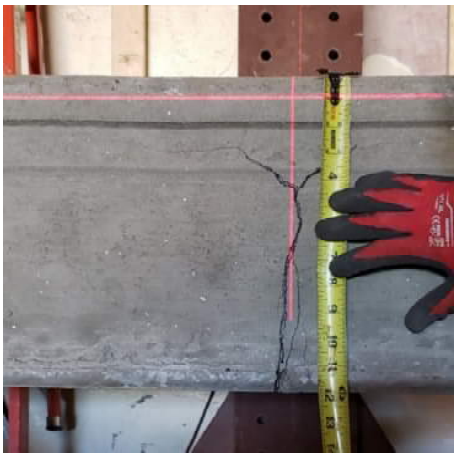

Figure E- 10. Center #1 center deflection.

Figure E- 11. Center #1 right end deflection.

Figure E- 12. Center #2 test frame setup.

Figure E- 13. Center #2 tension cracks.

Figure E- 14. Center #2 side cracks.

Figure E- 15. Center #2 side cracks.

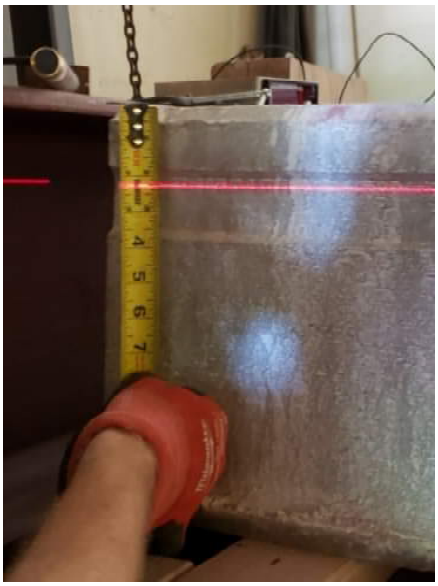

Figure E- 16. Center #2 left end deflection.

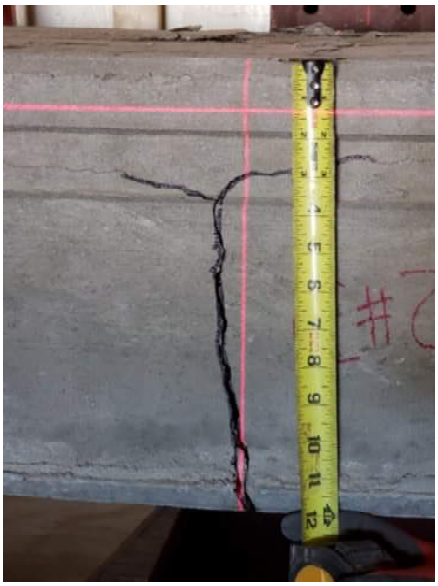

Figure E- 17. Center #2 center deflection.

Figure E- 18. Center #2 right end deflection.

Figure E- 19. Center #3 tension cracks.

Figure E- 20. Center #3 side cracks.

Figure E- 21. Center #3 side cracks.

Figure E- 22. Center #3 exposed strand in crack.

Figure E- 23. Center #3 left end deflection.

Figure E- 24. Center #3 right end deflection.

Figure E- 25. Offset #1 concentrated load location.

Figure E- 26. Offset #1 concentrated load location.

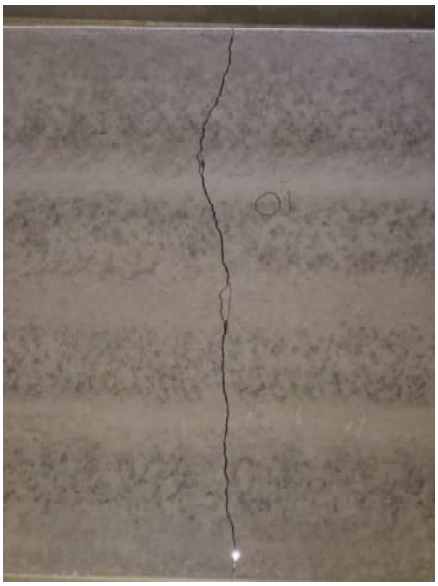

Figure E- 27. Offset #1 tension cracks.

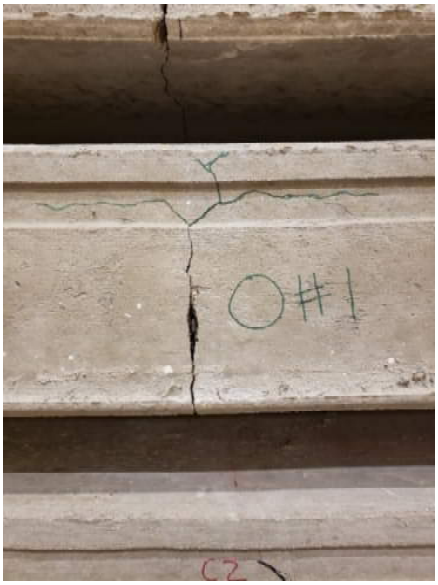

Figure E- 28. Offset #1 side cracks.

Figure E- 29. Offset #1 side cracks.

Figure E- 30. Offset #1 left end deflection.

Figure E- 31. Offset #1 middle deflection.

Figure E- 32. Offset #1 right end deflection.

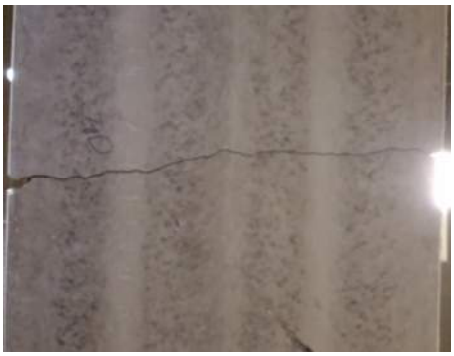

Figure E- 33. Offset #2 tension cracks.

Figure E- 34. Offset #2 side cracks.

Figure E- 35. Offset #2 side cracks.

Figure E- 36. Offset #2 left end deflection.

Figure E- 37. Offset #2 middle deflection.

Figure E- 38. Offset #2 right end deflection.

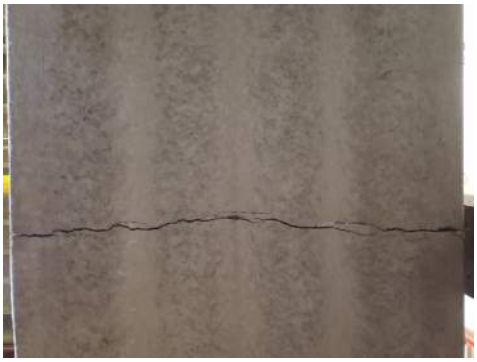

Figure E- 39. Offset #3 tension cracks.

Figure E- 40. Offset #3 side cracks.

Figure E- 41. Offset #3 side cracks.

Figure E- 42. Offset #3 left end deflection.

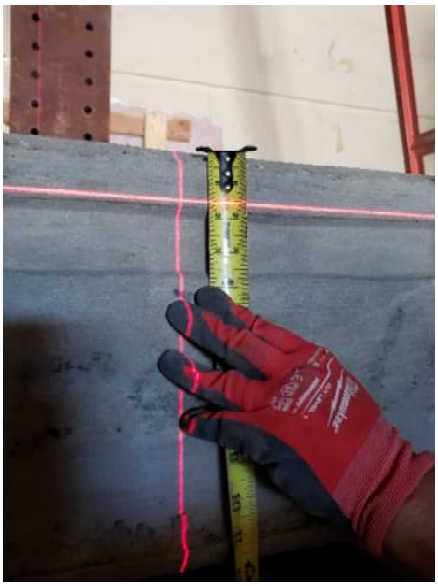

Figure E- 43. Offset #3 middle deflection.

Figure E- 44. Offset #3 right end deflection.

Figure E- 45. Offset #4 tension cracks.

Figure E- 46. Offset #4 side cracks.

Figure E- 47. Offset #4 side cracks.

Figure E- 48. Offset #4 left end deflection.

Figure E- 49. Offset #4 middle deflection.

Figure E- 50. Offset #4 right end deflection.

Architectural Engineering

Capstone Report Approval Form

Master of Science in Architectural Engineering – MSAE

Milwaukee School of Engineering

This capstone report, entitled "Behavior and Capacity of 12-Inch Hollowcore Under Concentrated Point Load," submitted by the student, Jenna J. Powers, has been approved by the following committee:

Faculty Advisor: _____ Date: 18 MAR 2021

Dr. Todd Davis, Ph.D.

Faculty Member: _____ Date: 3-17-2021

Dr. Christopher Raebel, Ph.D.

Faculty Member: _____ Date: 3-17-2021

Dr. Douglas Stahl, Ph.D.